

**SOAR: A MODEL FOR SCOPING OF OPTIONS
AND ANALYZING RISK VERSION 2.5
USER GUIDE**

Prepared for

**U.S. Nuclear Regulatory Commission
Contract No. 31310018D0001**

Prepared by

**U.S. Nuclear Regulatory Commission (NRC)
Washington, DC**

and

**Center for Nuclear Waste Regulatory Analyses (CNWRA®)
San Antonio, Texas**

April 2019

CONTENTS

Section	Page
FIGURES	iv
SOAR VERSION HISTORY	v
ACKNOWLEDGMENTS	viii
1 INTRODUCTION.....	1-1
1.1 What Is a Performance Assessment?	1-1
1.2 Purpose of the Scoping of Options and Analyzing Risk Performance Assessment Model	1-1
1.3 Objectives.....	1-2
2 OVERVIEW OF SCOPING OF OPTIONS AND ANALYZING RISK.....	2-1
2.1 Contents of Scoping of Options and Analyzing Risk	2-1
2.1.1 System Overview.....	2-1
2.1.2 Component Overviews	2-1
2.2 Model Development and Status	2-4
2.2.1 Model Conceptualization Process	2-4
2.2.2 Model Limitations.....	2-4
3 OVERVIEW OF MODEL ARCHITECTURE.....	3-1
3.1 Model Structure	3-1
3.2 Model Flexibility.....	3-2
3.2.1 Level-One Flexibility: GoldSim Dashboard Variables.....	3-3
3.2.2 Level-Two Flexibility: Modification of Default Parameter Values	3-3
3.2.3 Level-Three Flexibility: Modification of Model Structure	3-4
3.3 The GoldSim Modeling Environment.....	3-5
3.4 Quick Start Guide	3-5
4 MODEL COMPONENTS.....	4-1
4.1 Waste Form.....	4-1
4.1.1 Description.....	4-1
4.1.2 Model Implementation	4-1
4.1.3 Default Parameters.....	4-2
4.1.4 Flexibility.....	4-4
4.2 Waste Package	4-5
4.2.1 Description.....	4-5
4.2.2 Model Implementation	4-5
4.2.3 Default Parameters.....	4-10
4.2.4 Flexibility.....	4-11
4.3 Near-Field Environment	4-12
4.3.1 Description.....	4-12
4.3.2 Model Implementation	4-12
4.3.3 Default Parameters.....	4-18
4.3.4 Flexibility.....	4-19
4.4 Far Field	4-19
4.4.1 Description.....	4-19
4.4.2 Model Implementation	4-20
4.4.3 Default Parameters.....	4-23

4.4.4	Flexibility	4-24
4.5	Biosphere	4-24
4.5.1	Description.....	4-24
4.5.2	Model Implementation	4-25
4.5.3	Default Parameters.....	4-26
4.5.4	Flexibility.....	4-26
4.6	Alternative Failure Modes.....	4-27
4.6.1	Description.....	4-27
4.6.2	Model Implementation	4-27
4.6.3	Default Parameters.....	4-30
4.6.4	Flexibility.....	4-30
5	MODEL CONFIDENCE.....	5-1
6	REFERENCES.....	6-1

APPENDIX A—DEFAULT INPUT PARAMETERS

APPENDIX B—GLOSSARY

APPENDIX C—SUMMARY OF MODEL UPDATES AND VERIFICATION ACTIVITIES
FOR SOAR VERSION 2.0

APPENDIX D—TEST OF FEATURE PATHWAY TO SIMULATE A HUMAN INTRUSION
SCENARIO

APPENDIX E—INPUT PARAMETER DATABASE

FIGURES

2-1	Schematic Illustration of Disposal System Modeled in SOAR.....	2-2
3-1	Major Model Components in the SOAR Model	3-2
3-2	The SOAR Main Dashboard Allows Users to Exercise Level-One Model Flexibility by Selecting Predefined Parameter Sets for a Variety of Geologic Disposal System Configurations and Characteristics	3-4
3-3	SOAR Dashboard Menu for Waste Form Model Component Configuration Inputs	3-6
3-4	SOAR Dashboard Menu for Waste Package Model Component Configuration Inputs	3-7
3-5	SOAR Dashboard Menu for Near Field Model Component Configuration Inputs	3-8
3-6	SOAR Dashboard Menu for Far Field Model Component Configuration Inputs.....	3-9
3-7	SOAR Dashboard Menu for Biosphere Model Component Configuration Inputs.....	3-10
3-8	SOAR Dashboard Menu for Alternative Failure Mode Inputs.....	3-10
3-9	GoldSim Player Run Controller Can Be Used to Reset and Run the Model	3-11
3-10	SOAR Dashboard Menu for Viewing Model Results	3-11
3-11	SOAR Dashboard for Near Field Model Component Results	3-12
4-1	Example of Periods Considered in the Dynamic General Corrosion Model.....	4-7
4-2	Step Functions Used to Model Localized Corrosion Per Realization	4-8
4-3	Buffer Evolution Abstraction (Fraction of Buffer Open to Flow Versus Time)	4-15
4-4	Main and Feature Pathway Simulated in the Near Field Model	4-17
4-5	Characteristic Waste Package Failure Curves for the Three Abstractions Implemented in the Alternative Failure Modes Model Components.....	4-28

SOAR VERSION HISTORY

Version	Release Date	Authors and Summary of Revisions
1.0 (Original Version)	August 2011	<p><u>Authors:</u> Chris Markley, Osvaldo Pensado, Jin-Ping Gwo, James Winterle, Tae Ahn, Roland Benke, Tianqing Cao, Hipólito González, Anita Gray, Xihua He, Ronald Janetzke, Hundal Jung, Greg Oberson, Pavan Shukla, Timothy Sippel, Stuart Stothoff, Lynn Tipton</p>
1.1	May 2016	<p><u>Authors:</u> Chris Markley, Olufemi Osidele, Jin-Ping Gwo, Osvaldo Pensado, Jeanette Arce, Xihua He, Pavan Shukla</p> <p><u>Revisions:</u></p> <ul style="list-style-type: none"> • Expanded the radionuclide species list to include U-238 decay chain members: Th-230, Ra-226, Rn-222, and Pb-210. • Revised the default input parameters for the waste form, waste package, and near-field model components. • Revised the following GoldSim® elements to provide flexibility for future model revisions: <ul style="list-style-type: none"> — Radionuclide inventory data input formats for SNF, sMOX, HLWg, and HLWc — Function expressions for calculating the dry density of far-field rock materials, probabilities and breach area fractions for multiple waste package failure events, and the weighted average waste package breach area fraction • Revised the model dashboard to facilitate ease of use, including an adaptive dashboard feature that automatically disables dashboard options that conflict with other dashboard selections. • Revised the alternative failure mode calculations for multiple waste package failure events based on user-defined hazard curves for waste package failed fraction and breach area. • Revised the buffer degradation module (Near Field model component) based on user-defined piecewise linear functions defining buffer failure and damage as functions of time.

Version	Release Date	Authors and Summary of Revisions
2.0	February 2017	<p data-bbox="488 275 602 310"><u>Authors:</u></p> <p data-bbox="488 323 1105 359">Osvaldo Pensado, Jin-Ping Gwo, Chris Markley</p> <p data-bbox="488 371 992 407"><u>Revisions (see Appendix C for details):</u></p> <ul style="list-style-type: none"> <li data-bbox="488 420 1008 455">• Migrated the model to GoldSim 11.1. <li data-bbox="488 468 1382 539">• Consolidated the general corrosion model into a model with fewer model elements. <li data-bbox="488 552 1382 695">• Implemented an abstraction for dynamic corrosion, with different constant corrosion rates applied at different times depending on repository conditions (e.g., humid air, oxic groundwater, or anoxic groundwater after buffer saturation). <li data-bbox="488 707 1382 779">• Implemented a model for copper corrosion enhanced by hydrogen sulfide as part of the dynamic corrosion abstraction. <li data-bbox="488 791 1414 1031">• Developed a code to track the fraction of the buffer material open to flow as a function of time, which affects the following processes: <ul style="list-style-type: none"> <li data-bbox="586 875 1333 947">○ Corrosion of the copper canister, if hydrogen sulfide is assumed present in the groundwater <li data-bbox="586 959 1349 1031">○ Radionuclide transport through the buffer material, after failure of the waste packages <li data-bbox="488 1043 1382 1148">• Corrected a conceptual error in the computation of the waste package breach area fraction. In the revised computation, the breach area fraction is conditional on failure of the waste package. <li data-bbox="488 1161 1398 1295">• Updated the dashboards (user-friendly interfaces for input parameters) for the Waste Form, Waste Package, and Near Field components. Introduced new parameters for the buffer degradation abstraction and the hydrogen sulfide copper corrosion model. <li data-bbox="488 1308 1398 1413">• Updated the parameter database with consolidated distributions for the general corrosion model parameters and a new parameter for the hydrogen sulfide concentration in groundwater. <li data-bbox="488 1425 1382 1497">• Added an event probability factor to the computation of integrated releases (comparable to 40 CFR 191 cumulative release limits). <li data-bbox="488 1509 1398 1644">• Corrected a coding error that set the diffusion coefficient to zero in the region between the buffer material and the host rock for the radionuclides newly added in Version 1.1 (Th-230, Ra-226, Rn-222, and Pb-210).

Version	Release Date	Authors and Summary of Revisions
2.5	April 2019	<p data-bbox="488 279 602 310"><u>Authors:</u></p> <p data-bbox="488 323 911 354">Osvaldo Pensado, Jin-Ping Gwo</p> <p data-bbox="488 375 626 407"><u>Revisions:</u></p> <ul data-bbox="488 428 1417 1875" style="list-style-type: none"> <li data-bbox="488 428 1417 562">• The Far Field Transport Leg 1 was defaulted to reducing conditions when the dynamic corrosion model is enabled (the dynamic corrosion model assumes a transition from oxidizing to reducing conditions). <li data-bbox="488 583 1417 678">• Corrected a coding error that set the diffusion coefficient to zero in the buffer material for the radionuclides newly added in Version 1.1 (Th 230, Ra-226, Rn-222, and Pb-210). <li data-bbox="488 699 1417 833">• The boundary condition at the near-field terminus was extended to incorporate (1) a zero concentration condition (only case considered in Version 2.0) and (2) outgoing release equal to concentration \times flow rate (new condition enabled in Version 2.5). <li data-bbox="488 854 1417 1016">• Developed a Feature Pathway composed of (1) transport in a tunnel filled with bentonite clay, (2) discharge into a Feature (e.g., shaft, fault), (3) Feature transport simulated as an independent pipe, (4) dose computation for the Feature Pathway assuming the same human exposure as main pathway (i.e., drinking water). <li data-bbox="488 1037 1417 1199">• Updated the Near Field and Far Field dashboards to include parameters of the Feature Pathway. Visuals aids were added in the dashboard to clarify the meaning of input parameters. Results elements were updated for consistency with the Feature Pathway label, and new Feature Pathway results elements were added. <li data-bbox="488 1220 1417 1354">• Updated the Near Field flow model by introducing independent factors to define different flows through the buffer, transition region, and Feature Pathway. Corresponding changes were also incorporated in the dynamic general corrosion model. <li data-bbox="488 1375 1417 1509">• Aggregated total releases in units of activity (e.g., Curie or Becquerel) and removed total releases in units of mass. Added total release curves allowing for comparisons of releases from different waste forms. <li data-bbox="488 1530 1417 1665">• Due to numerical artefacts, GoldSim may output negative near-field releases that, when output to far-field GoldSim pipes, makes the SOAR model crash. This GoldSim bug was corrected by forcing releases from the Near Field component to be positive or zero. <li data-bbox="488 1686 1417 1875">• Updated Alternative Failure Modes dashboard to include more intuitive inputs for the Linear Failure Rate mode. The failure time for the Single Failure Event mode is sampled from a truncated exponential distribution (in Version 2.0, it was sampled from a uniform distribution, which is only an approximation to the truncated exponential distribution in the limit when the recurrence rate is low).

ACKNOWLEDGMENTS

Several members of the U.S. Nuclear Regulatory Commission (NRC) and Center for Nuclear Waste Regulatory Analyses (CNWRA®) staffs are recognized for their current and past contributions to development of the Scoping of Options and Analyzing Risk (SOAR) model. For SOAR Version 2.5, D. Speaker assisted with independent testing of modifications. For SOAR Version 2.0, T. Ahn, R. Fedors, and X. He assisted with technical discussions and identification of reasonable input parameter values, as well as development of the copper corrosion and buffer degradation abstractions. For SOAR Version 1.1, T. Ahn, R. Fedors, R. Janetzke, C. Manepally, J. McMurry, S. Stothoff, and L. Tipton assisted with technical discussions and feedback, while J. Gwo, J. Rubenstone and D. Pickett provided overall management support. For SOAR Version 1.0, K. Compton, B. Hill, and T. McCartin are recognized for their technical advice; K. Axler, H. Basagaoglu, J. Bradbury, D. Brooks, R. Fedors, C. Manepally, J. McMurry, B. Meyers, J. Myers, J. Pohle, and S. Self contributed to technical discussions; and J. Guttman and D. Pickett provided overall management support.

This report is an independent product of the CNWRA under Contracts No. 31310018D0001 and NRC–HQ–12–C–02–0089 and does not necessarily reflect the view or regulatory position of the NRC. The NRC staff views expressed herein are preliminary and do not constitute a final judgment or determination of the matters addressed or of the acceptability of any licensing action that may be under consideration at NRC. The activities reported here were performed on behalf of the NRC Office of Nuclear Material Safety and Safeguards, Division of Spent Fuel Management. The authors would like to acknowledge reviews by G. Wittmeyer and D. Pickett. The authors also appreciate L. Neill and A. Ramos for providing word processing support in preparation of this document.

QUALITY OF DATA, ANALYSES, AND CODE DEVELOPMENT DATA

DATA: The SOAR model was developed outside a formal quality control program for software development [CNWRA Technical Operating Procedure (TOP)–18]. However, simplified procedures (mutually agreed upon by NRC and CNWRA staffs) were implemented for model development that included version control and verification testing. Some input data to SOAR documented in this report are primarily experimental observations obtained from other publicly available sources. Each data source is cited in this report and should be consulted for determining the level of quality for those cited data. Scientific Notebooks 1038E (Stothoff, 2010) and 1036E (Tipton, 2010) document model development in work areas related to the waste form and near-field components of SOAR Version 1.0.

ANALYSES AND CODES: SOAR was developed using GoldSim Version 11.1 (GoldSim Technology Group, LLC, 2016). As previously stated, SOAR development did not follow TOP–18, but a simplified procedure for version control and software verification. The SOAR model utilizes the Microsoft® Access® Database [part of Microsoft Office Professional Plus 2010 (Microsoft Corporation, 2010)] for database management.

REFERENCES

GoldSim Technology Group, LLC. “GoldSim Probabilistic Simulation Environment User’s Guide.” Vols. 1 and 2. <<https://www.goldsim.com>>. Issaquah, Washington: GoldSim Technology Group, LLC. 2016.

Microsoft Corporation. "Microsoft Office Professional Plus 2010." Redmond, Washington: Microsoft Corporation. 2010.

Stothoff, S. "Integrated Spent Fuel Management Program Analyses." Scientific Notebook No. 1038E. San Antonio, Texas: Center for Nuclear Waste Regulatory Analyses. 2010.

Tipton, E.L. "Flexible Performance Assessment—Scoping of Options and Analyzing Risk (FPA–SOAR)." Scientific Notebook No. 1036E. San Antonio, Texas: Center for Nuclear Waste Regulatory Analyses. 2010

1 INTRODUCTION

1.1 What Is a Performance Assessment?

In the context of long-term geologic disposal of high-level radioactive waste (HLW), a performance assessment is a systematic analysis that quantifies the risk triplet questions.

- What can happen?
- How likely is it?
- What are the consequences?

In general, a performance assessment

- Identifies the features, events, processes, and sequences of events and processes that might affect the geologic disposal system and their probabilities of occurring
- Examines the effects of those features, events, processes, and sequences of events and processes upon the performance of the geologic disposal system
- Estimates some quantitative performance metric, weighted by its probability of occurrence, be it a dose to a receptor or radionuclide releases

1.2 Purpose of the Scoping of Options and Analyzing Risk Performance Assessment Model

The U.S. Nuclear Regulatory Commission (NRC) developed a performance assessment model named Scoping of Options and Analyzing Risk (SOAR). The model is intended to help the NRC staff with development of timely risk and performance insights for a variety of potential HLW disposal options. The model is based on relatively simple or generic representations of features, events, and processes that can be parameterized or modified to allow consideration of a variety of alternative waste form characteristics, engineered barrier materials, and geologic, hydrologic, and geochemical settings. Since the release of SOAR Version 1.0 (Markley et al., 2011), a number of changes have been incorporated into the model, including revisions to functional expressions to enhance flexibility of use, expansion of the radionuclides considered and associated decay chains, and an abstraction to evaluate buffer material performance. Additional complexity may be added to model components that represent specific site characteristics or processes. The modular structure and analytic approach of the model are designed to accommodate this additional complexity and more detailed process-level models if needed.

The SOAR model is not intended to be used as a tool to evaluate information associated with licensing actions, but as a support tool to gain insights. Due to the abstracted representation of features, events, and processes, results of the SOAR model are intended to be applied for scoping analyses, and should be used with caution. Specific limitations of SOAR are discussed in Section 2.2.2.

The SOAR model is designed with the goal of maximizing flexibility to allow considering a variety of disposal options. The simplified model abstractions and associated parameter inputs

are built upon the knowledge and experience gained by the NRC staff, the Center for Nuclear Waste Regulatory Analyses (CNWRA®), and from other domestic and international performance assessments for a variety of geologic disposal options. The model is parameterized with data available in the literature of international disposal programs for a variety of engineered concepts and geologic settings. The default parameter distributions and generic technical bases are listed in Appendix A, and their use in the model calculations is detailed throughout Chapter 4. Many of the input parameters are stochastically sampled from broad ranges of values to account for uncertainty and variability. This sampling approach permits evaluating effects of parameter uncertainties on radionuclide release and receptor dose estimates.

1.3 Objectives

The objectives of the SOAR model are to

- Provide analytic capabilities that assist the NRC staff to develop an effective and efficient regulatory program for reviewing and licensing a disposal site in any geologic medium
- Enhance the NRC staff's technical capabilities by creating a model in an intuitive, icon-based, software development environment [GoldSim™ (registered trademark of GoldSim Technology Group, LLC)] that enhances model transparency
- Develop a generic scoping tool to provide initial risk and performance insights for a wide variety of HLW disposal options
- Develop an efficient computational tool for future expansion or implementation of alternative descriptions of processes

As indicated previously, flexibility is a key element in several of the model objectives. A detailed discussion of how flexibility is built into the model is provided in Section 3.2.

The objectives of this SOAR User Guide are to

- Provide an overview of the technical bases, equations, input, output, and assumptions of the model
- Provide an overview of the modeling environment, key flexibilities, and general guidance for using the model
- Provide an overview of the key aspects of the model components
- Summarize activities conducted to provide confidence in SOAR results

2 OVERVIEW OF SCOPING OF OPTIONS AND ANALYZING RISK

2.1 Contents of Scoping of Options and Analyzing Risk

2.1.1 System Overview

The Scoping of Options and Analyzing Risk (SOAR) model is a conceptualization of a hypothetical geologic nuclear waste disposal system. The SOAR model is designed to quantify radionuclide releases to the environment and doses to a human receptor given containment breach scenarios. Figure 2 illustrates the general conceptualization implemented in the SOAR model. The engineered portion of the system comprises the waste form, waste package, engineered buffer or backfill material,¹ and deposition tunnels, which are all part of the subsystem referred to as the near field. The far-field comprises the natural subsystem. The waste form may consist of different volumes of (i) commercial spent nuclear fuel (SNF), (ii) high-level waste glass (HLWg), (iii) high-level waste ceramic (HLWc), and (iv) spent mixed-oxide (sMOX) fuel waste forms, which degrade by different mechanisms at different rates. Failure of waste packages is implemented as gradual failure over time (i.e., distributed failure) and instantaneous failure of a given number of waste packages at specified times (i.e., stepwise failure). These two failure abstractions allow flexibility to represent different waste package materials and failure mechanisms.

Three additional user-defined waste package failure abstractions are available to represent various alternative failure modes (Alternative Failure Modes model component), referred to as Linear Failure Rate, Single Failure Event, and Multiple Failure Events. Radionuclides released from degraded waste forms migrate out of the waste package, through a buffer or backfill region, and into the surrounding natural system or into some large-scale feature (such as emplacements shafts or intercepting faults). The natural system is represented by three “legs” with characteristics specified to represent transport pathways through up to three types of geologic media. Radionuclide transport through each leg can be either through porous rock; fractured, low-permeability rock; or unconsolidated sediments. The inset in Figure 2 indicates that the concept for radionuclide release and transport need not be constrained to a horizontal system layout. Modeled radionuclide releases from the natural system into the biosphere are used to assess the performance of a system as a whole. Performance metrics include cumulative radionuclide release and annual dose to human receptors from drinking water.

2.1.2 Component Overviews

The main model components of the SOAR model are

- Waste Form
- Waste Package
- Near Field (engineered and disturbed zones)
- Far Field (natural system)
- Biosphere
- Alternative Failure Modes

¹The terms “buffer” and “backfill” in this User Guide refer to any engineered material (e.g., bentonite clay, cement, or crushed rock) placed between the waste package and the host rock or used to seal tunnels.

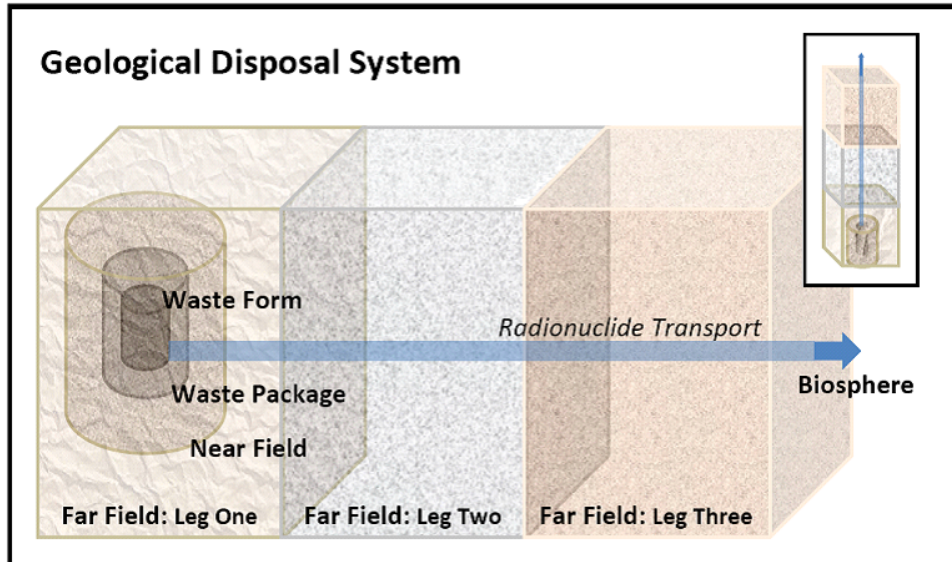


Figure 2-1. Schematic illustration of Disposal System Modeled in SOAR

The model components are briefly described in the following paragraphs. More detailed descriptions of the computational approaches and input parameters for each of the six model components are presented in Chapter 4.

The SOAR Waste Form model component includes up to four types of waste forms

- Commercial SNF
- HLWg
- HLWc
- sMOX fuel

The user can define the total inventory of each waste form. Both matrix-bound and unbound radionuclide inventories can be considered. Matrix-bound radionuclides are those that are embedded in a waste form matrix (e.g., glass, SNF matrix) and are released at a rate controlled by the rate of waste form matrix degradation or dissolution. Unbound radionuclides are not embedded in the waste form matrix or are loosely bound (e.g., radionuclides accumulated in waste form grain boundaries or in the gap between spent fuel pellets and cladding), and are assumed instantly released after breach of the waste package and contact with groundwater. Waste form degradation is assumed to occur at a constant rate, calculated based on the type of waste form and chemical environment.

The Waste Package model component includes abstractions to compute the waste package failure time. Two models for general corrosion are available. The first model implements constant-in-time corrosion rates that can vary from waste package to waste package (randomly sampled according to input distribution functions). In the second model, constant corrosion rates are applied during different periods to simulate humid air corrosion, corrosion in oxic water, and general corrosion in anoxic groundwater. (For example, at the time the buffer bentonite material is saturated and fully expanded, anoxic conditions are assumed to be established.) Corrosion rates for the different periods are randomly sampled for each waste package, but are assumed constant within the period. In addition, as part of the dynamic

general corrosion model (model two), if the waste package material is copper, an option is available to simulate enhancement of corrosion rates due to the presence of hydrogen sulfide in the groundwater. The general corrosion rate is increased by a factor proportional to the water flow rate per waste package and the concentration of hydrogen sulfide in the groundwater. Only one model—either the constant-in-time general corrosion rate (model one) or the dynamic general corrosion rate (model two)—can be enabled during a simulation. If model two is enabled, it is assumed that the repository is located at depth in reducing host rock, with transitory oxidizing conditions after repository closure. The hydrogen sulfide copper corrosion enhancement is part of model two. Both models output a distribution of failure times within a single realization to define the fraction of waste packages failed as a function of time.

An additional waste package failure abstraction implements failures as a step function (e.g., 10 percent of waste packages fail at once at some time). This abstraction is used to account for localized corrosion, which affects passive metals and progresses relatively fast when it occurs. This model is enabled only when the waste package material is stainless steel. The timing, number of failures, and breach area are defined based on the waste package material selected, stochastically sampled input parameters such as general corrosion rates, and parameters defined in the waste package dashboard. With appropriately modified inputs, the time of failure and breach area could be adapted to approximate other failure mechanisms, such as stress corrosion cracking and mechanical damage.

The fraction of waste packages failed as a function of time, used as input to compute radionuclide releases, is a combination of the distribution of failure times by general corrosion and the fraction of waste packages failed by localized corrosion. It is assumed that these failure mechanisms operate independently of each other.

The Near Field model component includes advective and diffusive radionuclide transport through a breach in the waste package, a surrounding diffusive barrier, and a zone of surrounding host rock connected to a flow path in the Far Field. The diffusive barrier is used to represent engineered buffer or backfill, and the user can specify its presence or absence. A dynamic evolution abstraction is available to account for openings in buffer where groundwater could form paths and contact the waste package. Buffer made of bentonite clay may expand when saturated with water and those openings may close, such that the buffer becomes a predominantly diffusive barrier afterwards. At later times, the buffer material might erode or degrade and advective flowpaths could again form. The dynamic evolution buffer abstraction is coupled to the waste package corrosion model when the material is copper. The rate of supply of hydrogen sulfide is assumed dependent on openings in the buffer material. If the buffer material is a diffusive barrier, it is assumed that hydrogen sulfide does not react with copper (as minerals in the buffer material may react with hydrogen sulfide). A transition region between the buffer material and the far field is included with the model, and the user has the option to take credit for sorption and retention in this transition zone. In Version 2.5, a Feature Pathway was added, including diffusion through buffer material, advection and diffusion through a tunnel, and discharge into a large-scale feature such as an emplacement shaft or excavated disturbed zone around it, or a major fault. The majority of the parameters of the Feature Pathway are input in dashboards. The Feature Pathway can be enabled and disabled in the dashboard.

The Far Field model component accounts for radionuclide transport through groundwater pathways in the natural system. The term “far field” refers to radionuclide transport in a region far from the engineered and disturbed zones. The Far Field model component is divided into three distinct zones, referred to as transport legs, used to represent the potential transition of groundwater pathways through different types of geologic environments. Each of the three

transport legs can be specified to be either fracture-dominated (e.g., granite rock) or matrix-dominated (e.g., clay, alluvium) transport pathways. The user can define the length of each transport leg. In Version 2.5 an independent far-field leg was added, referred to as far-field Feature Pathway, receiving input releases from the near-field Feature Pathway. The Feature Pathway is intended to represent a major feature such as an emplacement shaft or a major water conducting fault. Transport parameters for the Feature Pathway are controlled in the Far Field dashboard.

The Biosphere model component is used for the computation of doses to a hypothetical human receptor that drinks groundwater from a well that captures radionuclides at the end of the main Far Field transport pathway, and from the Feature Pathway. This model component only calculates ingestion doses from contaminated drinking water.

The Alternative Failure Modes module is used to define alternatives for waste package failure. Waste packages can be specified as linearly failing with time, within a time window up to a plateau (Linear Failure Rate mode); or a single failure event can be postulated to occur in a single realization, between the start and end of the simulation (Single Failure Event mode); or multiple events can be postulated to occur in a single realization (Multiple Failure Events mode) with “event intensities” controlled by inputs in a dashboard. Both the Single Failure and Multiple Failure events are simulated as Poisson processes. The Alternative Failure Modes module allows flexibility to consider waste package failure by mechanisms such as seismic events, human intrusion, and defective waste packages. Appendix D, for example, includes a human intrusion example exercising the Alternative Failure Modes module.

2.2 Model Development and Status

2.2.1 Model Conceptualization Process

Performance assessment models are usually based upon a detailed site-specific scenario analysis. Because SOAR is a scoping tool to support regulatory programs that incorporate performance and risk insights in a variety of potential disposal systems, a detailed scenario analysis was not conducted. Rather, the general conceptual approach described in Section 2.1 was developed to allow flexibility to consider a variety of engineered and natural system features and processes.

2.2.2 Model Limitations

A thorough development of a performance assessment model traditionally starts from a compilation of features, events, and processes (FEPs), and screening arguments to include or exclude those FEPs in the model. Only a limited number of FEPs from the Nuclear Energy Agency (NEA, 2006) list are explicitly included in SOAR. The U.S. Nuclear Regulatory Commission staff and the Center for Nuclear Waste Regulatory Analyses selected FEPs that represent common elements of international performance assessment models. The SOAR model was designed to afford the flexibility to incorporate additional features, events, and processes when needed. The following potentially significant processes are not included in this version of the SOAR model:

- The SOAR model does not explicitly consider the geometric and dimensional variations for each waste package due to different waste package designs, locations within the disposal system, tunnel orientations, and distance to nearest groundwater flow paths. Rather, the analytical approach is designed to reflect average or representative

geometric and spatial properties, and representative waste packages. Because of this limitation, the model would not be appropriate for evaluating small-scale system properties, such as fracture patterns. However, the staff's extensive experience with developing and evaluating previous performance assessments supports the principle that using a representative waste package and transport pathway approach is appropriate and reasonable in a variety of applications.

- The SOAR model does not consider other biosphere pathways, such as ingestion of contaminated crops and animal products, inhalation of radionuclides on dust resuspended in air, or external exposure to radiation emitted from radionuclides on the ground surface (groundshine). It only considers ingestion of contaminated groundwater in dose calculations, which in many systems is found to be a dominant pathway.
- The SOAR model does not explicitly model geochemical processes and coupled thermal-hydrologic-mechanical-chemical processes that can affect waste package corrosion, waste form degradation, and radionuclide sorption and solubility in the buffer or backfill, and in the geologic host media. Alternate geochemical environments can be considered by comparing model results for alternative parameter sets developed for specific geochemical environments. Options are available for alternative parameter sets (e.g., waste form dissolution rates, sorption coefficients, and corrosion rates) intended to provide the users a choice of oxidizing or reducing geochemical environments in fractured granite or other porous media.
- The SOAR model does not consider gaseous transport of radionuclides and enhanced transport by reversible or irreversible attachment to colloids. Only aqueous phase transport of dissolved radionuclides is considered. Aqueous phase transport of radionuclides is typically considered the dominant pathway in most repository environments.
- The SOAR model does not model complex groundwater flow and transport processes (e.g., splitting of flow paths, time-varying velocity, or varying geochemical conditions).
- Disruptive events in the SOAR model are assumed to cause damage to waste packages. Other effects, such as changes in water flow paths, are disregarded.

3 OVERVIEW OF MODEL ARCHITECTURE

3.1 Model Structure

The Scoping of Options and Analyzing Risk (SOAR) model is composed of five component models that were developed using the GoldSim probabilistic simulation environment software. The GoldSim simulation environment permits modular icon-based model development providing visualization of connections (influences and dependencies) between model elements. The six main model components (Waste Form, Waste Package, Alternative Failure Modes, Near Field, Far Field, and Biosphere) are each grouped in separate GoldSim “containers”, as illustrated in Figure 2. These components were developed modularly to facilitate further modifications. For example, if a more detailed Waste Package module were needed, a specific container could be changed with minimal impact on the other model components. The user can take advantage of the visual display of dependencies and influences to follow the flow of information in the computations. The GoldSim user manuals (GoldSim Technology Group, LLC, 2016a,b) describe the various types of specialized GoldSim elements. Following is a brief introduction to the model components of SOAR. See the corresponding section for each model component in Chapter 4 for additional details.

The Waste Form Component includes the radionuclide inventory and the Waste Form degradation rates. The considered waste forms in SOAR are spent nuclear fuel (SNF), high-level waste glass (HLWg) and/or high-level waste ceramic (HLWc) from reprocessed SNF, and spent mixed-oxide (sMOX) fuel. Both oxic and anoxic Waste Form degradation rates are considered. Degradation rates are assumed to be constant in time.

The Waste Package Component includes the type of waste package material, abstractions for electro chemical degradation mechanisms (i.e., corrosion), and the potential opening or breach areas on the waste package when failure occurs. The waste package materials considered in the model are copper, stainless steel, carbon steel, and titanium. The main degradation process implemented is general corrosion, which computes corrosion failures for either oxic or anoxic environments, as selected by the user. An abstraction for localized corrosion is implemented for stainless steel only. A dynamic general corrosion abstraction is available for considering different constant corrosion rates during different periods (e.g., humid air corrosion, oxic and anoxic conditions). As part of the dynamic general corrosion model, if the material is copper, corrections can be applied to include enhancements due to the reaction of hydrogen sulfide in groundwater with copper.

The Alternative Failure Modes model component of SOAR can be used to consider additional waste package failure mechanisms not included in the Waste Package model component. The Alternative Failure Modes model component specifically models three additional waste package failure abstractions: Linear Failure Rate, Single Failure Event, and Multiple Failure Events.

The Near Field Component includes the characteristics of and radionuclide transport through waste package internals, any surrounding buffer or backfill, and the disturbed zone within the geologic host formation.

The assigned properties of the buffer or backfill are for a bentonite material for which diffusion is expected to be the dominant transport mechanism. A dynamic evolution abstraction is available to account for swelling of clay as buffer material is saturated with water. The user must specify transition times (e.g., from unsaturated to saturated conditions) and fractions of the buffer

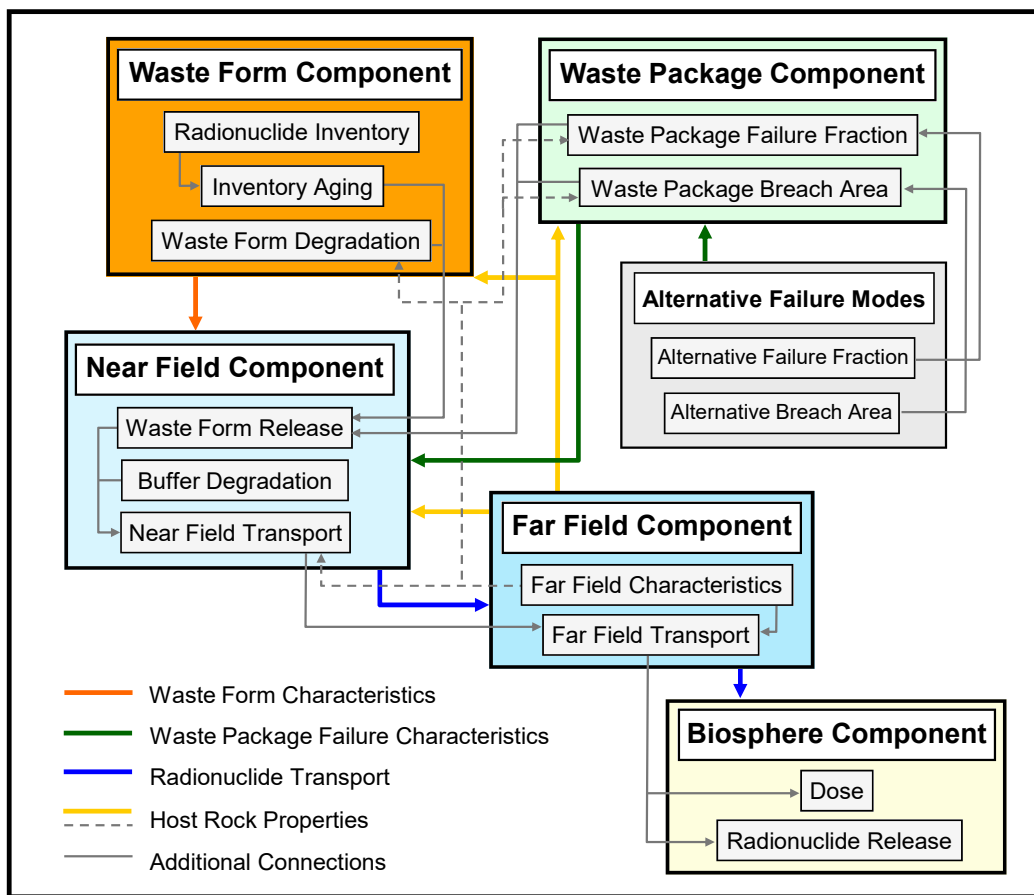


Figure 2-1. Major model components in the SOAR model. Arrows indicate transfer of information

material volume open to free water flow. The user also specifies properties of the surrounding disturbed zone to be either crystalline rock (e.g., fractured granite); porous rock (e.g., clay, porous medium); or unconsolidated sediments.

The Far Field component includes the geologic media and the radionuclide transport pathways of the natural system. The geologic media were selected to encompass a range of transport pathways (e.g., matrix-dominated and fracture-dominated transport). In the model, the input parameters for the far field are assigned to approximate transport through fractured rock, porous rock, or unconsolidated sediments. The parameters of the Feature Pathway are defined in both the Near Field and Far Field dashboards. The Feature Pathway can be enabled in the Near Field dashboard to simulate radionuclide transport in tunnels and eventual discharge to a large scale feature (e.g., an emplacement shaft or a major water conducting fault) that could discharge radionuclides to the biosphere faster than the main pathways.

The Biosphere Component includes the radionuclide exposure and dose assessment. The dose pathway is limited to a drinking-water ingestion pathway.

3.2 Model Flexibility

Three levels of model flexibility were incorporated into SOAR. Level one flexibility is afforded by the user-selected parameter options in the “dashboard” interfaces of SOAR (see Figure 3-2).

Level two flexibility is the ability to modify the default parameters controlled in a database. Level three flexibility is the ability to modify the modeling elements and algorithms. To exercise Level two and three changes, access to GoldSim professional is required.

3.2.1 Level-One Flexibility: GoldSim Dashboard Variables

Level-one flexibility is incorporated into dashboards, allowing only a limited set of parameter combinations to be considered for simulations. Figure 3-2 shows the overall layout of the SOAR main dashboard. The main dashboard provides access to level-one parameter settings for the Waste Form, Waste Package, Near Field, Far Field, Biosphere, and Alternative Failure Modes. Selecting one of these options takes users to a menu of module-specific settings accessible from secondary dashboards. The level-one parameters allow simulation of a wide range of potential combinations of disposal system configurations and characteristics. For example, the user may modify the waste form degradation-rate multiplier to emulate the effect of cladding protection on waste form degradation; the Alternative Failure Modes allows postulating failure times to examine a range of “what-if” scenarios. Note also that an adaptive dashboard feature is implemented to assist users to avoid inconsistent or ineffective inputs. For example, defining dimensions of the buffer material in the Near Field dashboard would be ineffective if the buffer is bypassed (i.e., results would be independent of or insensitive to buffer material dimensions). For such situations, the adaptive dashboard feature automatically hides options that are ineffective, inconsistent, or redundant with other dashboard settings. Notwithstanding the provision of this adaptive feature, users should always check the reasonableness of options selected on the SOAR dashboard. The dashboard also contains a set of Master Controls for running the model, viewing the model architecture, accessing this user guide and other useful information, resetting default parameters, and viewing model results. Level-one flexibility can be exercised using the GoldSim Player software, which is available at no charge from www.goldsim.com.

3.2.2 Level-Two Flexibility: Modification of Default Parameter Values

Level-two flexibility involves modifications to default model input parameter values or uncertainty distribution types. The default input parameters provided with SOAR are listed and described in Appendix A. Default values and distribution types are managed through a Microsoft Access database file, *FPA-SOAR.accdb*. GoldSim Pro allows download on-demand of input parameters. The GoldSim User’s Guide describes the procedure for linking a database file to a GoldSim model file (GoldSim Technology Group, LLC, 2016a, Appendix F). Appendix E of this document provides brief description the controlled Excel files for SOAR to build a database, and steps to connect the *FPA-SOAR.accdb* file to the SOAR model. If parameters are modified in the database, the database information must again be downloaded to the SOAR model file. The parameters can also be modified directly in the SOAR model file, but modified Goldsim elements become disconnected from the database.

To exercise level-two flexibility, access to GoldSim Pro is required (the free GoldSim Player software does not allow for model file modifications, including modifications to stochastic and data elements defining input parameters). To change model default parameter values, users need to locate the data or stochastic GoldSim element within the model, and revise the input values or distribution type as desired. For both level-one and level-two parameter modifications, there are two general classes of model parameter inputs considered in SOAR: physical and parametric. Physical-based model inputs rely on some scientific basis or measurable quantity, such as physical dimensions of engineered barrier system (EBS) components, metal corrosion rates, diffusion coefficients, solubilities, and sorption coefficients. Modifications to inputs of this

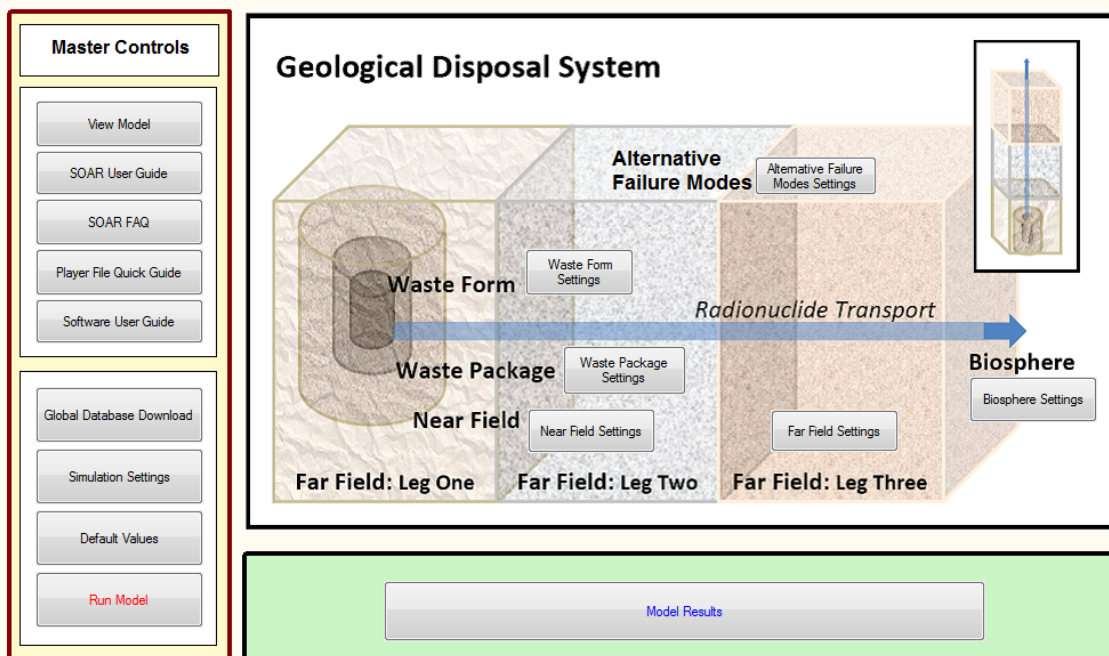


Figure 3-2. The SOAR main dashboard allows users to exercise level-one model flexibility by selecting predefined parameter sets for a variety of Geologic Disposal System configurations and characteristics

kind need an appropriate technical basis. The physical inputs are controlled mostly in the SOAR database. Changes to those parameters represent level-two changes to SOAR.

Parametric model inputs are intended to give flexibility to the model and account for model abstraction uncertainties. Generic enhancement factors for what-if analyses are examples of parametric inputs. The parametric inputs are controlled mostly in dashboards. Changes to those parameters represent mostly level-one changes.

A user may obtain corrosion rates for a specific alloy, use the GoldSim Pro software to input those corrosion rates in SOAR (level-two change), and analyze consequences of using different waste package materials in the system. Low solubility limits for actinides in the near-field may be considered to examine consequences of assumed limited mobilization of heavy elements. Solubility may control the amount of an actinide available for transport between engineered barrier system (EBS) components and between the near-field and the far-field. A user may exercise level-two flexibility to change radionuclide solubility that depends on factors such as chemical environment, temperature, and pH, and study the effects of these factors on the movement of radionuclides between repository system components.

3.2.3 Level-Three Flexibility: Modification of Model Structure

Level-three flexibility involves modification of the model structure by adding, removing, or replacing model elements. For example, a user may develop a submodel that explicitly tracks

radionuclide transport through a large fracture network. Such a model could be readily incorporated into SOAR, provided its inputs were available or implementable in SOAR. As previously stated, model structure modification requires the GoldSim Pro software.

3.3 The GoldSim Modeling Environment

SOAR was developed using the GoldSim Probabilistic Simulation Environment (GoldSim Technology Group, LLC, 2016a). The GoldSim graphic simulation environment allows users to visualize model dependencies and influences. Models developed in GoldSim can be executed in Monte Carlo mode to account for uncertainty in model inputs (specified as distribution functions), such as waste package corrosion rates or radionuclide sorption coefficients. The radionuclide transport module of GoldSim provides, for example, elements to calculate radionuclide ingrowth and decay and elements implementing solutions to the advection-dispersion mass balance equation. For system requirements and additional information about GoldSim, see the GoldSim User Guide (GoldSim Technology Group, LLC, 2016a).

GoldSim allows designing dashboards for quick access to selected model inputs and simulation settings. Dashboard interfaces facilitates the use of GoldSim models. Dashboard interfaces also are accessible with the GoldSim Player. The main dashboard for SOAR, shown in Figure 3-2, allows users to access the level-one flexibility inputs. The SOAR dashboard includes links to documents with more detailed instructions on model use.

The SOAR model was developed using simplified models and abstractions to represent key features, events, and processes associated with geologic disposal. GoldSim has broad capabilities to incorporate internal-model documentation. Where appropriate in SOAR, additional text, figures, and hyperlinks to external documents have been provided. GoldSim allows users to control parameter inputs by providing the capability to link to an external database. SOAR uses this feature by linking to a controlled Microsoft Access database (file named *FPA-SOAR.accdb*). In SOAR, only physical-based parameters are controlled via the database. Flexibility parameters are directly input in dashboards or in GoldSim data elements.

3.4 Quick Start Guide

The most direct way to learn to use the SOAR model is to explore a model file starting from the main dashboard. The model is provided in two formats: a GoldSim player file with a *.gsp* file name extension and a GoldSim model file with a *.gsm* file name extension. Users requiring only level-one flexibility (see Section 3.2.1) may modify dashboard parameters, run the model, and access model results of the *.gsp* file using the free GoldSim Player software. Users who require level-two and level-three flexibility (Sections 3.2.2 and 3.2.3) must work with a *.gsm* file, which requires access to the GoldSim Pro software to make changes to model files.

Regardless of which model format is used, opening the model and clicking on the “Model Home” button will take the user to the main dashboard interface illustrated in Figure 3-2. The user may then set up the desired geologic disposal system configuration to be modeled by clicking on the buttons for waste form, waste package, near field, far field, biosphere, and alternative failure modes. These buttons take the user to the respective input menus illustrated in Figures 3-3 through 3-8. Moving the cursor over any of the input entries of these dashboard menus produces a pop-up text box with a description of the parameter.

The default values for the dashboard parameters can be restored at any time by returning to the main dashboard and clicking the “Default Values” button on the Master Controls panel (see Figure 3-2). If the model has previously been run and has stored results, the model will be in “Results Mode” and the user will not be able to make parameter changes until the model is reset. When working with the GoldSim Player version, the model can be reset by clicking the

Waste Form

Return to Home Waste Form Settings Waste Package Settings Near Field Settings Far Field Settings Biosphere Settings Alternative Failure Modes Settings

Geochemical conditions of the Near Field are defined by redox properties of Far Field Leg One.
 Waste Form oxic conditions are used when the Near Field is under oxidizing conditions.
 Waste Form anoxic conditions are used when the Near Field is under reducing conditions.

Waste Form Results Home Waste Form Results View Component

Total Number of Waste Packages: 11650
 SNF: 7500 HLWg: 4000
 sMOX: 50 HLWc: 100

	Spent Nuclear Fuel	Spent Mixed-Oxide Fuel	High-Level Waste (glass)	High-Level Waste (ceramic)
Radionuclide Inventory (Total Waste Mass in Metric Tons):	75000	500	4000	100
Total Disposed Mass per Waste Package (Metric Tons): (Rad. mass, no substrate)	10	10	1	1
Fraction of Initial Inventory Available for Release:	1	1	1	1
Waste Form Degradation Rate Multiplier:	1	1	1	1
Enable Combined Oxic/Anoxic Degradation Rates:	<input type="checkbox"/> Check to Enable	<input type="checkbox"/> Check to Enable	Not Applicable	Not Applicable

Figure 3-3. SOAR Dashboard Menu for Waste Form Model Component Configuration Inputs

“Reset” button at the bottom of the GoldSim Run Controller, which appears as a separate popup outside the main dashboard whenever the model file is open (see Figure 3-9). There is no reset option in GoldSim Pro. Changes made using GoldSim Pro may result in different model versions. Thus, when working with .gsm files, users should exercise careful version control to avoid making unintended changes to default settings.

After making desired changes in dashboard controlled entries, users can click the “Return to Home” button at the top of each menu to return to the main dashboard interface. From the main dashboard menu, the model then can be run by clicking the “Run Model” button. The model can also be run by clicking the “Run” button on the GoldSim Run Controller. If previous model results have been stored, the user will receive a warning message giving the opportunity to abort the run before overwriting previous model results. If users do not wish to overwrite a previous model, then the model with revised dashboard inputs can be saved and run in a separate folder.

After running a model, displays of model results can be viewed by clicking the “Model Results” button on the main dashboard, which will take the user to the Model Results menu shown in Figure 3-10. As can be seen in this figure, the results are grouped by the main five model components. Figure 3-11 is an example of the dashboard results of the near field model component. Results are provided in graphical formats, but tabular results are also available within the results elements and can be directly copied to spreadsheets if needed.

Waste Package

Return to Home
Waste Form Settings
Waste Package Settings
Near Field Settings
Far Field Settings
Biosphere Settings
Alternative Failure Modes Settings

Geochemical conditions of the Near Field are defined by redox properties of Far Field Leg One. Waste Package oxic conditions are used when the Near Field is under oxidizing conditions. Waste Package anoxic conditions are used when the Near Field is under reducing conditions.

Waste Package

Results Home
Waste Package Results
View Component

Waste package material:

Copper
 Carbon Steel
Stainless Steel
 Titanium

Check to define waste package thickness: (default values used if unchecked)

Waste package thickness (cm):

Disable general corrosion

Disable localized corrosion (stainless steel WP)

Water volume inside the waste package (m3):
 Used to define radionuclide concentrations.
 The same volume is used for all waste forms.

Additional failure options are available in the Alternative Failure Modes dashboard

General Corrosion Settings

The breach area due to general corrosion is uniformly sampled between min and max values (used also for hydrogen sulfide copper corrosion)

	Min Value	Max Value
GC breach area fraction	0.2	0.8

Enable dynamic general corrosion

Enable dynamic hydrogen sulfide Cu-corrosion

The buffer Variable Openings case must be also enabled in the Near Field Settings dashboard for HS Cu-corrosion to affect waste package failure times

Hydrogen sulphide concentration factor (distribution controlled from the parameter database)

Parameters log-uniformly sampled between min and max values

	Min Value	Max Value
Humid air corrosion factor	1	10
Transition to aqueous corrosion [yr]	10	50

Hydrogen sulphide copper corrosion is assumed to contribute to general corrosion. The corrosion rate is proportional to buffer flow rates (controlled in the Near Field Settings dashboard).

The transition time from oxic to anoxic conditions is controlled by the buffer saturation time in the Near Field Settings dashboard

Figure 3-4. SOAR Dashboard Menu for Waste Package Model Component Configuration Inputs

Near Field

- Return to Home
- Waste Form Settings
- Waste Package Settings
- Near Field Settings
- Far Field Settings
- Biosphere Settings
- Alternative Failure Modes Settings



- Results Home
- Near Field Results
- View Component

Geochemical conditions of the Near Field are defined by redox properties of Far Field Leg One

Buffer, Zone 2

Buffer case: See diagram below for Variable Openings case

	Value
Length [m]	0.5
Inner radius [m]	0.5
Reference height [m]	0.5
Flow factor	1

Buffer Geometry Picture

Flow factor with respect to far-field leg-one flow

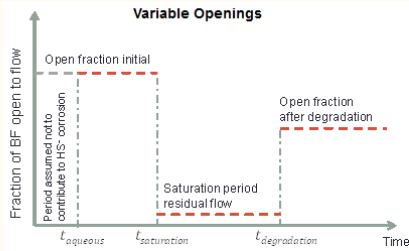
Buffer parameters for Variable Openings case

Parameters sampled from log-uniform distributions between min and max values

	Min Value	Max Value	
Open BF fraction initial	0.01	0.1	The following times must be in increasing order: 1. Transition time from humid air to aqueous corrosion 2. Buffer saturation time 3. Buffer degradation time If there is any potential cross-over, the simulation will be stopped.
Open BF fraction after saturation	0.001	0.05	
BF degradation time [yr]	10000	100000	
Open BF fraction after degradation	0.001	0.1	

The humid air transition time is controlled in the Waste Package Settings dashboard.

The BF saturation time is assumed to be the same as the transition time from oxic to anoxic conditions in the dynamic general corrosion model



Transition region (buffer to far field), Zone 3

Zero length transition region *Checked: zero length region (Zone 3 bypass)
Unchecked: Zone 3 length defined from fracture separation*

Zero concentration far-field discharge cell
*If checked, the far-field discharge cell is fixed at zero concentration.
If unchecked, the discharge rate to the far-field is controlled by the flow rate.
The discharge cell is conceptualized as a fracture if the host rock is fractured rock*

Enable radionuclide sorption *If enabled, Kd=far-field host rock Kd
If disabled, Kd=0 and porosity=1*

Cross section factor with respect to the buffer cross section. Volume of Zone 3 and diffusive exchange are proportional to this factor. Setting to 0 is equivalent to Zone 3 bypass (Zone 3 volume = 0).

Flow factor with respect to far-field leg-one flow

Feature Pathway

Enable Feature Pathway

BF diffusive length [m]	1	Additional diffusive path in buffer to reach the tunnel
Tunnel length [m]	10	
Tunnel cross section [m ²]	1	
Enable sorption (0, 1)	1	<i>If disabled, Kd=0 and porosity=1. If enabled, Kd=buffer Kd</i>

Feature Pathway Picture

Zero concentration far-field discharge cell
*If checked, the far-field discharge cell is fixed at zero concentration.
If unchecked, the discharge rate to the far-field is controlled by the flow rate.*

Define flow through the tunnel of the NF Feature Pathway
*If checked, user-defined flow is selected (next field)
If unchecked, the flow is computed based on the FF Leg 1 flux. Flow factor used to modify the flow*

Flow rate (m³/yr)

Flow factor *When 1, the flow velocity equals the FF Leg 1 flux*

Figure 3-5. SOAR Dashboard Menu for Near Field Model Component Configuration Inputs

Return to Home
Waste Form Settings
Waste Package Settings
Near Field Settings
Far Field Settings
Biosphere Settings
Alternative Failure Modes Settings



Note that Far Field Leg One defines the flow and redox conditions of the repository Near Field.

Far Field
Results Home
Far Field Results
View Component

Far Field Leg One

Geologic Medium:
Unconsolidated Sediments
Fractured Rock
Porous Rock

Redox Condition:
(defaulted to reducing if dynamic general corrosion is enabled)

Oxidizing

Reducing

Transport Length (km):

Hydraulic Gradient:

Effective Porosity Reduction Factor (Water Saturation):

Water Travel Time:

Far Field Leg Two

Geologic Medium:
Unconsolidated Sediments
Fractured Rock
Porous Rock

Redox Condition:

Oxidizing

Reducing

Transport length (km):

Hydraulic Gradient:

Effective Porosity Reduction Factor (Water Saturation):

Water Travel Time:

Far Field Leg Three

Geologic Medium:
Unconsolidated Sediments
Fractured Rock
Porous Rock

Redox Condition:

Oxidizing

Reducing

Transport length (km):

Hydraulic Gradient:

Effective Porosity Reduction Factor (Water Saturation):

Water Travel Time:

Feature Pathway (e.g., shaft, fault, tunnel)

The Feature Pathway (FP) is an independent pathway with direct release to the biosphere. Water flows through the FP are independently defined by the user. The host rock is assumed consistent with the Leg One host rock. The Near Field FP must be enabled in the Near Field dashboard to activate the Far Field Feature Pathway.

	Value
Length [m]	100
Dispersivity/Length	0.1
Aperture [m]	0.1
Width [m]	1
Flow velocity [m/yr]	1
Enable matrix diffusion? (0-no, 1-yes)	0
Enable sorption? (0-no, 1-yes)	1

*The aperture controls mass transfer with the matrix, if enabled.
 Width is perpendicular to the aperture.*

Water travel time

Figure 3-6. SOAR Dashboard Menu for Far Field Model Component Configuration Inputs

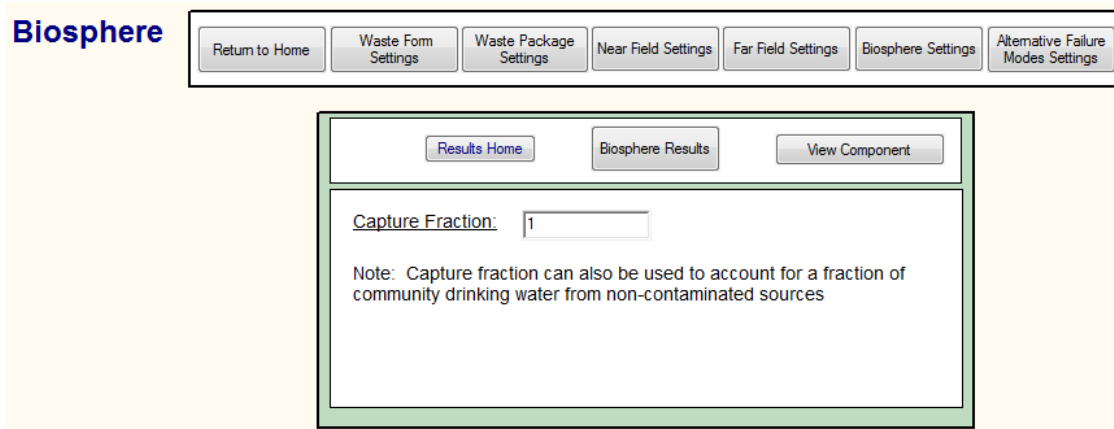


Figure 3-7. SOAR Dashboard Menu for Biosphere Model Component Configuration Inputs

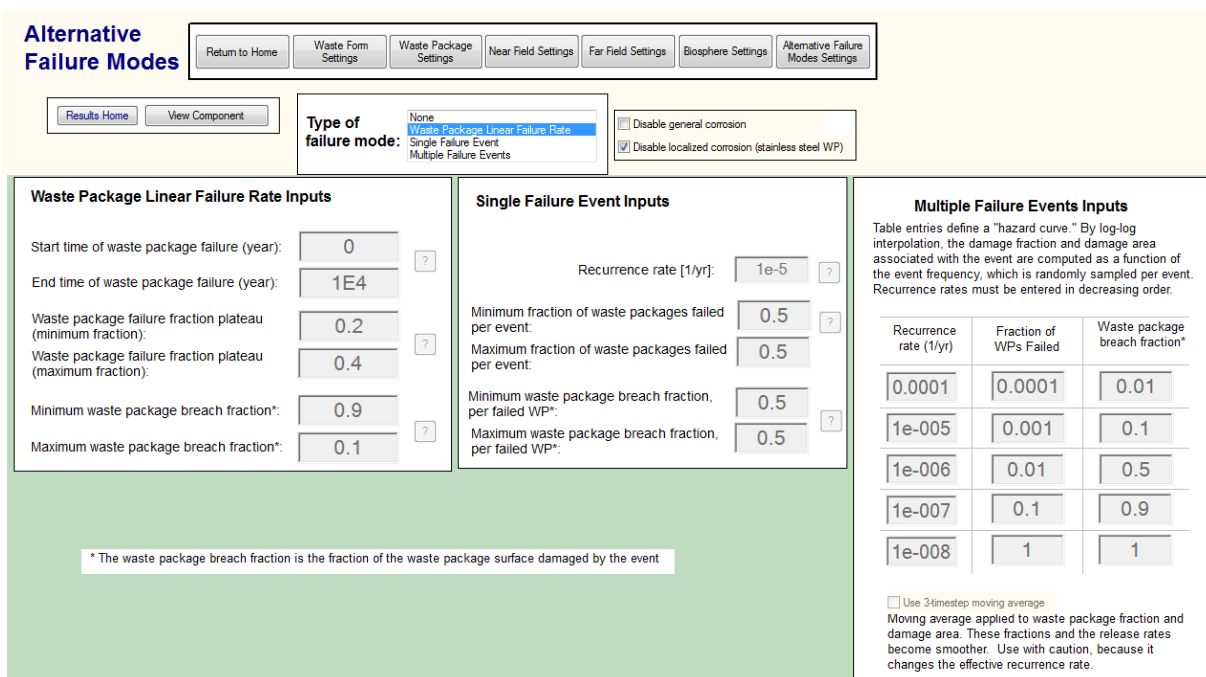


Figure 3-8. SOAR Dashboard Menu for Alternative Failure Mode Inputs. Alternative Fields Are Enabled Depending on the Failure Mode.



Figure 3-9. GoldSim Player Run Controller Can Be Used to Reset and Run the Model

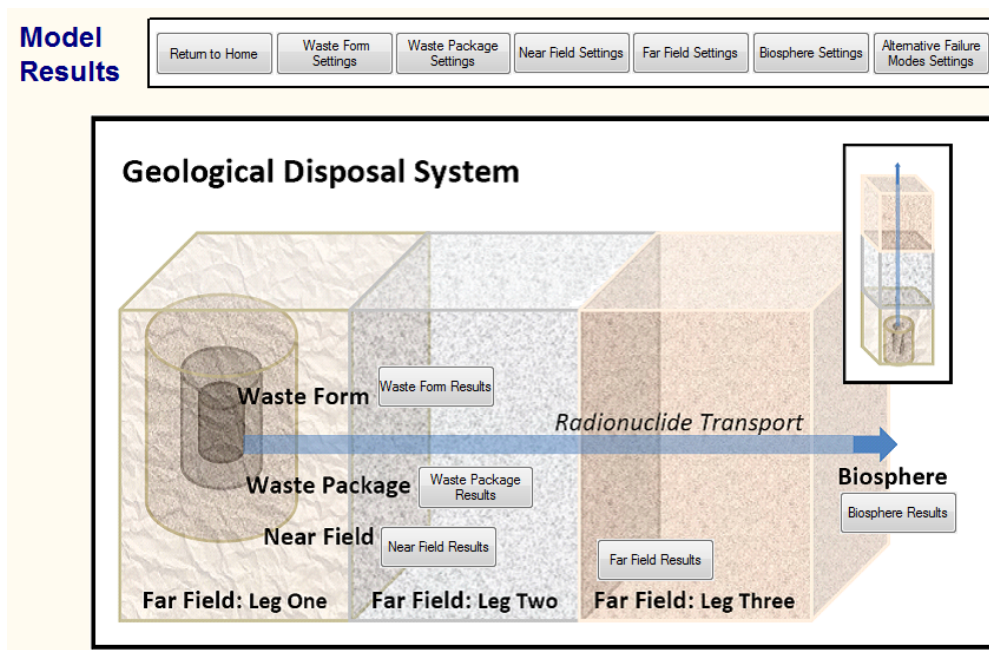


Figure 3-10. SOAR Dashboard Menu for Viewing Results

Near Field Results

[Return to Home](#)
[Waste Form Settings](#)
[Waste Package Settings](#)
[Near Field Settings](#)
[Far Field Settings](#)
[Biosphere Settings](#)
[Alternative Failure Modes Settings](#)

[Results Home](#)
[Waste Form Results](#)
[Waste Package Results](#)
[Near Field Results](#)
[Far Field Results](#)
[Biosphere Results](#)


Near Field [View Near Field Component](#)

	Spent Nuclear Fuel	Spent Mixed-Oxide Fuel	High-Level Waste (glass)	High-Level Waste (ceramic)	Comparison
Concentration of Radionuclides in Water in Waste Package Internals:	Radionuclide	Radionuclide	Radionuclide	Radionuclide	
Precipitated Mass in Waste Package Internals:	Radionuclide	Radionuclide	Radionuclide	Radionuclide	
Release Rates from the Waste Package (Zone 1):	Radionuclide	Radionuclide	Radionuclide	Radionuclide	Total per WF
Release Rates from the Buffer (Zone 2):	Radionuclide	Radionuclide	Radionuclide	Radionuclide	Total per WF
Release Rates to Far Field (Zone 3):	Radionuclide	Radionuclide	Radionuclide	Radionuclide	Total per WF
Buffer Integrity:	Open Fraction	BF Flow			
Release comparison: Includes WF and AP	Total	Total	Total	Total	All Forms
Feature Pathway (FP)					
Release from buffer into Near Field FP:	Radionuclide	Radionuclide	Radionuclide	Radionuclide	Total per WF
Main and FP comparison:	Total	Total	Total	Total	
Release rate into FF Feature Pathway:	Radionuclide	Radionuclide	Radionuclide	Radionuclide	Total per WF
Main and FP comparison:	Total	Total	Total	Total	
Flow rate:	Distribution				

Figure 3-11. SOAR Dashboard for Near Field Model Component Results

4 MODEL COMPONENTS

4.1 Waste Form

4.1.1 Description

The Waste Form model component of Scoping of Options and Analyzing Risk (SOAR) considers inventories and waste form dissolution or degradation processes to define the source term (i.e., the amount and type of radionuclides released) for radionuclide transport computations. The waste forms are emplaced inside waste packages and may be protected by cladding materials (i.e., an outer layer protecting the nuclear fuel rods to provide structural support). The Waste Form model component specifically considers the type of solid waste form, important radionuclides, initial radionuclide inventory, and degradation of the waste form following exposure to an aqueous environment after waste package breach. The Waste Form model component is linked with the Waste Package model component and the Near Field model component. It receives waste package failure times from the Waste Package model component and the number of waste packages breached as a function of time, which determines when water would contact the waste and the total radionuclide inventory that may be released. The Waste Form model component outputs radionuclide release rates as functions of time to the Near Field component.

4.1.2 Model Implementation

The model computes the amount of radionuclides dissolved from the waste form, which is then input to the Near Field component. Twenty radionuclide species are considered (Pu-238, 239, 240, 242; U-232, 233, 234, 235, 236, 238; Np-237; C-14; Cs-135; I-129; Tc-99; Se-79; Th-230; Ra-226; Rn-222; and Pb-210). Four of these species (Th-230, Ra-226, Rn-222, and Pb-210) are members of the U-238 decay chain and are assumed to have zero inventory in the initial waste form. The radionuclides were chosen to represent an appropriate variety of geochemical behavior (e.g., solubility of radionuclide-bearing solid phases) and potential waste form inventories for commercial spent nuclear fuel (SNF), spent mixed-oxide (sMOX) fuel, high-level waste glass (HLWg), and high-level waste ceramic (HLWc) waste forms, based on performance assessment results in both oxidizing and reducing environments (Bechtel SAIC Company, LLC, 2004; Leslie et al., 2007; Marivoet et al., 2001). Each of the four waste forms (as defined in the Waste Form model) is an individual GoldSim source element of the Near Field component. Six different radionuclide inventories are available to represent these four distinct waste forms. These inventories consist of the matrix-bound inventory for SNF, sMOX, HLWg, and HLWc, and the unbound inventory for SNF and sMOX. The matrix-bound inventory requires the waste form to degrade before the radionuclides are dissolved and released. Each matrix-bound radionuclide inventory has a characteristic dissolution rate. The unbound inventories for SNF and sMOX fuel include C-14, Cs-135, I-129, Tc-99, and Se-79 radionuclide species. These unbound inventories are instantly available for transport when the waste package breaches and are intended to represent gap and grain boundary inventories. The SOAR model is flexible and additional radionuclides could be added, if needed.

The basic equation describing the degradation rate of matrix materials is

$$\frac{dM}{dt} = -r \quad (4-1)$$

where M [kg] is the mass of the matrix materials and r [kg/yr] is the degradation rate, considered constant in SOAR. The release of matrix-bound radionuclides from the waste matrix is computed by GoldSim source elements by assuming congruent release with degradation of the waste form matrix. Eq. (4-1) can also be expressed as

$$\frac{dM}{dt} = -r = -g M_o = -R A M_o \quad (4-2)$$

where M_o is the initial mass of the waste form matrix and $g (=R A)$ [1/yr] is the initial fractional degradation rate. R [g/(cm²-yr)] is the matrix dissolution rate, and A [cm²/g] is the initial specific area of the waste form exposed to an aqueous environment. Experimental values for the dissolution rate, R , and initial specific area, A , reported in the literature for various waste forms were considered to compute initial fractional degradation rates, g , which are inputs to the Waste Form model component. The input parameter database tracks values and distributions of the fractional degradation rate, g . From the fractional degradation rates, the waste form lifetime is computed as $1/g$. Use of the constant degradation rate, r , simplifies the calculation procedure and the number of required assumptions without underestimating radionuclide release from the waste form. Otherwise, the matrix dissolution rate, R , and the specific surface area, A , would need to be explicitly described. The parameters R and A could vary over time for different waste forms, environmental conditions, and geometrical considerations, and data are insufficient to support long-term models for R and A .

GoldSim source elements use the waste form lifetime (computed as $1/g$) to define waste form dissolution rates to the water inside the waste package (water assumed immediately present after waste package failure). The dissolution rate of each radionuclide is determined by the fraction of each radionuclide in the waste form based on the congruent dissolution assumption. Complexities in the mass conservation equation arise because of the gradual waste package failure, which increases the releasable inventory. See the Contaminant Transport Module User Guide for a more general description of the equations solved by the GoldSim source term element (GoldSim Technology Group, LLC, 2016b, Appendix E). The GoldSim source element implements a double convolution algorithm, accounting for waste form dissolution over time per failed waste package, and failure of multiple waste packages over time.

The four distinct waste forms selected are considered representative of potential future waste forms. Experimental data on the performance of these future waste forms are limited and are not sufficiently characterized to develop an accurate model.

4.1.3 Default Parameters

A complete list of default parameter values, distribution types, and technical bases for the Waste Form model component is provided in Appendix A, Table A-1. The Waste Form model component assigns default values to the radionuclide inventory, instant release fraction of unbound inventory (i.e., fission and activation products), and fractional rate of waste form degradation.

All input data used in the Waste Form model are primarily based on published data on representative waste forms from domestic and international geologic disposal programs. To enhance traceability, data from NRC investigations are used as the initial input values when practicable, such as the instant release fraction of unbound inventory (Leslie et al., 2007; Jain et al., 2004; NRC, 2008).

Radionuclide Inventory

For the four waste forms (commercial SNF, spent mixed-oxide, high-level waste glass, and high-level waste ceramic), the initial radionuclide inventories are assigned based on literature data, with an additional projection based on representative values for commercial SNF, sMOX fuel, HLWg, and HLWc. Level 2 flexibility (see Section 3.2.2) allows the user to modify the default initial inventory values. Situations that may require such modification include aging of the initial inventory to account for the time that elapses before disposal system closure (e.g., HLWc with various waste loading from reprocessing) and additional waste inventory that is generated before disposal system closure. Modified inventory values may be generated from calculations performed outside the SOAR model.

Instant Release Fraction of Unbound Inventory

For the unbound inventory (fission and activation products), instant release fractions for commercial SNF and sMOX fuel are based on the values in Leslie et al. (2007) and Jain et al. (2004). Unbound radionuclides are available for transport as soon as the waste package is breached. For higher burnup (e.g., >60 GWd/MTU) commercial SNF or sMOX fuel, the instant release fractions may increase. High burnup spent fuel may lead to higher estimated dose rates at earlier times; however, data on unbound radionuclides for higher burnup waste forms are very limited.

Degradation of Waste Form

The Waste Form model component assumes the matrix-bound radionuclides are released into the water contacting the waste form at the rate of waste form dissolution or degradation. For commercial SNF, the model considers radionuclides from the matrix-bound inventory are released at the same rate as UO₂ matrix dissolution (Wilson and Gray, 1990). In an oxidizing environment, the UO₂ matrix dissolves electrochemically as soluble species with the aid of oxidants, such as dissolved oxygen or hydrogen peroxide (Shoemith, 2000). In a reducing environment, the UO₂ matrix dissolves chemically as soluble species (Sunder and Shoemith, 1991). The degradation rate of sMOX fuel is approximated by commercial SNF degradation rates (due to limited data on sMOX fuel degradation), given similarities in sMOX fuel material properties and the UO₂ matrix in commercial SNF. For HLWg, it is assumed that the HLWg matrix will dissolve chemically, where the process is controlled by the concentration of dissolved silica compound in both oxidizing and reducing environments (Bechtel SAIC Company, LLC, 2004). HLWc has been studied only in laboratories; there is no yet prototype HLWc. A variety of HLWc waste forms have been considered (e.g., SYNROC, titanates, zirconolites). The HLWc typically have lower degradation rates than HLWg (Wang, 2009). From the limited laboratory data (Reeve, et al., 1989; Vance, et al, 1997; Wang, 2009), the rate of degradation of HLWc is considered to be a factor of 0.01 lower than HLWg degradation.

To determine the fractional degradation rate for each specific waste form, upper and lower bounds for waste form dissolution rate were considered for both oxic and anoxic conditions and for various pH conditions, based on representative values in the literature (e.g., NRC, 2008; Van Iseghem, 2007; Ferry et al., 2005; Bechtel SAIC Company, LLC, 2004). These bounding values for the dissolution rate were then multiplied by the specific surface area of the waste form, accounting for the waste form density and surface roughness factors (NRC, 2008). In computing fractional degradation rate inputs to the Waste Form model component, specific surface areas were considered, using a characteristic waste form length (e.g., associated with the diameter of grains) of 0.1 cm [0.04 in] for commercial SNF and sMOX

fuel (NRC, 2008) and 10 cm [4 in] for HLWg (Bechtel SAIC Company, LLC, 2004). The densities are 10.6 g/cm³ [0.38 lb/in³] for commercial SNF and sMOX fuel (NRC, 2008) and 2.7 g/cm³ [0.1 lb/in³] for HLWg (Ahn, 2003). The resulting fractional degradation rates were used to define upper and lower limits for log-uniform distributions, which are sampled once per realization to account for uncertainty in fractional degradation rates for each waste form. The inventory depletion time was simply computed as the inverse of the fractional release rate, and input to GoldSim source elements.

In the Waste Form model component, a constant-in-time degradation rate is assumed [see Eq. (4-1)] for each waste form. This assumption simplifies the calculation procedure without underestimation of radionuclide release from the waste form. The dissolution rate and specific surface area, however, could vary over time for different waste forms, environmental conditions, and geometrical considerations. Time-dependent data on waste form degradation rates for the range of potential environmental conditions and future waste form types are limited and should be evaluated further, to incorporate key uncertainties in future performance assessment models.

4.1.4 Flexibility

In addition to the default parameterization, the Waste Form model has several significant flexibilities. For example, the user can modify the default parameter values for the waste form inventories; fractional degradation rates of commercial SNF, sMOX fuel, HLWg, and HLWc; and unbound fractions for SNF and sMOX fuel.

The Waste Form settings on the user interface dashboard (see Figure 3-3) allow users flexibility to specify and evaluate alternative model scenarios without the need to revise the input parameter distributions. Specifically, the dashboard provides users with options to make the following changes:

- Specify the total mass of waste disposed for each of the four waste form types.
- Change the total disposed mass per waste package for each of the four waste forms. These parameters are used in calculating the number of waste packages, and affect the calculation of the waste package failure distribution. The user can modify these values to study the effects of waste package mass loading and varied number of waste packages on system performance. However, the key variable is the total disposed mass. Results will be similar for systems with a different number of waste packages if the total disposed mass is the same. Differences arise only due to the fact that GoldSim source elements track integers for the number of waste packages failing as a function of time. Those differences become minor when the total number of waste packages is large.
- Modify the releasable fraction of the initial radionuclide inventory for each waste form, which is the fraction of the waste form mass available for mobilization. This fraction decreases the inventory available for transport (which may be used to simulate the effects of potential cladding protection or changes to local redox conditions).
- Modify the fractional rate of waste form degradation using a multiplier applied to the bound inventory degradation rate for each waste form. This parameter can be used to approximate effects that may either increase or decrease the bound inventory degradation rates (e.g., the user could assume different waste form fragment sizes and modify the degradation rate accordingly).

- Enable a combined oxic/anoxic degradation rate switch to allow sampling from the full range of degradation rates, mixing oxic and anoxic conditions. This feature could be used for sensitivity studies.

4.2 Waste Package

4.2.1 Description

The Waste Package model component of SOAR specifically models waste package electrochemical degradation (i.e., corrosion) processes that may lead to waste package failure. Additional waste package failures caused by alternative failure modes are modeled independently in the Alternative Failure Modes model component, as described in Section 4.6. The Waste Package model component calculates waste package failure times and the extent of damage on the waste package surface for geologic disposal systems located in either oxidizing or reducing host media, where the redox condition of the geologic media is defined by the first leg of the Far Field component. The Waste Package model component is integrated with the Alternative Failure Modes, Waste Form, and Near Field model components. The Waste Package model component receives the fraction of waste packages failed by alternative failure modes and the associated breach area fraction from the Alternative Failure Modes model component, and combines them with those analogous outputs from this Waste Package model component to calculate a combined breach area. The Waste Package model component provides the waste package failure times to the Waste Form model component to initiate computations of waste form degradation for each failed waste package and the total breach areas to the Near Field model component for radionuclide transport calculations.

4.2.2 Model Implementation

The Waste Package model component calculates the fraction of waste packages failed as a function of time and breach area fractions due to corrosion in aqueous environments, representing potential geologic disposal system settings. The calculation considers the following attributes of the Waste Package model component.

Waste Package Specifications

It is assumed the disposal system will include waste packages made of a single metallic material. The Waste Package model component considers general corrosion for stainless steel, carbon steel, titanium, or copper. In addition, stainless steel is considered to be also affected by localized corrosion. These materials were selected to represent a range of materials that could be susceptible to corrosion or corrosion resistant. Depending on the material type and chemical environment (oxidizing or reducing) the user selects on the dashboard interface, the model will choose the appropriate set of parameter values to use in calculating the fraction of waste packages failed as a function of time and breach areas.

Failure Mechanisms (General Corrosion and Localized Corrosion)

The Waste Package model component models two waste package failure mechanisms representing general corrosion and localized corrosion. General corrosion is modeled to represent progressive failures of waste packages distributed over time. Conversely, localized corrosion is modeled to breach a fraction of the surface of the waste packages at discrete times. Other degradation processes (e.g., stress corrosion cracking, microbial influenced corrosion, hydrogen embrittlement, creep, and susceptibility to corrosion as a function of metal and

container fabrication processes) are not explicitly considered in the model. The following paragraphs describe the calculation process for general and localized corrosion.

General corrosion is a gradual material thinning process proceeding in a relatively slow and uniform manner, compared to localized corrosion. Two different descriptions for general corrosion were implemented: constant-in-time corrosion rate and "dynamic" corrosion rate. In the former case, the waste package failure time is calculated as the time at which the corrosion front penetrates the material thickness, using the equation

$$t_{gc} = \frac{L}{R_{gc}} \quad (4-3)$$

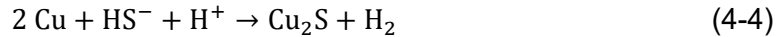
where t_{gc} is the waste package failure time, L is the thickness of waste package material, and R_{gc} is the general corrosion rate in units of length/time. Distributions of general corrosion rates for the respective waste package materials and repository settings are inputs to both general corrosion models. Using the constant-in-time corrosion rate option, in a realization, each waste package is considered to exhibit a single corrosion rate. (As discussed later, in the dynamic corrosion rate case, the corrosion rate changes at specific timesteps.) However, the constant corrosion rate varies from waste package to waste package. Waste packages are computed to fail at different times within a realization, depending on their corrosion rate. The output of the model is the fraction of waste packages failed as a function of time. The constant corrosion rate is selected based on long-term oxidizing or reducing conditions of the repository. Those conditions are imposed by the "far field leg one" selected in the Far Field Settings dashboard.

In the dynamic general corrosion model, the corrosion rates are assumed to change with time at specific times. **Error! Reference source not found.** shows an example of potential periods with different corrosion rates. For example, after closure of the repository, humid air may contact waste package materials resulting in relatively high oxygen levels, and humid air corrosion rates may act during that time. At a later time, after a level of water saturation of buffer materials is attained, water with residual oxygen may contact the waste package. Aqueous general corrosion rates are applied during that time. Eventually, buffer materials may become fully saturated with water and clay materials may expand and fill open spaces. It is assumed that, at that time, the water is oxygen depleted, and anoxic aqueous corrosion would operate. The residual oxygen may react with minerals in the rock and the buffer material, and become depleted prior to buffer material saturation with groundwater. Oxic general corrosion rates are higher than anoxic corrosion rates; thus, assuming a longer aqueous oxic period is conservative. The input parameter database tracks distributions for oxic and anoxic corrosion in aqueous environments. To define the humid air corrosion rates, an enhancement factor to the aqueous corrosion rates is applied. The range of the enhancement factor is defined in the Waste Package Settings dashboard, and a log-uniform distribution is used to sample this enhancement factor between the minimum and maximum user-defined limits. The transition time from humid air to oxic aqueous conditions is uncertain. The Waste Package Settings dashboard allows for user-defined values for minimum and maximum transition times. The transition time is also sampled from a log-uniform distribution with those limits.

The transition time from oxic to anoxic conditions is defined in the Near Field Settings dashboard as part of the buffer material evolution abstraction.

If the waste package material is copper, an option is available to simulate enhancement of corrosion rates due to hydrogen sulfide, HS^- , in the groundwater. HS^- may be produced by

sulfate reducing bacteria or dissolution of pyrite (He et al., 2015). HS^- combines with copper according to the reaction



It is assumed that the reaction is fast or instantaneous. Thus, the corresponding copper corrosion rate is related to the rate of supply of HS^- to the waste package surface, which is proportional to the HS^- concentration and to the water flow rate. In addition, the corresponding corrosion rate is inversely proportional to the area of the spread of the HS^- attack on the waste package surface. The concentration of HS^- is defined in the parameter database. The rate of supply is assumed proportional to the flow rate through the buffer material, which in turn is assumed proportional to the extent of openings in the buffer. After the buffer is saturated with water, if there are no residual openings or gaps, it is assumed that HS^- would not contact the waste package (HS^- is likely to react with minerals in the buffer material before reaching the waste package surface). Finally, the area of the HS^- attack is defined in the Waste Package Setting dashboard. This area is used to compute the total general corrosion damage area. The HS^- copper corrosion model is part of the dynamic general corrosion abstraction (corrosion model two). The alternative general corrosion model (constant-in-time corrosion rates — corrosion model one) does not provide an option to account for HS^- enhancement of copper corrosion.

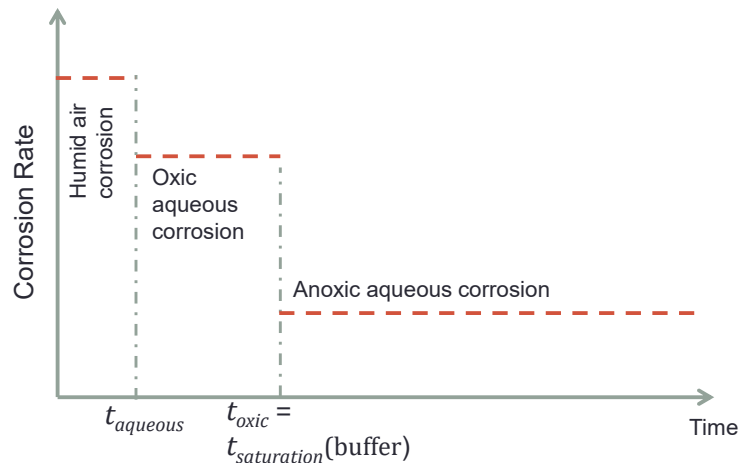


Figure 4-1. Example of periods considered in the dynamic general corrosion model

Note that the leg one is defaulted to reducing conditions when the dynamic general corrosion model is enabled; the redox condition option for the leg one is hidden in the Far Field Settings dashboard. The Far Field dashboard includes a note alerting the user of the default redox state (i.e. reducing) for leg one when the dynamic general corrosion model is enabled.

Localized corrosion is a relatively fast degradation process compared to general corrosion. Only stainless steel, a passive metal, is assumed to exhibit localized corrosion. No explicit models for initiation and propagation of localized corrosion are implemented. Instead, failure times are directly sampled from input distributions. Localized corrosion is assumed to cause simultaneous failure of multiple waste packages at one or two discrete times, depending on whether the geologic disposal system is located in reducing or oxidizing host media.

For a disposal system located in reducing host media, an initial transient oxidic period (referred to as Period I) is considered before stable reducing conditions are established (referred to as Period II). The initial transient oxidizing period will be relatively short (tens to hundreds of years), lasting until the initial oxygen in the disposal system is consumed by the corrosion process, reaction with minerals, or consumed by microbes. For this type of disposal system, a two-step function defining the fraction of waste packages affected by localized corrosion (f_{lc}) as a function of time is constructed for each realization (**Error! Reference source not found.**). Two distributions to define the waste package failure time by localized corrosion (t_{lc})—one each for Periods I and II—are provided as inputs to the Waste Package model component. Other inputs to the Waste Package model component are the fractions of waste packages affected by localized corrosion during Periods I and II. During Period I, the affected fraction is sampled from a distribution for f_{lc} , which was selected based on the probability that a waste package would exhibit localized corrosion under the transient oxidic conditions.

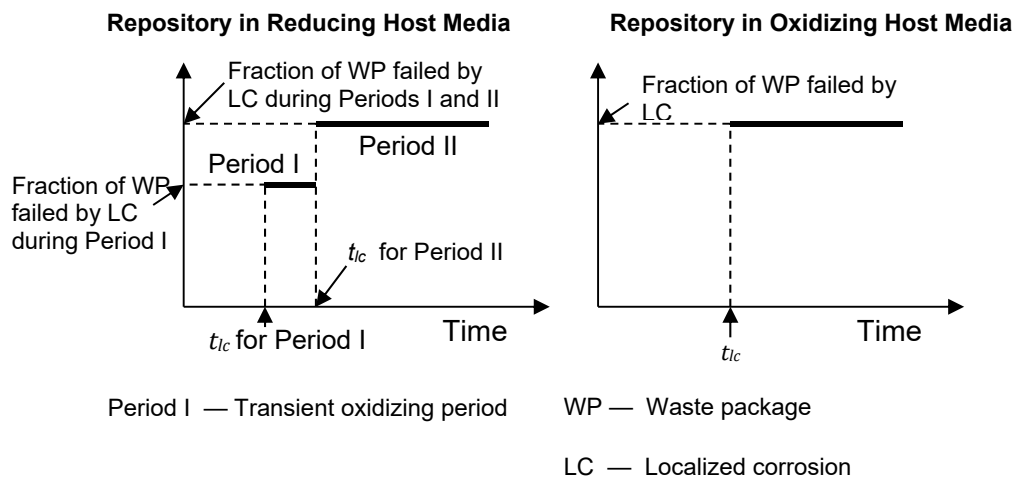


Figure 4-2. Step Functions Used to Model Localized Corrosion Per Realization

During Period II, it is assumed that waste packages that did not fail in Period I could still exhibit localized corrosion. The fraction of waste packages failed during Period II is also sampled from a distribution based on the probability for a waste package to exhibit localized corrosion under reducing conditions. For any realization, groups of waste packages are assumed to fail at two discrete times. The total number of waste packages that fail by localized corrosion is the sum of the number of failed waste packages during Periods I and II (**Error! Reference source not found.**).

In the case of a disposal system in oxidizing host media, only one failure time distribution is provided as an input to the Waste Package model component, along with the corresponding distribution for the fraction of waste packages affected by localized corrosion. With these inputs, a single-step function defining the fraction of waste packages failed by localized corrosion as a function of time is constructed for each realization (**Error! Reference source not found.**). The fraction of waste packages failed by localized corrosion is sampled from a distribution based on the probability for a waste package to exhibit localized corrosion under oxidizing conditions. This distribution function is defined in the input parameter database.

Waste Package Breach Area

An output of the Waste Package model component is the combined waste package breach area from corrosion processes and alternative failure modes, described in Section 4.6, as a function of time. This breach area is provided as input to the Near Field component. Diffusive radionuclide releases into the region surrounding the waste packages are proportional to the breach area (see Section 4.3.2 for a discussion on advective radionuclide releases). SOAR considers three distinct breach area fractions: one for localized corrosion, one for general corrosion, and one for alternative failure modes. For waste package radionuclide release computations, however, a combined breach area per failed waste package is computed at each timestep as a function of the independent breach areas and the number of waste packages failed.

If F_{GC} , F_{LC} , and F_{AF} are the fractions of waste packages failed by general corrosion, localized corrosion, and alternative failure modes, respectively, then the fraction of non-failed waste packages (by any mechanism), assuming independent degradation mechanisms, is $(1 - F_{GC})(1 - F_{LC})(1 - F_{AF})$. The combined fraction of failed waste packages, F_{WP} , is computed as

$$F_{WP} = 1 - (1 - F_{GC})(1 - F_{LC})(1 - F_{AF}) \quad (4-5)$$

Similarly, if $f_{A,GC}$, $f_{A,LC}$, and $f_{A,AF}$ are the corresponding breach fractions per failed waste package by general corrosion, localized corrosion, and alternative failure modes, respectively, then the total area fraction (i.e., the fraction of the area of all waste packages in the system) not affected by any degradation mechanism is $(1 - f_{A,GC}F_{GC})(1 - f_{A,LC}F_{LC})(1 - f_{A,AF}F_{AF})$. The total breach area fraction, F_A , is then

$$F_A = 1 - (1 - f_{A,GC}F_{GC})(1 - f_{A,LC}F_{LC})(1 - f_{A,AF}F_{AF}) \quad (4-6)$$

The quantity F_A is the total area fraction accounting for failed and non-failed waste packages. The average breach area per failed waste package is defined as

$$A_{WP} = \frac{F_A}{F_{WP}} A \quad (4-7)$$

where A is the total area of the waste package. The quantities F_{AF} and $f_{A,AF}$ are described in Section 4.6.2. For example, if waste packages fail only by general corrosion (i.e., $F_{LC}=F_{AF}=0$), then the ratio F_A/F_{WP} equals $f_{A,GC}$, and $A_{WP} = f_{A,GC} A$, as expected. If the majority of the waste packages fail due to general corrosion (and only a few due to localized corrosion or alternative failure mechanisms), the breach area per failed waste package is closer to the breach area associated with general corrosion. As more waste packages fail due to alternative failure modes at later times, the breach area per failed waste package, A_{WP} , approaches the breach area associated with the alternative failure modes.

Waste Package Counting

An output of the Corrosion and Alternative Failure Modes model components is the fraction (ranging from 0 to 1) of waste packages that fail due to corrosion and due to the alternative failure modes, respectively. These fractions are passed as inputs to the GoldSim source term elements to compute total radionuclide releases from the engineered barrier system (EBS). The GoldSim source term computes the total number of waste packages failed by combining the

failure fractions under the assumption that these fractions are independent. For example, if the fraction of waste packages failed by corrosion is 0.5 and the fraction of waste packages failed by alternative failure modes is 0.7, the total fraction of waste packages failed is 0.85, derived as follows. The fraction of waste packages not failed by corrosion is $1 - 0.5 = 0.5$; the fraction of waste packages not affected by alternative failure modes is $1 - 0.7 = 0.3$. The fraction of waste packages not affected by any failure mode is $0.5 \times 0.3 = 0.15$. Thus, the fraction of waste packages affected by at least one failure mode is $1 - 0.15 = 0.85$. This example computation is consistent with Eq. (4-5). The GoldSim source term element performs these computations automatically and generalizes these computations for the case when multiple (two or more) independent failure modes are considered. GoldSim tracks an integer numbers of waste packages: GoldSim rounds the product (fraction of failed waste packages) \times (total number of waste packages) to the nearest lowest integer. This rounding to integers causes radionuclide releases rate curves (versus time) to manifest oscillations and sharp jumps in some instances, especially when those releases are associated with a small number of waste packages.

4.2.3 Default Parameters

A list of default parameter values, distribution types, and technical bases for the Waste Package model component is provided in Appendix A, Table A-2. The default parameters in the Waste Package model component assign values to assess consequences of general corrosion and localized corrosion of the waste package. General corrosion affects all waste package materials in both oxidizing and reducing conditions, while localized corrosion is assumed to affect stainless steel only.

For the general corrosion model, the key input parameters are the general corrosion rates for each waste package material for geologic disposal systems in oxidizing or reducing media [R_{gc} in Eq. (4-3)] represented as probability distributions to reflect uncertainties in the disposal system environmental conditions. Environmental conditions affecting general corrosion (e.g., temperature, solution pH, and solution chemical composition) are not explicit inputs to calculate general corrosion rates. Nevertheless, their influence is implicitly accounted for by the specified ranges of the corrosion rate distributions (i.e., the lower and upper bounds for the distributions are obtained from literature data representing benign and aggressive environmental conditions). Other general corrosion inputs include the thickness of each waste package material [L in Eq. (4-3)] and general corrosion breach area fraction [$f_{A,GC}$ in Eq. (4-6)] sampled from the user-defined breach area fraction range for general corrosion on the dashboard interface. In the dynamic general corrosion model, the user is required to input transition times from humid air to aqueous conditions (**Error! Reference source not found.**) in the Waste Package Settings dashboard, and the transition from oxic to anoxic conditions in the Near Field Settings dashboard (the latter time is conservatively assumed equal to the buffer material saturation time). For the HS^- enhancement of the general corrosion rate for copper, the distribution of the HS^- groundwater concentration is specified in the SOAR parameter database. The Waste Package Settings dashboard includes a HS^- concentration factor that is directly applied to the sampled concentration to enhance or decrease the HS^- groundwater concentration. The dashboard concentration factor is a practical term to support sensitivity analyses.

For the localized corrosion model, probability of waste package failure by localized corrosion differs for the four materials considered in the SOAR default parameter set. For example, the titanium waste package material is assumed to be alloyed with noble metals (e.g., palladium or ruthenium), effectively preventing localized corrosion of this material (e.g., Revie, 2000). Accordingly, localized corrosion is disregarded for this material. For copper and carbon steel,

localized corrosion in the form of pitting corrosion is possible. However, localized corrosion of these materials is modeled not explicitly but indirectly, by adjusting the input general corrosion rates—pitting corrosion of these materials tends to be widespread and manifest more as enhanced general corrosion (e.g., Revie, 2000). The localized corrosion model is enabled only for the stainless steel waste package material. Other inputs to the localized corrosion model include localized corrosion failure time (t_{lc} in Figure 4-1) and the localized corrosion breach area fraction [$f_{A,LC}$ in Eq. (4-6)].

The parameter values used in the waste package component were primarily obtained by literature review of waste container design and corrosion testing results from domestic and international geologic disposal programs. Independent analyses and engineering judgment were also used where data were lacking, such as to establish the probability and breach area fraction for localized corrosion of stainless steel.

4.2.4 Flexibility

In addition to the default parameterization, the Waste Package model component has several flexibilities to consider alternative geologic disposal system configurations. Where appropriate technical data are available, the user can modify the general corrosion rates to assess performance of other waste package materials (see discussion of level-two flexibility in Section 3.2). These corrosion rates can be modified to constrain uncertainty where environmental conditions in the disposal system are better characterized or to analyze different environmental regimes (e.g., potentially increasing the rates due to higher temperatures). The user can modify the distributed (general corrosion) and stepwise (localized corrosion) failure to approximate additional failure mechanisms beyond general and localized corrosion. Given that any waste package failure mechanism can be characterized by two quantities—the failure time and the extent of damage to the waste package surface—the user can adjust the default input parameters to evaluate consequences of other failure mechanisms. For example, consequences of stress corrosion cracking could be evaluated, provided technical data were available to define the extent of waste package surface damage and other input parameters selected to cause failure in defined time frames. Similarly, the user can modify the stepwise failure time, probability, and breach area fraction to approximate discrete events, such as early failure, human intrusion, or other alternative failure modes. Note that because SOAR is an abstracted model with limited consideration of coupling among processes leading to waste package failure and radionuclide release to the environment, the results should be carefully interpreted.

The Waste Package menu of the user interface dashboard (see Section 3.4) allows users additional flexibility to evaluate alternative model concepts without the need to revise the input parameter distributions. Specifically, the dashboard provides users with the options to

- Select the waste package material from the list of options (copper, carbon steel, stainless steel, titanium)
- Define a waste package thickness, thus overruling default thickness values for each specific material (see Appendix A, Table A-2 for default values)
- Disable general corrosion or localized corrosion degradation modes

- Select reducing or oxidizing geochemical environment (selection made under the Far Field Settings dashboard), and select general corrosion rates constant in time consistent with the reducing or oxidizing conditions
- Enable general corrosion rates that change at discrete times (e.g., humid air corrosion, oxic aqueous corrosion, and anoxic aqueous corrosion)—if this general corrosion model two is enabled, the geologic setting, reducing or oxidizing mentioned in the previous bullet, is ignored
- Define the breach area fraction range for general corrosion

4.3 Near-Field Environment

4.3.1 Description

The Near Field component of SOAR considers transport of radionuclides from within the waste package, through the disturbed zone outside the waste package, and into the undisturbed natural system. A Feature Pathway can be enabled to account for parallel transport through tunnels or excavated disturbed zones and eventual discharge into a major feature of the Far Field (e.g., an emplacement shaft or a major fault). The Near Field component of SOAR specifically considers dissolved radionuclide transport through any engineered buffer or backfill materials accounting for the effects of advection, dispersion, diffusion, sorption, and mineral precipitation and dissolution. The Near Field model component receives dissolved radionuclide release rates from the Waste Form model component (which are also a function of the number of waste packages failed as a function of time), and the breach area from the Waste Package model component, and outputs dissolved radionuclide releases to the Far Field model component.

4.3.2 Model Implementation

The Near Field model component implements a one-dimensional diffusive and advective transport approach with sorption, mineral precipitation, and dissolution. Conceptually, the model considers dissolved radionuclide transport from the near field to the far field through three distinct transport zones: (i) Zone 1, from the waste package internals through the breach area; (ii) Zone 2, from the surface of the waste package through any engineered buffer or backfill material; and (iii) Zone 3, a transition region from the buffer or backfill material to a far-field groundwater transport pathway. A Feature Pathway is available to simulate diffusion through engineered buffer material, advection-dispersion through a backfilled tunnel or excavated disturbed zone, and discharge to a large feature such as an emplacement shaft or a major water-conducting fault. If the Feature Pathway is enabled, the Main and Feature Pathways operate in parallel.

For each waste form type, the SOAR model includes four independent subsystems: (i) waste form dissolution, (ii) solubility and precipitation, (iii) contaminant transport through the buffer or backfill material, and (iv) contaminant transport through the transition region and the Feature Pathway (if enabled). The combined fraction of waste packages failed as a function of time computed by the Waste Package and Alternative Failure Modes model components [Eq. (4-5)] is used in the four subsystems. The combined breach area per failed waste package as a function of time, computed according to Eq. (4-7), is used in subsystems (iii) and (iv) [subsystems (i) and (ii) do not require this information]. Zones 1, 2, and 3, and the Feature Pathway, common to the four waste forms, are discussed next.

Zone 1: Waste Package Internals

In Zone 1, two processes are considered. First, dissolved concentrations of radionuclides released from the waste form are computed. For radioactive species with relatively low solubility (e.g., uranium and plutonium), solid phases may precipitate from solution and constrain the dissolved concentration to the solubility limit. Concentrations of highly soluble radionuclides (e.g., cesium and iodine) are unlikely to reach their solubility limits, and concentrations and releases into Zone 2 are controlled only by the waste form degradation rate. The second process considered in Zone 1 is radionuclide releases into Zone 2. Mass balance equations governing advection, dispersion/diffusion, and radionuclide decay are solved using the GoldSim cell pathway implementation to compute releases into Zone 2 (GoldSim Technology Group, LLC, 2016b).

The radionuclide release rates are computed based on flow rates (advective transport), concentration difference (diffusive transport), and the cross-sectional area of the breaches in the degraded waste packages [i.e., the average breach area per failed waste package; Eq. (4-7)] using the GoldSim cell pathway representation of the mass balance equation

$$f_{bs} = c_s q + D_s (c_s - c_b) \quad (4-8)$$

where f_{bs} is the release rate (g/yr), q is the flow rate out of the waste package (m^3/yr), c_s is the radionuclide concentration in water inside the waste package (g/m^3), c_b is the radionuclide concentration in water outside the waste package (g/m^3), and D_s is the diffusive conductance (m^3/yr). The diffusive conductance term in Eq.(4-5) is calculated as follows

$$D_s = \frac{A_{WP}}{\frac{L_i}{n_i D_{is} \tau_i} + \frac{L_b}{n_b D_{bs} \tau_b}} \quad (4-9)$$

where A_{WP} is the waste package breach area per failed waste package (m^2); L_i and L_b are the diffusive lengths of the mixing cell immediately inside and outside the waste package, respectively (m); n_i and n_b are the porosity of the mixing cells i and b , respectively; D_{is} and D_{bs} are the diffusivity of species s in the water of mixing cells i and b , respectively (m^2/yr); and τ_i and τ_b are the tortuosity of the porous medium within mixing cells i and b , respectively. The term A_{WP} is the combined breach area that includes contributions from general corrosion, localized corrosion, and alternative failure modes [Eq. (4-7)].

Radionuclide release rates may be constrained by solubility limits. The solubility constraints on concentration are enforced within the GoldSim mixing cell representing the waste package internals. This mixing cell tracks the mass of radionuclides released from the waste form as well as the mass transferred to Zone 2. The GoldSim mixing cell keeps track of the precipitated mass, which can be dissolved back when the concentration falls below the solubility limit. The net effect of the solubility limit is to increase the residence time of radionuclides in the mixing cell representing the waste package internals. Solubility constraints are also enforced in cells representing buffer or backfill materials (Zone 2 and the Feature Pathway); however, because concentrations tend to decrease away from Zone 1, solubility limits outside Zone 1 have minor influence on release and dose estimates.

Equation (4-8) accounts for both advective and diffusive release mechanisms. For calculation of advective release, it is assumed that water can flow through the waste package (i.e., $q > 0$) only if the diffusive barrier capability of the buffer or backfill (Zone 2) is degraded or absent. Hence,

there is no advective transport in Zone 1 as long as Zone 2 is intact (see Zone 2 discussion in next paragraph). Diffusive release occurs regardless of the state of Zone 2. Therefore, in simulations for which the dynamic buffer evolution abstraction is not enabled, diffusive transport is the only mechanism for release away from the waste package.

Zone 2: Buffer Material

In Zone 2, dissolved radionuclides are transported through the engineered buffer or backfill material. For sorbing radionuclides, transport is delayed by sorption onto the buffer material. Solubility constraints are also applied to the radionuclide concentrations in Zone 2, although, as previously stated, they are less influential there because concentrations decrease away from the waste form. Three cases for the treatment of the barrier capability of the buffer are available through settings in the dashboard via a pull-down menu: (i) intact (i.e., diffusive barrier), (ii) variable openings over time, or (iii) bypass. For the intact case (default case), radionuclide transport occurs only by diffusion in the direction of the concentration gradient. If “variable openings over time” is selected in the Near Field dashboard, the user must define additional parameters related to the fraction of the buffer volume open to flow at emplacement, the residual open fraction after saturation, and the open fraction after long-term degradation. These fractions also require corresponding transition times, to define a stepwise buffer open fraction as a function of time (**Error! Reference source not found.**).

Degraded buffer units would exhibit cracks or openings, and direct contact of groundwater carrying corrosive species (such as HS^-) with the waste package surface cannot be ruled out. It is assumed that water flows through those openings and cracks, and causes corrosion of waste package materials such as copper. Radionuclides are transported away from the waste form by those water flows and by diffusion. Advective transport of radionuclides from the waste package internals to the buffer is proportional to the waste package breach area and the flow rate through the buffer. For simplicity, the flow rate is assumed proportional to the total volume fraction of openings in the buffer units. In reality, flows are controlled by pressure gradients; the sole presence of gaps, cracks, and openings alone does not imply water flows if pressure gradients are missing.

Error! Reference source not found. shows two transition periods. Initially the buffer material may have openings that would seal after saturation (water saturation causes bentonite clay to expand). Some residual openings may remain after saturation. After a long time, degradation or erosion could occur and cause openings in the buffer units. The abstraction in **Error! Reference source not found.** is only an example; the Near Field Settings dashboard allows flexibility to change the open fractions and transition times to incorporate alternative evolutions. Note that the buffer evolution abstraction is independent of the repository geologic medium and redox state (which is controlled by the leg one pathway in the Far Field Settings dashboard). The user should exercise caution, because the buffer evolution model is highly simplified, and some transitions may not occur, for example, in a repository in oxidizing media. Note also that the transition time to saturation is used in the dynamic general corrosion model to define the transition from oxic to anoxic conditions.¹ This is a cautious (i.e., conservative) approximation, because anoxic conditions may be established before complete saturation. Also, assuming advection through openings proportional to the buffer open fraction is a simplification. As

¹ If the dynamic general corrosion model is enabled, the far-field leg-one redox state is defaulted to reducing. The dynamic general corrosion model assumes the existence of a transition from oxidizing to reducing conditions.

previously stated, water flows are dependent on pressure gradients, which are dependent on large-scale, repository scale, and tunnel- and deposition hole-scale factors (and not solely dependent on the presence of gaps in the buffer).

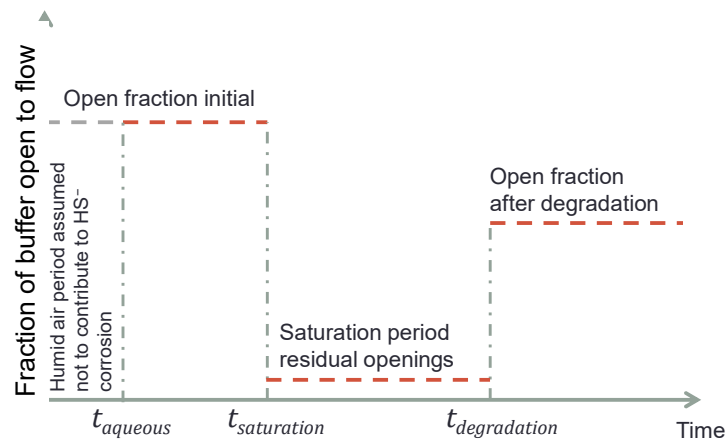


Figure 4-3. Buffer evolution abstraction (fraction of buffer open to flow versus time)

In the buffer bypass option, flowing water is assumed to contact the waste form at the Zone 3 flow rate. Radionuclides are transported directly from Zone 1 (waste package internals) to Zone 3. If dynamic general corrosion is enabled (in the Waste Package Settings dashboard), the rate of supply of HS^- to the copper waste package surface is also proportional to the Zone 3 flow.

Zone 3: Transition Region

In Zone 3, or the transition region, dissolved radionuclides are transported from Zone 2 to the closest fracture (for a disposal system in fractured host rock) or to the rock matrix (for a disposal system in porous rock) via diffusion and advection. The following paragraphs describe how transport through Zone 3 is represented differently, depending on whether the host rock is fractured rock or porous medium.

If the host rock is a porous medium, the transport distance for Zone 3 is set to an extremely low value and releases from Zone 2 effectively go directly to the far field (i.e., first transport leg of the far field). For a fractured host rock, the Zone 3 length (i.e., the effective diffusive transport distance to the far-field pathway) is a function of the fracture separation, which is adjusted by a fractional parameter that is randomly sampled to account for the random location of waste packages with respect to the nearby fracture planes. The Near Field dashboard includes an option to set the Zone 3 length as zero to bypass Zone 3, for sensitivity analyses.

Two different boundary conditions are implemented at the terminus of Zone 3. In the default boundary condition, release rates are defined as $c \times q$, where c is the radionuclide concentration at the terminus cell and q is the Zone 3 flow rate. In the boundary condition two, the Zone 3 terminus is set at a zero concentration. The default boundary condition is preferred to examine the competition of the Main Pathway and the Feature Pathway. The operating boundary condition is user-selectable in the Near Field dashboard. The dashboard also includes a check to enable or disable sorption for Zone 3.

Zone 2 and Zone 3 Flows

The Zone 2 and Zone 3 flows are computed as follows. First, a near-field reference flow rate is defined on the basis of the Far Field Leg 1 Darcy flux (see Section 4.4 for description of the Far Field model component). If the Far Field Leg 1 is fractured rock, the near-field reference flow is the flow rate carried in one fracture intercepting one buffer unit. If the Far Field Leg 1 is porous rock, the reference flow is computed as the leg-one Darcy flux times a buffer cross section. This near-field reference flow is used to define flow rates through Zones 2 and 3. Flow factors, available in the Near Field dashboard, are used to multiply the reference flow to define the Zones 2 and 3 flow rates. The Zone 3 flow rate is also proportional to a cross section factor. This dashboard-controlled cross section factor changes the size of the Zone 3 cross section with respect to the Zone 2 cross section. The Zone 3 cross section factor is used as well to define the Zone 3 volume and cross sections for calculations of radionuclide transport by diffusion.

The SOAR model is not a water balance model, but it allows incorporation of information from a detailed water balance model. For example, a large-scale regional flow model could be implemented to solve for far-field flows. Far-field flows and pressures could be used as boundary condition input to a near-field water flow balance model, with a more refined scale and explicit representation of the repository system. A detailed flow model would account for variable hydraulic conductivity on the different parts of the system (e.g., impermeable waste canisters and waste forms, less permeable host rock, and permeable bentonite, backfilled tunnels, and excavated disturbed zones). Near-field flows computed with such a detailed model may be considered to define inputs to SOAR, recognizing that SOAR employs a single representative waste package concept requiring definition of average flows per waste package. In general it is difficult to simply predict near-field flows as function of far-field flows without a detailed water balance model. For example, most of the flow may occur in connected zones of high hydraulic conductivity (e.g., backfilled tunnels and excavated disturbed zones), and very limited or no flow through buffer units enclosing impermeable waste packages. The SOAR model implements simple assumptions, scaling the far-field flow to define near-field flows. The Near Field model includes independent flow factors to change a reference flow to define the flow through the buffer (Zone 2), transition region (Zone 3), and the Feature Pathway. These three factors offer flexibility to implement flows consistent with a detailed flow model.

Feature Pathway

An optional Feature Pathway model is available parallel to the Main Pathway (Main Pathway: Zone 1 → Zone 2 → Zone 3 → Far Field Leg 1). The Main and Feature Pathways are depicted in the diagram in **Error! Reference source not found.** The Feature Pathway includes an additional buffer segment with diffusion-only transport, connected to the main buffer pathway (Zone 2) and to a tunnel region, considered backfilled with bentonite clay (the same material as the buffer). Radionuclide transport in this region occurs by diffusion and advection.

Radionuclides eventually discharge to a large-scale feature (for example representing an emplacement shaft), independently simulated in the Far Field component. In similitude to Zone 3, two boundary conditions are available: release rate equal to $c \times q$ as default option, and zero concentration as option two. The Feature Pathway can be enabled or disabled from the Near Field dashboard. If disabled, transport is constrained to the Main Pathway (Zone 1 → Zone 2 → Zone 3 → Far Field Leg 1). The Main and Feature Pathways are coupled; enabling the Feature Pathway causes a reduction in radionuclide releases from the Main Pathway. The Near Field dashboard includes entries to define dimensions of the Feature Pathway, a check to enable or

disable radionuclide sorption (K_d distribution coefficients are the same as the buffer material K_d 's), and a flow factor. The flow

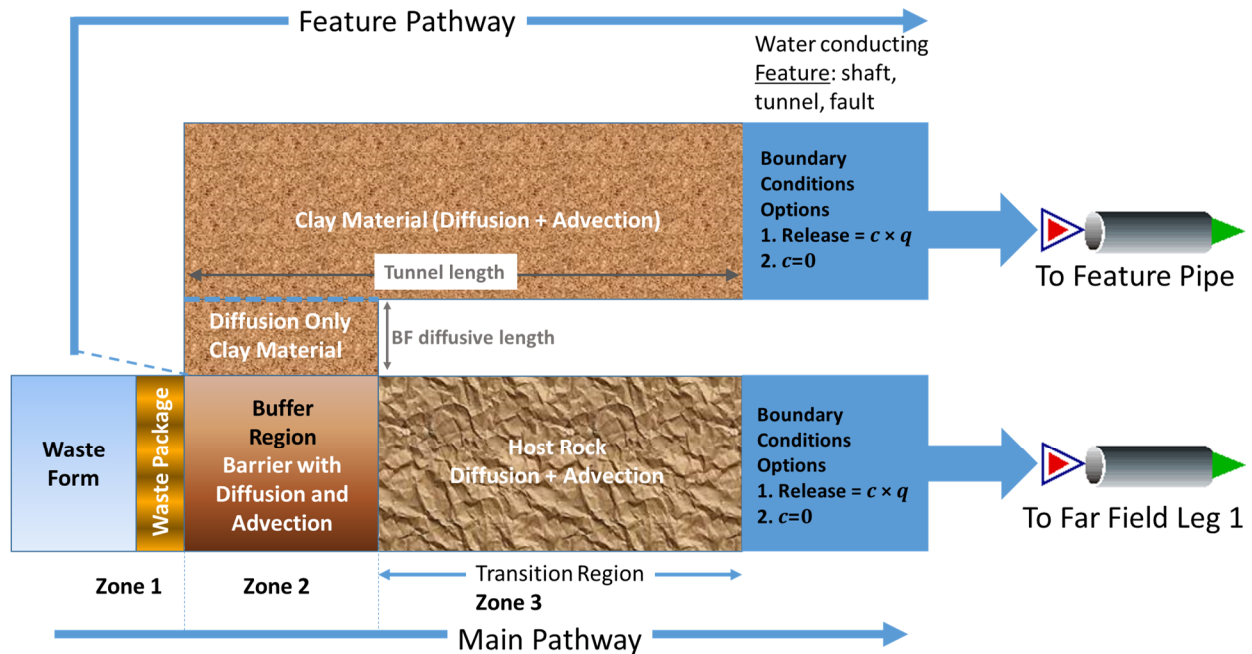


Figure 4-4. Main and Feature Pathway Simulated in the Near Field Model

factor is used in the same way as the Zone 2 and Zone 3 flow factors, to change the flow rate with respect to the reference near-field flow rate.

Modeled Scenarios

The Near Field model component allows flexibility to explore different scenarios with appropriate selection of settings and parameters. For example, bypassing the Zone 3 represents a case of a water-conducting fracture directly intercepting the buffer material. Selecting the buffer reference height to a small value simulates a case where radionuclide transport in the buffer is constrained to a narrow region, for example due to localized failure of the waste package surface. The Zone 3 and Feature Pathway could be used to emulate transport in the excavation damaged zones (EDZ), with relative high water flows. The Zone 3 and the Feature Pathway differ in the K_d values; the Zone 3 implements host-rock K_d 's, and the Feature Pathway, bentonite material K_d 's. Thus, different K_d alternatives exist to simulate EDZs. The Zone 3 and Feature Pathway flow factors may be used to examine the relevance of constrained flows. In some international performance assessments (e.g. performance assessment models of geologic repositories in Japan and Sweden), significant constraint of near-field radionuclide release rates arise from very small flows through fractures in the host rock and very few fractures intercepting waste package deposition holes. Such cases can be simulated in SOAR selecting a zero-length Zone 3 with a small Zone 3 flow factor, and an advective release boundary condition (i.e. radionuclide release rate = $c \times q$) at the Zone 3 terminus.

Model Assumptions

The following assumptions are inherent to the simulation approach for near-field flow and radionuclide transport:

- Sorption of dissolved radionuclides onto solid material occurs instantaneously and is described by an equilibrium partition coefficient (k_d , also referred to as the distribution or sorption coefficient) for a specified environment (i.e., it is an instantaneous equilibrium linear sorption model).
- Precipitation/dissolution reactions are reversible. A single mineral phase controls the solubility for each element for a specified set of geochemical conditions. Radioisotopes of a single element share the same solubility constraint. For example, the concentration of dissolved uranium in water leaving the waste package is computed by adding all the concentrations of the uranium isotopes present at that time. If the total concentration exceeds the solubility limit, then uranium minerals form that include proportional amounts of the uranium isotopes.
- The pH, ionic strength, pCO_2 , and oxidation state do not vary spatially or temporally in the near field. For a specified geochemical environment, a range of these parameter values can be considered using a distribution of solubility constants and partition coefficients.
- Flow rates in the buffer are assumed proportional to the volume of openings in the buffer.
- A single representative system is modeled of waste package/buffer material/host rock. Flow rates and other extensive quantities (e.g., cross section, volumes) of the near field are specified *per waste package*.

4.3.3 Default Parameters

A complete list of default parameter values, distribution types, and technical bases for the Near Field model component is provided in Appendix A, Table A-3.

The diffusion coefficient, dispersivity, solubility limit, and partition coefficient parameter values or ranges of values used for various engineered barrier materials in the Near Field model component were primarily obtained by literature review of engineered barrier designs, laboratory testing, and geochemical modeling results from domestic and international geologic disposal programs. Based on the user's selection of redox conditions for a simulation, the model will select representative input data distributions for radionuclide-specific solubility limits and partition coefficients for either oxidizing or reducing conditions. Diffusion coefficients are also radionuclide specific and assumed not dependent on redox conditions.

For calculating transport through the buffer or backfill in Zone 2, inputs include a reference height and an inner radius to compute the cross-sectional area and volume of the diffusive transport pathway, and a length parameter to specify transport distance. For transport in Zone 3, the distance is calculated based on the far-field fracture separation and a factor to account for uncertainty in the location of the waste package with respect to the nearest flowing fracture. The Zone 3 diffusive transport calculation also includes a parameter to permit increasing or decreasing the diffusive cross-sectional area relative to that calculated for the Zone 2 transport pathway. For fractured rock, a near-field flow factor is specified through the Near Field Settings dashboard to adjust the near-field flow velocity (by default equal to the velocity in the first leg of

the far field) to support sensitivity analyses. For the Feature Pathway, geometry parameters controlled from the Near Field dashboard include an additional buffer diffusive distance, the tunnel length or tunnel distance to the large-scale feature, and the tunnel cross section. A flow factor is available to individually adjust the water Darcy flux and flow velocity, for sensitivity analyses.

4.3.4 Flexibility

Through careful selection or modification of input parameter sets and individual parameter values, the SOAR model has the flexibility to evaluate engineered barrier material properties, such as diffusion coefficients, diffusive area, and barrier thickness; evaluate geochemical properties, such as solubility constants and partitioning coefficients; and implicitly evaluate effects such as variability in pH, ionic strength, and pCO₂ by selecting input data sets for either reducing or oxidizing environments. The model also is capable of evaluating buffer evolution (Zone 2) over time. Given the appropriate technical data, sorption coefficient could be modified to represent materials other than bentonite (e.g., cement or other forms of clays).

The Near Field model component of the user interface dashboard allows users additional flexibility to evaluate alternative model concepts without the need to revise the input parameter distributions. Specifically, the dashboard provides users with the options to

- Bypass the near-field Zones 2 and 3, to examine their combined effect on radionuclide transport
- Enable or disable sorption in the Zone 3 and the Feature Pathway, to examine the isolated importance of radionuclide sorption
- Specify the volume of water inside the waste, to examine effects of solubility limits to constrain radionuclide releases
- Specify different near-field flow factors for Zone 2, Zone 3, and the Feature Pathway, to explore flow effects
- Specify a different transport pathway cross sections for Zone 2, Zone 3, and the Feature Pathway, to examine the effect of pathway dimensions on radionuclide releases
- Explore different options for the boundary condition to compute radionuclide releases at the terminus of Zone 3 and at the terminus of the Feature Pathway
- Specify alternatives for the evolution of the buffer material.
- Adjust near field flow factors independently to match flow rates derived from detailed process-level water flow balance models.

4.4 Far Field

4.4.1 Description

The Far Field model component of SOAR considers transport of radionuclides within the natural-system barrier component from the engineered barrier system to the biosphere. The Far Field model component specifically considers transport of radionuclides through geologic media,

accounting for the effects of advection, diffusion, dispersion, decay, and sorption. The Far Field model component receives radionuclide releases from the Near Field model component and provides radionuclide releases to the Biosphere model component. The Far Field model does not implement a detailed water-balance model. Instead, it computes Darcy water fluxes simply as the product of the effective hydraulic gradient (user-defined input in the Far Field dashboard) and the effective hydraulic conductivity of the rock.

4.4.2 Model Implementation

The Far Field component considers a range of geologic media using a simplified representation for flow and transport. It includes two pathways: Main Pathway and Feature Pathway. The Main Pathway is a series of three transport legs, and it is connected to the Near Field Main Pathway. The Far Field Feature Pathway is connected to the Near Field Feature Pathway.

Entries in the Far Field dashboard provide flexibility to assign either a fracture-dominated or a matrix-dominated transport model to each of three transport segments (legs) of the Main Pathway. The type of host rock and redox condition of the first leg of the Far Field model component defines the host rock and redox condition for Zone 3 of the Near Field component. If the dynamic general corrosion model is enabled in the Waste Package dashboard, the redox condition is defaulted to anoxic or reducing for the first leg.²

The Feature pathway is a fourth independent leg, transporting radionuclides in parallel to the three-leg Main Pathway. This parallel pathway is intended to simulate a large-scale feature such as emplacement shafts, tunnels, or major water-conducting faults. The type of host rock for the first leg of the Main Pathway defines the values of K_d 's for the computation of matrix diffusion of the Feature Pathway.

The Far Field component is based on the concept of one-dimensional advection-dispersion transport with equilibrium sorption mass exchange with the rock matrix and first-order decay and ingrowth of radionuclides, as defined next in Eq. (4-10). In this conceptual model, radionuclides released from the Near Field component are carried by water moving through the geologic media within a sequence of adjacent flow paths, conceptually referred to as stream-tube bundles. Each leg within the three-leg sequence of the Main Pathway, and the Feature Pathway, is an effective stream tube that represents the many pathways in a complete bundle. The parameters for the effective stream tube represent the average flow and transport parameters of the bundle.

The conceptual model is mathematically represented by the expression describing transport of a radionuclide species in the mobile zone

² In the dynamic general corrosion model it is assumed a transition from an early oxidizing state (associated with a transitory period following repository closure) to a long-term reducing state (after depletion of oxygen). In other words, the dynamic general corrosion model assumes the repository is located in a medium that eventually becomes reducing.

$$n R \frac{\partial c}{\partial t} = -\frac{Q}{A_{cs}} \frac{\partial c}{\partial x} + \left(\frac{\alpha Q}{A_{cs}} + D \right) \frac{\partial^2 c}{\partial x^2} + n R \left[-\lambda c + \sum_p c_p \lambda_p f_p S_p \frac{W R_p}{W_p R} \right] - \frac{F_{md}}{A_{cs}} \quad (4-10)$$

where n is the effective porosity [unitless] of the mobile zone medium ($n = 1$ for a fracture without any infill medium), R is the retardation factor (unitless) of the mobile zone medium, c is solute concentration (kg/m³), Q is volumetric flow rate of water (m³/yr), A_{cs} is the cross-sectional area (m²) perpendicular to the flow direction, α is dispersivity (m), D is effective diffusivity (m²/yr), λ is decay rate (1/yr), f is the fraction of the parent species that decays into the species (unitless), S is the stoichiometric ratio of moles produced per mole of parent (unitless), W is atomic weight (kg/mole), F_{md} represents diffusive mass flux per unit length of pathway (kg/yr/m) from water flowing in fractures (mobile zone) into stagnant water (immobile zone) within the adjacent rock matrix, t is time (yr), and x is the position coordinate along the pathway (m). To make parameters dimensionally consistent, unit conversions are handled internally by the GoldSim software. A subscript p represents a parent species in a decay chain.

The flux into matrix diffusion zones is considered only for the conceptual model of fracture-dominated flow and is represented by

$$F_{md} = -P f_{im} D_{im} \left. \frac{\partial c}{\partial z} \right|_{z=0} \quad (4-11)$$

where P is the pathway perimeter [m], f_{im} is the fraction of the perimeter with matrix diffusion (unitless), D_{im} is the effective diffusivity of the matrix diffusion zone (m²/yr), and z is distance into the matrix diffusion zone (m) perpendicular to the x direction.

From Eq. (4-11) it can be seen that the rate of diffusive transport into the stagnant matrix diffusion zone is controlled by the solute concentration gradient at the rock fracture–interface ($z = 0$) perpendicular to the flow direction. The time-dependent solute concentration within the matrix diffusion zone is calculated in GoldSim from

$$n_{im} R_{im} \frac{\partial c_{im}}{\partial t} = D_{im} \frac{\partial^2 c_{im}}{\partial z^2} + n_{im} R_{im} \left[-\lambda c_{im} + \sum_p c_{im,p} \lambda_p f_p S_p \frac{W R_{im,p}}{W_p R_{im}} \right] \quad (4-12)$$

where the symbols are the same as in Eq. (4-7), except that the im subscript denotes the immobile region. The GoldSim software assumes the effective diffusion coefficient, D_{im} , to be proportional to the porosity of the matrix, n_{im} . The porewater diffusivities (equal to D_{im}/n_{im}) are input through the SOAR database; GoldSim internally multiplies the porewater diffusivity and the porosity to compute the effective diffusivity of the matrix, D_{im} .

The retardation factor for each radionuclide species is calculated as

$$R = 1 + \frac{\rho_b K_d}{\theta} \quad (4-13)$$

where ρ_b is the dry bulk density of the porous medium or rock matrix (kg/m³), K_d is the radionuclide-specific equilibrium partition coefficient (m³/kg), and θ is the saturated porosity of

the porous medium or rock matrix (unitless). For uniform flow in porous media, θ is equal to n in Eq.(4-10). For fracture flow with diffusion into a stagnant matrix zone, θ is equal to n_{im} in Eq. (4-12). Users are referred to GoldSim Technology Group, LLC (2016b) for a thorough explanation of underlying solute transport modeling methods and assumptions used in the GoldSim pipe elements, as well as solution algorithms of the mass-balance differential equations. The Far Field component provides the capability to treat flow in each transport leg of the three main legs as either single porosity or dual porosity. A single-porosity flow leg represents uniform flow through a homogenous medium. A dual-porosity flow leg represents a heterogeneous system, such as fractured rock, where nearly all flow occurs in a small portion of the total porosity that can exchange mass by diffusion into the relatively stagnant water that occupies the remaining porosity of the unfractured rock mass. The type of model used and the associated parameters in the transport calculations depend on the medium selected. For calculating water flow rates in a single-porosity medium, the volumetric water flux per unit area is calculated according to Darcy's Law by multiplying the hydraulic gradient and the bulk hydraulic conductivity. For flow in a dual-porosity system fractured medium, Darcy's Law is also used to represent volumetric water flux per unit area. In this case, however, two sampled parameters—effective fracture aperture and average flowing fracture separation—are used to calculate an equivalent hydraulic conductivity using the cubic law for flow between parallel plates. The cubic law relates the average volumetric flux to the cube of the aperture. The effective fracture aperture is the aperture that yields the same average volumetric flux as the actual aperture distribution. The fracture length density describes the total length of flowing fractures per unit rock area in the plane perpendicular to flow direction. The effective porosity is assumed to be the product of effective equivalent or representative aperture and fracture length density. The fracture length density and perimeter for exchange with the matrix diffusion zones are calculated using the conceptual model of parallel flowing fractures, each extending the height of the stream-tube bundle and separated by an average distance. With this conceptual model, the fracture length density is the inverse of the average separation distance.

The Feature Pathway is a dual porosity system. It is assumed that water flows through open space (this open space could simulate a system of fractures) exchanging radionuclide mass with the rock matrix. The rock matrix is assumed to be of the same material (same K_d 's, rock density, and porosity) as the first leg of the basecase far-field pathway. The matrix diffusion thickness is assumed equal to half the fracture separation if the host rock is fractured rock, or semi-infinite if the host rock is porous rock. Transport parameters of the Feature Pathway such as the length, dispersivity, fracture aperture, fracture width, and flow velocity are controlled in the Far Field dashboard. The Feature pathway is simulated using a GoldSim pipe element, in similitude to the three transport legs of the Main Pathway. It is intended to simulate a physical feature relatively close to the disposal system, and of flow rates different to flows of the Main Pathway. An example of applicability of the Feature pathway is in the simulation of a major water-conducting fault (MWCF). In a performance assessment model for a geological disposal system in Japan, a MWCF with discharge to an aquifer on the surface (JNC, 2000) was considered. The MWCF was evaluated as a potential pathway that could release radionuclides to the biosphere sooner than other groundwater paths, such as a network of fractures in granitic rock (JNC, 2000). The Main Pathway could be used to simulate transport in the background groundwater flow, and the Feature Pathway could be set to simulate transport in the MWCF. In general, the Feature Pathway includes flexible settings in the Far Field dashboard to emulate other scenarios such as radionuclide transport through vertical shafts or tunnels, under the premise that related flows are different (different magnitude and discharge) than background groundwater flows.

Some inherent assumptions and key processes represented by the described computational approach include the following:

- Flow in fractures and porous media is assumed slow and laminar, such that Darcy's Law (i.e., flow rate is proportional to hydraulic gradient) is a valid approximation, and time-dependent and local acceleration as well as turbulent flow effects can be neglected. Information from detailed water-balance models can be incorporated through careful selection of the user-defined hydraulic gradients input in the Far Field dashboard.
- Longitudinal contaminant dispersion during transport that results from variability in flow velocities within adjacent flow pathways is assumed to be proportional to the average water velocity, with a proportionality constant called the dispersivity. The resulting smearing of transport times caused by dispersion is in general dominant over the effect of molecular diffusion. The dispersivity (α) is assumed to be scale dependent and is calculated as a fraction of the transport path length (e.g., 10 percent in the basecase parameter set).
- When fractured rock is selected as the geologic medium for a transport leg, the model considers the flowing fractures to be a mobile zone with adjacent immobile zones representing both the low-permeability rock matrix and any nonflowing fractures. The GoldSim software is capable of representing up to three different geometric configurations for the interface between mobile and immobile zones. These geometries include (i) a slab (diffusive area is constant with distance into the matrix), (ii) a sphere (diffusive area decreases with distance into the matrix, like a matrix block between bounding fractures), and (iii) a slot (diffusive area increases exponentially with distance into the matrix). Each immobile zone may occupy a fraction of the fracture perimeter and extend halfway to the next flowing fracture. The default setup for the Far Field components (i.e., the Main Pathway and Feature Pathway) calculates matrix diffusion flux using the slab geometry with no "skin zone" enabled (skin zone refers to a thin zone at the fracture surface that permits instantaneous sorption).
- Some radionuclides can be sequestered onto the surface of solid particles for long periods of time by sorption. The Far Field component represents sorption using the assumption that the ratio of sorbed radionuclides to dissolved radionuclide concentration rapidly establishes a single fixed value regardless of concentration (i.e., equilibrium linear sorption). This fixed ratio equals the product of the partition coefficient, K_d , and the dry density, ρ_b . Conceptually, sorption describes attachment of a radionuclide molecule to one of many sites on the solid surface. For some radionuclides, the partition coefficient may differ by orders of magnitude with different values of pH, salinity, redox potential, dissolved-species concentrations, and specific surface area (surface area per unit volume). The SOAR model only considers sorption to fixed static surfaces (i.e., colloidal transport is not included). When a porous medium is selected for a transport leg, sorption is assumed to occur throughout the porous medium. When a fractured medium is selected, sorption is assumed to occur only within the stagnant rock matrix.
- The transport model does not account for precipitation or dissolution. Each radionuclide is assumed to have concentrations no greater than the ambient solubility limit. This assumption is reasonable, as concentrations decrease away from the source.

4.4.3 Default Parameters

A complete list of default parameter values, distribution types, and technical bases for the Far Field component is provided in Appendix A, Table A–4. Parameter sets were developed for three types of transport media: fractured rock, unconsolidated sediments, and porous rock. Radionuclide-specific sorption coefficients (K_d), bulk density (ρ_b), effective porosity (θ), and matrix porewater diffusion coefficients were selected based on literature reviews of laboratory and field testing from domestic and international geologic disposal system programs. Properties for fracture-dominated flow systems were selected to be consistent with flow in granitic rock (SKB, 2006). Properties for unconsolidated sediments were based on studies of alluvium for the Yucca Mountain project (DOE, 2008). Properties for the porous rock medium are based on a variety of sources for properties of clays suitable for geologic disposal sites (NEA, 2005; Nirex Limited United Kingdom, 2003; SKB, 1997).

4.4.4 Flexibility

With appropriate selection or modification of input parameters such as radionuclide distribution coefficients and hydraulic conductivity, the Far Field component is capable of representing flow and transport through a wide range of porous or fracture-dominated natural media. For example, with modification of these parameters, one could represent transport through basalt, sandstone, or clay. The Far Field component provides default parameters for each equivalent stream tube. The default parameters for porous medium legs are representative of oxidizing conditions in typical alluvium. The default parameters for fractured medium legs are representative of reducing conditions in typical fractured granite.

The Far Field component of the user interface dashboard allows users additional flexibility to evaluate alternative model concepts without the need to revise the input parameter distributions. Specifically, the dashboard provides users with the options to

- Select the conceptual models for flow (fracture dominated or matrix dominated) and geochemical environment (oxidizing or reducing). The combination of these two conditions affects the selection of radionuclide sorption coefficients and the rock matrix diffusion coefficients used in the transport calculations
- Specify the transport path length for each of the three transport legs
- Specify the effective flow porosity in each of the transport legs, for example to selectively change the water travel time
- Specify the hydraulic gradient independently for each of the three main legs (water fluxes are proportional to the hydraulic gradient)
- Specify key parameters of the Feature Pathway such as length, dispersivity, fracture aperture and width, and flow velocity.
- Enable and disable matrix diffusion and sorption in the Feature Pathway, to examine the individual relevance of those processes. When sorption is enabled, the K_d 's are the same as leg one of the Main Pathway.

4.5 Biosphere

4.5.1 Description

The Biosphere model component converts radionuclide mass arrival rates from the Far Field model component into radiological dose to a person (receptor) in the biosphere. Biosphere considerations were simplified to only address the drinking water pathway. No other dose pathways are considered. Integrated radionuclide release is also calculated to provide a second, optional metric of system performance. The same dose pathway is used for the Main Pathway and the Feature Pathway.

4.5.2 Model Implementation

The Biosphere component computes radiological dose in the following manner

$$E = \sum_i m_i \frac{CF}{Q} a_i I d_i \quad (4-14)$$

where E [Sv/yr] is the annual effective dose; m_i (g/yr) is the mass arrival rates from the Far Field component for radionuclide i ; CF (unitless) is the contaminant plume capture fraction; Q (m^3/yr) is the water flow rate to the biosphere; a_i (Bq/g) is the specific activity for radionuclide i ; I (m^3/yr) is the water consumption rate; and d_i (Sv/Bq) is the dose coefficient for ingestion of radionuclide i .

The calculation of radiological dose involves the following steps:

- Radionuclide mass concentrations in water (g/m^3) are calculated by multiplying radionuclide mass arrival rates output by the Far Field component (g/yr) by a capture fraction (unitless) and dividing by the annual water flow rate to the biosphere (m^3/yr).
- Radionuclide mass concentrations in water are converted to radionuclide activity concentrations in water (Bq/m^3). This conversion applies internal specific activity definitions (Bq/g) for individual radionuclide species internally tracked in GoldSim.
- Annual radionuclide dose to the receptor is calculated by multiplying the radionuclide activity concentration in water with the product of annual water consumption rate (m^3/yr) and the radionuclide dose coefficient for ingestion (Sv/Bq). Doses are calculated for ingestion of drinking water only.
- The total annual dose (Sv/yr) is calculated by summing the annual dose contributions from the individual radionuclides. Individual radionuclide doses and the total dose from all radionuclides are computed. Doses to individual organs are not calculated.

Radionuclide and total dose results are computed as in Eq. (4-14) and also weighted by the probability of alternative failure events. Section 4.6 on Alternative Failure Modes presents three optional models: (i) waste package failure rate, (ii) single failure event, and (iii) multiple failure event. Options (ii) and (iii) require specification of an event frequency, f (1/yr). The weight factor is the probability of occurrence of at least one event during the simulation time, T (yr):

$$P = 1 - e^{-f T} \quad (4-15)$$

This probability, P , is used as a weight factor adjustment to the dose, and is applied only when mode (ii), single failure event, is enabled in the Alternative Failure Modes Settings dashboard.

The integrated release is calculated as described in 40 CFR Part 191, Appendix A, Subpart B, Table 1. This calculation in SOAR assumes that the initial inventory falls into the category of 40 CFR Part 191, Subpart B, Table 1, Note 1(a), where the waste form is based on a burnup rate of 25,000–40,000 MWd/MTHM. The probability weight in Eq. (4-15) is also applied to the computation of integrated releases when alternative failure mode (ii) is enabled.

4.5.3 Default Parameters

The Biosphere component includes four input parameters related to the water flow to the biosphere, plume capture fraction, water consumption rate, ingestion dose coefficients. The default parameter values, distribution types, and technical bases for the default parameters of the Biosphere component are listed in Appendix A, Table A-5.

Parameter distributions for sampling the water flow rate to the biosphere and amount of contaminated water the receptor consumed were selected to generically account for variability and uncertainty in regional irrigation practices, community water usage, and individual habits regarding water consumption from a well or natural surface-water source (e.g., spring). Constant values are used for the other biosphere parameters.

The water flow rate to the biosphere is used to calculate radionuclide concentrations in water available at the interface between the far field and the biosphere. Irrigation practices were used to establish groundwater usage for a small farming community, consisting of four farms of average size with respect to number of acres irrigated by groundwater. The parameter distribution accounts for variability in groundwater usage based on different water resource regions of the contiguous 48 states of the United States. The data source for this parameter value is U.S. Department of Agriculture (2010, Table 11).

A plume capture fraction modifies the concentration of radionuclides in water and accounts for the fraction of water accessible to the biosphere that is contaminated or the fraction of total radionuclide mass from the far field that is transferred to the biosphere. There is no specific data source. A default value of unity for this parameter does not change the concentration calculation and implies that all radionuclide mass transported to the end of the Far Field is completely transferred to the Biosphere.

The water consumption rate is the population-averaged consumption rate of community water for adults in the United States. The data source for this parameter value is the U.S. Environmental Protection Agency (2004, Table A1, Appendix E, p. E-4). Because the selected source data accounted for both direct (water ingested as a beverage) and indirect (water added to foods and beverages during final preparation) intake, the distribution was based on reported survey data up to the 95th percentile.

Ingestion dose coefficients provide the radiological dose to an adult from the ingestion of a unit radionuclide activity. The ingestion dose coefficient parameter is implemented as a tabular array with separate values for each radionuclide. The data source for these parameter values is the International Commission on Radiological Protection (1996, Table A.1).

4.5.4 Flexibility

As described in the default parameter section, the parameter distribution for water flow to the biosphere was determined from data on groundwater usage for irrigation. Alternative distributions for this parameter could be specified to represent water practices for a specific region or regions as candidate disposal sites.

A capture fraction parameter adds flexibility in the biosphere for calculating radionuclide concentrations in water that are representative of the annual intake of contamination by an average member of a critical group. This parameter can be used to account for the situation where water access and usage by a nearby community include water from other sources that is not contaminated with radionuclides. The parameter also can account for the incomplete transfer of radionuclides from the far field to the biosphere (e.g., if plume dimensions exceed well capture zones).

4.6 Alternative Failure Modes

4.6.1 Description

The Alternative Failure Modes model component of SOAR (i) allows for consideration of additional waste package failure mechanisms not explicitly included in the Waste Package model component (such as initially defective waste packages, human intrusion, seismic events, and igneous events), (ii) includes three additional waste package failure abstractions, and (iii) receives no inputs from other SOAR components (i.e., it is independent of other SOAR components; all of the relevant inputs are defined in the corresponding dashboard). The Alternative Failure Modes model component outputs (i) the fraction of waste packages failed as a function of time to the Waste Form model component to initiate computations of waste form degradation/dissolution, (ii) the breach area per failed waste package to the Waste Package model component, and (iii) the probability of at least one failure event to the Biosphere component.

4.6.2 Model Implementation

The Alternative Failure Modes component provides three waste package failure abstractions: (i) a defined waste package linear failure rate, (ii) a single failure event, (iii) or multiple failure events (**Error! Reference source not found.**). Only one of these three options can be used within a simulation. The options are described as follows.

Waste Package Linear Failure Rate Abstraction

As an alternative or in addition to the corrosion mechanisms described in Section 4.2, the user may specify a linear failure rate for waste packages. Waste packages are assumed to fail linearly with time between a start time and end time, up to a plateau fraction. This option requires three sets of inputs provided through the dashboard: the period during which the failure occurs (specified as start and end times—**Error! Reference source not found.**), the plateau waste package failure fraction (**Error! Reference source not found.**), and the waste package breach fraction (i.e., extent of damage to the waste package surface). The fraction plateau is sampled once per realization from a uniform distribution, with minimum and maximum values defined by the user in the Alternative Failure Modes Settings dashboard. The user defines the start and end times of the waste package failure process. Outside this interval, waste packages no longer fail (i.e., the total fraction of waste packages failed is 0 at time less than the start time,

and equal to the plateau fraction at times greater than the end time—**Error! Reference source not found.**). The user also defines a minimum and maximum breach area fraction. This fraction is assumed to follow a uniform distribution, sampled once per realization.

Single Failure Event Abstraction

The single failure event abstraction is provided to quantify consequences of rare events (i.e., an event that may or may not occur within the simulation time). A single failure event is forced to occur once in each realization at a random time, uniformly sampled between 1 year and the simulation time. The dose consequences and integrated releases are weighted by the probability of an event happening within the simulation time.

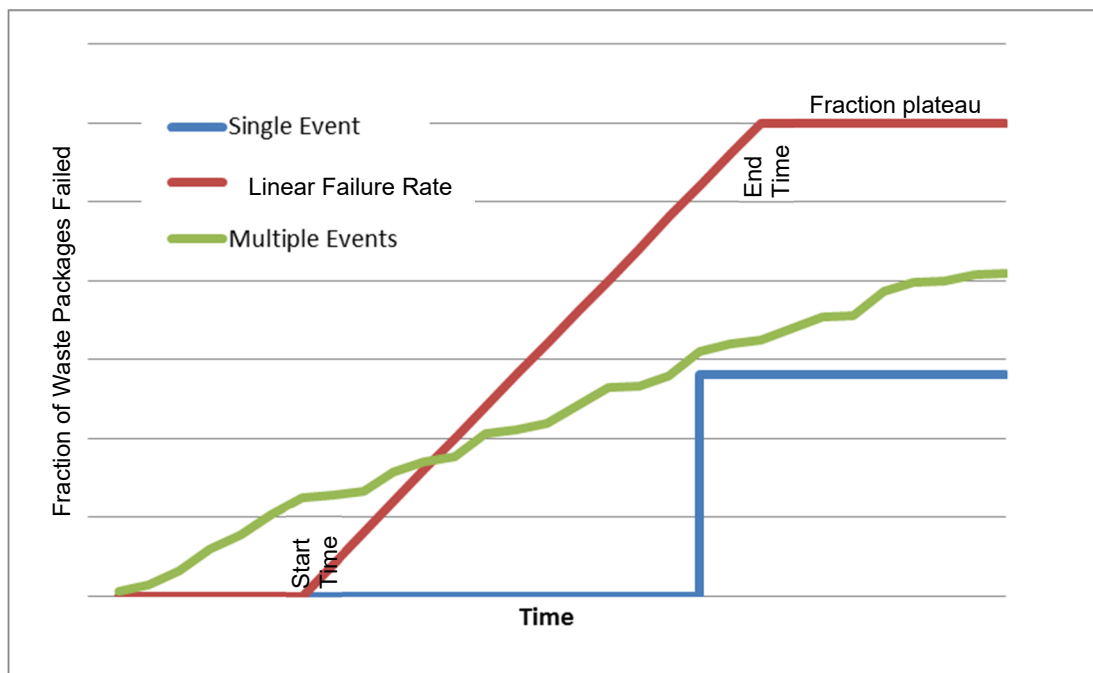


Figure 4-5. Characteristic Waste Package Failure Curves for the Three Abstractions Implemented in the Alternative Failure Modes Model Component

The single failure event abstraction requires three inputs for implementation in SOAR: the fraction of waste packages damaged by the event, the extent of damage (i.e., breach area fraction) per failed waste package, and the recurrence rate or frequency of the event (i.e., the number of events per year).

The user defines a minimum and maximum fraction of waste packages damaged after the event. The fraction of failed waste packages is assumed to follow a uniform distribution between those limits. One fraction is sampled per realization.

The waste package damage is defined as the fraction of the waste package surface breached that no longer provides a barrier to radionuclide release. The user defines a minimum and maximum waste package breach fraction, which also is assumed to follow a uniform distribution, sampled once per realization.

The event recurrence rate or event frequency, defined by the user, is used to compute the consequences of low probability events. In general, the probability of having one or more events of recurrence rate f (1/yr) in a simulation time T is equal to $P = 1 - \exp(-f T)$. This probability is used as a dose modification factor to expedite convergence. For example, if the simulation time is 10,000 years, and the recurrence rate is 10^{-6} 1/yr, then the probability of at least one event is $P=1-\exp(-0.01)=0.00995$. An event sampled at its actual recurrence rate would occur only in approximately 1 of every 100 realizations. Many realizations would be needed to capture the effect of the rare event. Instead, to avoid computing many realizations, an event is forced to occur in each realization, but the dose consequences are weighted with the event probability within the simulation time. This event probability is also used in the computation of integrated releases to compare to 40 CFR 191 limits. The weight or probability factor is not applied to other intermediate results. Thus, caution should be exercised in interpreting intermediate results which do not include probability weights.

This alternative failure mode is useful for exploring consequences of low-frequency (i.e., low-recurrence rate) events. For high-frequency events multiple events may occur within the simulation time. An alternative abstraction is available to simulate consequences of multiple events, which is discussed in the following paragraphs. The multiple event abstraction should be enabled for high-frequency events.

Multiple Failure Event Abstraction

The multiple event abstraction is available to analyze consequences of high-frequency events. High-frequency events may occur multiple times, and cause failure of waste packages at different discrete times, in a single realization. The events are assumed to occur randomly via a Poisson process. The multiple failure event abstraction requires two inputs for implementation in SOAR: the fraction of waste packages damaged for a given event and the damage area per waste package for the event.

SOAR utilizes a Timed Event element to generate each event that has the potential to impact the waste packages. The timing of these events is generated following a Poisson process (i.e., the time interval between events follows an exponential distribution). The recurrence rate (from which the event intensity is defined) is sampled from a uniform distribution between 10^{-8} yr⁻¹ and 10^{-4} yr⁻¹ (the user has flexibility to modify these 10^{-8} yr⁻¹ and 10^{-4} yr⁻¹ bounds through the dashboard). For each order of magnitude change in recurrence rate, the user can define a fraction of waste packages that are assumed to fail and the waste package surface damage fraction, or breach area fraction, to create a hazard curve. Values for the event impact (i.e., the number of waste packages affected by an event of a given sampled recurrence rate) are interpolated from the user-defined hazard curve. Events with a recurrence rate greater than 10^{-4} yr⁻¹ are assumed to have no impact on waste package integrity, while events of less than 10^{-8} yr⁻¹ are assumed to have the same impact as the 10^{-8} yr⁻¹ recurrence rate events. As an example, seismic events that occur with a frequency of 1 in 10,000 years, or more often, are assumed to have peak ground velocities and peak ground accelerations that do not cause major damage to the waste packages. Events with a frequency of 1 in 100 million years (or even less frequent) are assumed to be destructive and damage the majority of the waste packages. In the model, consequences of those high intensity events are restricted to waste package damage. However, extreme events could have other large effects on the system, such as changes to the landscape and water flow paths. Other potential alternative effects are not included in the model. This multi-event model does not need a probability weight, as the single-event model, because the events are sampled within a realization at the actual recurrence rate.

Waste packages fail at discrete times in the multiple failure event abstraction. These discrete events tend to cause oscillations in the radionuclide release rate versus time curves. The Alternative Failure Modes dashboard includes a flag to enable computing the number of waste packages failed and the average waste package damaged area versus time as three-timestep moving averages (e.g., the number of waste packages failed is computed as an average of the current value and values at the two previous timesteps). Enabling the moving average causes smoother near-field radionuclide release curves. The moving average was introduced predominantly for testing, to identify the reason of oscillations in radionuclide release rates, and it should be used with caution. The moving average changes the effective magnitude of the events (e.g., an event at a timestep is averaged with two previous timesteps without events; therefore, the resulting three-timestep average event is less intense), and care should be exercised in interpreting results.

Waste Package Breach Area

The waste package breach area calculated from the three additional alternative failure modes abstractions described previously [denoted as symbol $f_{A,AF}$ in Eq. (4-6)] is combined with the breach area from the corrosion processes modeled in the Waste Package model component described in Section 4.2 [denoted as symbols $f_{A,GC}$ and $f_{A,LC}$ in Eq. (4-6); the prefix *GC* is for general corrosion and *LC*, for localized corrosion]. Section 4.2.2 describes the computation of the combined breach area.

Waste Package Counting

As previously stated, only one of the three alternative failure events can be executed in a simulation. In addition, a simulation can include waste package failure due to corrosion. Section 4.2.2 includes a description of how the GoldSim source term elements compute the total number of failed waste packages by combining the failure fractions due to corrosion and the selected alternative failure mode. The fraction of waste packages failed output by the Alternative Failure Modes module is denoted with the symbol F_{AF} in Eq. (4-5).

4.6.3 Default Parameters

The default parameters for the Alternative Failure Modes model component were arbitrarily chosen to cover a broad range of values. As such, no values have been documented in Appendix A or the SOAR database.

4.6.4 Flexibility

With appropriate selection or modification of input parameters, such as event recurrence rate, waste package damaged fraction, and breach area fraction, the Alternative Failure Modes component is intended to represent a variety of approximations of alternative waste package failure mechanisms.

The Alternative Failure Modes component of the user interface dashboard allows users additional flexibility to evaluate alternative model concepts. Specifically, the dashboard provides users with the options to

- Select and activate one of the additional waste package failure abstractions described in this section. (Specific inputs are discussed in Section 4.6.2.)

- Specify the damage area fraction for the failed waste packages

5 MODEL CONFIDENCE

This section discusses activities aimed at enhancing confidence in the models implemented in Scoping of Options and Analyzing Risk (SOAR). Activities conducted on SOAR Version 1.0 to build confidence in the model components remain valid for the updated Version 2.0. A formal verification report was published in 2012, documenting various tests on the SOAR code based on the activities described in this section (Janetzke et al., 2012). A code regression test was conducted between SOAR Versions 1.0 and 1.1 to confirm that updates included in Version 1.1 did not introduce unintended differences and errors in the functioning of SOAR. Results from this test are provided in Appendix C of this User Guide. The update to Version 2.0 addressed an error in the computation of the combined breach area fraction. Radionuclide release rates increased slightly due to this change. A regression test was also implemented to compare outputs of Version 2.5 to Version 2.0 outputs. By disabling the alternative path in the Near Field component, setting the boundary condition at the Near Field terminus to zero concentration, and disabling the three-timestep moving average in the Alternative Failure Modes dashboard, the results of SOAR Version 2.0 are approximately the same as those output by Version 2.5. Results from Version 2.5 and 2.0 differ because Version 2.5 addressed bugs (e.g., missing dispersion coefficients associated with the uranium decay series introduced in Version 1.1) and implemented different Near Field flows, which slightly changed results.

The model review and testing conducted to gain model confidence are summarized in the following bullets.

- All GoldSim model elements (e.g., data elements, mixing cells, pipe pathways, selectors, results elements) were visually inspected to ensure correct computations and algorithms were implemented, correct units were used, and inputs and outputs connected to the correct elements. For most model elements, text descriptions were added to help users understand the purpose of the element.
- Individual realizations were run using high and low input parameter values, and results were inspected to ensure intermediate outputs and system-level response were reasonable. For example, the model was run using the highest and lowest waste form degradation rate and results compared against the expectation that higher waste form degradation rates resulted in proportionally higher release.
- Different combinations of waste form, waste package material, and geochemical environment were run, and intermediate-level and system-level outputs were evaluated to verify that the model selected the correct inputs and computational algorithms appropriate to the model settings.
- The initial inventory of radionuclides was varied from very small to very large values to check a proportional output response.
- In addition to these initial testing efforts, developers at the U.S. Nuclear Regulatory Commission (NRC) and the Center for Nuclear Waste Regulatory Analyses (CNWRA®) performed a more detailed verification effort. The effort included development of a number of test plans, test reports, and a status spreadsheet and focused on testing all of the major model components.

The SOAR code was developed with the GoldSim language, which is an icon-based, high-level programming language. As such, it does not lend itself to traditional verification techniques

associated with sequential languages (e.g., FORTRAN, C++). However, GoldSim automatically performs many of the checks required for a sequential language. For example, GoldSim automatically checks for proper parameter types, consistent units of physical quantities, and meaningful syntax, and establishes a proper connection between functional elements. Given the automatic availability of these features, a number of verification activities focused on performing visual inspections of equations in the GoldSim elements, determining their logical relationship to other programming elements, and analyzing results. In general, performed tests relied on qualitative comparison of results with respect to expected values.

Different analysts developed the multidiscipline models, or model components, in SOAR. When each team member is able to work on any of the model components, there is an opportunity to check the work of other team members. Many self-checks of this nature were performed during the development of the code, including visual inspection of equations and review of the logical structure of each model component. A first level of confidence in the code was attained during development using this self-checking technique. Also, the availability of intermediate values and outputs enabled the inspection of the output response of each component to changes in input values.

A model that represents a physical process, with the associated uncertainties, requires the ability to vary the value of model parameters to represent ranges of possible conditions. Flexible parameter values are also required to investigate relevant scenarios that may differ from base models. Parameters are also used to implement specific features of the model or otherwise control the operation of the model during execution. In general, modification of input parameters in a model component of SOAR does not affect the functionality of another independent model component. Therefore, in general, tests on a particular model component were not repeated when input parameters for other model components changed. Numerous preliminary input parameter values were used in development testing. Documented selection of input parameter values are supplied with the different releases of the SOAR code.

During the code development process, repeated tests were commonly executed by inputting many different values for the relevant parameters to check the behavior of the component being constructed. This process frequently used the dashboards to enter the new values, with the intention to test the dashboard interface, as well as the corresponding model component. In this way the mechanics of the parameter entry dialog and the propagation of the parameter value to the model components were evaluated. The dashboard interface also enabled the convenient testing of parameter minimum and maximum value limits. During the development of the code, no formal documentation was prepared to establish agreement with external calculations; however, the output was continually checked to ensure self-consistency. Qualitative testing was also performed on input values and mode selectors available in the dashboards.

The SOAR model has the ability to consider up to four different waste form types. While the model components for each waste form type share similarities, separate independent tests were performed for each type. Integrated tests were also performed to test the capability of the model to handle cases with simultaneous presence of multiple waste forms. These kinds of tests were performed during the development of the Waste Form model component and during formal testing phases.

Once the model was considered to be relatively mature, formal verification tests were implemented. These formal verification tests were mostly high-level tests that focused on one specific model component at a time. Each test was documented in a test report summary. These formal tests exercised the operation of model component dashboards, input parameter

values, and switches. These tests included the qualitative analysis of intermediate output values by the particular model component. By studying the qualitative trends of outputs, or changes in outputs in response to changes in inputs, a conclusion was attained on whether an aspect of a model was appropriately implemented. The SOAR model was revised when necessary to address issues identified during the formal testing phase.

Formal tests were organized into six groups:

- Waste Form
- Waste Package
- Near Field
- Far Field
- Dashboard
- Disruptive Events¹

Each group tested one or more aspects of the target component. To isolate the aspect/parameter for a test, it was frequently necessary to configure other parameters or switches in a way that would disable parts of the model that could potentially impose conditions that would influence the results more than the aspect being tested. The testing of a particular aspect was, in general, compared to a reference run and to several runs with different inputs than the reference run.

Documentation for the verification effort was maintained as Microsoft Word and Excel® files on a drive shared by NRC and CNWRA developers. The documentation consisted of test plans, test reports, and a status spreadsheet. The test plan identified the test objective, specified the criteria for a successful test, and was generated prior to each test. The results of the test were documented in a test report summary that displayed the data in text or chart form as output by SOAR, as well as the status of the test.

Exhaustive testing of modeling software can be time consuming and difficult to design. The design of the tests performed to verify the SOAR model balanced time available by testers with the level of confidence desired in the code performance (taking into account that SOAR is intended as a generic tool for scoping computations). This resulted in the execution of a limited number of tests. Further tests for internal consistency could be aimed at database value propagation, convergence of statistical results as a function of increasing number of realizations, and dependence of results on timesteps. Quantitative tests can be defined; for example, the SOAR model could be compared to external codes that perform a subset of similar calculations. This type of test is time consuming to implement because inputs must be identical for results to match, the model or code used as comparison must be thoroughly understood, and SOAR and the comparison code must be adjusted to yield comparable outputs. Although difficult to implement, this type of test is feasible, and results of few international performance assessments are available to be used as benchmarking.

¹The Disruptive Events component was renamed Alternative Failure Modes in SOAR Version 1.1.

6 REFERENCES

Ahn, T.M. "Compendium of HLW Solidification Process." ML033450471. Washington, DC: U.S. Nuclear Regulatory Commission. 2003.

Bechtel SAIC Company, LLC. "Defense HLW Glass Degradation Model." ANL-EBS-MD-000016. Rev. 02. ACN 001, ERD 001, ERD, 002. Las Vegas, Nevada: Bechtel SAIC Company, LLC. 2004.

DOE. "Total System Performance Assessment Model/Analysis for the License Application." MDL-WIS-PA-000005. Rev. 00. Washington, DC: U.S. Department of Energy. 2008.

Ferry, C., C. Poinssot, V. Broudic, C. Cappelaere, L. Desgranges, P. Garcia, C. Jégou, P. Lovera, P. Marimbeau, J.P. Piron, A. Poulesquen, D. Roudil, J.M. Gras, and P. Bouffioux. "Synthesis on the Spent Fuel Long Term Evolution." CEA-R-6084. Saclay, France: Commissariat A L'énergie Atomique. 2005.

GoldSim Technology Group, LLC. "GoldSim Probabilistic Simulation Environment User's Guide." Vols. 1 and 2. Issaquah, Washington: GoldSim Technology Group, LLC. 2016a.

———. "GoldSim Contaminant Transport Module." Issaquah, Washington: GoldSim Technology Group, LLC. 2016b.

He, X., T. Ahn, and J. McMurry. "Copper Corrosion in Simulated Granitic Groundwater." Proceedings of the 2015 International High-Level Radioactive Waste Management Conference (IHLRWM). Charleston, South Carolina, April 12–16, 2015. La Grange Park, Illinois: American Nuclear Society. 2015.

International Commission on Radiological Protection. "Age-Dependent Doses to Members of the Public From Intake of Radionuclides: Part 5, Compilation of Ingestion and Inhalation Dose Coefficients." Publication 72. Tarrytown, New York: Elsevier Science, Inc. 1996.

Jain, V., G. Cragolino, and L. Howard. "A Review Report on High Burnup Spent Nuclear Fuel-Disposal Issues." ML043020321. San Antonio, Texas: Center for Nuclear Waste Regulatory Analyses. 2004.

Janetzke, R., C. Markley, O. Pensado, K. Compton, G. Adams, R. Nes, and S. Mohanty. "SOAR Model Verification Report." ML12052A022. San Antonio, Texas: Center for Nuclear Waste Regulatory Analyses. 2012.

JNC. "H12: Project to Establish the Scientific and Technical Basis for HLW Disposal in Japan. Supporting Report 3 – Safety Assessment of the Geological Disposal System." Tokai-Mura, Japan: Japan Nuclear Cycle Development Institute (JNC). 2000.

Leslie, B., C. Grossman, and J. Durham. "Total-System Performance Assessment (TPA) Version 5.1 Module Description and User Guide." ML072710060. San Antonio, Texas: Center for Nuclear Waste Regulatory Analyses. 2007.

Marivoet, J., X. Sillen, D. Mallants, and P. De Preter. "Performance Assessment of Geological Disposal of High-Level Radioactive Waste in a Plastic Clay Formation." Scientific Basis for Nuclear Waste Management XXIV. B.P. McGrail and G.A. Cragolino, eds. Materials Research

Society Symposium Proceedings. Vol. 713. Paper No. J.J4-4. Warrendale, Pennsylvania: Materials Research Society. 2001.

Markley, C., O. Pensado, J.-P. Gwo, J. Winterle, T. Ahn, R. Benke, T. Cao, H. Gonzalez, A. Gray, X. He, R. Janetzke, H. Jung, G. Oberson, P. Shukla, T. Sippel, S. Stothoff, and L. Tipton. "SOAR: A Model for Scoping of Options and Analyzing Risk: Version 1.0, User Guide." San Antonio, Texas: Center for Nuclear Waste Regulatory Analyses. August 2011.

NEA. "International Features, Events, and Processes Database, Version 2.1." Paris, France: Organisation for Economic Co-operation and Development, Nuclear Energy Agency. 2006.

NEA. "Clay Club Catalogue of Characteristics of Argillaceous Rocks." Radioactive Waste Management ISBN 92-64-01067, NEA No. 4436, OECD 2005. Paris, France: Nuclear Energy Agency. 2005.

Nirex Limited United Kingdom. "Generic Repository Studies: Generic Postclosure Performance Assessment." Report No. N/080. Oxfordshire, United Kingdom: Nirex Limited United Kingdom. July 2003.

NRC. NUREG-1914, "Dissolution Kinetics of Commercial Spent Nuclear Fuels in the Potential Yucca Mountain Repository Environment." ML083120074. Washington, DC: U.S. Nuclear Regulatory Commission. 2008.

Reeve, K.D., D.M. Levins, B.W. Seatonberry, R.K. Ryan, K.P. Hart, and G.T. Stevens. "Fabrication and Leach Testing of SYNROC Containing Actinides and Fission Products." Materials Research Society Symposium Proceedings. Vol. 127. Warrendale, Pennsylvania: Materials Research Society. pp. 223-230. 1989.

Revie, R.W., ed. *Uhlig's Corrosion Handbook*. 2nd Edition. Pennington, New Jersey: John Wiley & Sons, Inc. 2000.

Shoesmith, D.W. "Fuel Corrosion Processes Under Waste Disposal Conditions." *Journal of Nuclear Materials*. Vol. 282. pp. 1-31. 2000.

SKB. "Data Report for the Safety Assessment SR-Can." Technical Report TR-06-25. S. Kärnbränslehantering, ed. Stockholm, Sweden: Swedish Nuclear Fuel and Waste Management Company. 2006.

SKB. "Compilation of Radionuclide Sorption Coefficients for Performance Assessment." R-97-13. S. Kärnbränslehantering, ed. Stockholm Sweden: Swedish Nuclear Fuel and Waste Management Co. September 1997.

Sunder, S. and D.W. Shoesmith. "Chemistry of UO₂ Fuel Dissolution in Relation to the Disposal of Used Nuclear Fuel." AECL-10395. Pinawa, Canada: Atomic Energy of Canada Limited. 1991.

U.S. Department of Agriculture. "2008 Farm and Ranch Irrigation Survey, Vol. 3, Special Studies, Part 1, 2007 Census of Agriculture." National Agricultural Statistics Service. 2010. <http://www.agcensus.usda.gov/Publications/2007/Online_Highlights/Farm_and_Ranch_Irrigation_Survey/fris08.pdf> (30 April 2010).

U.S. Environmental Protection Agency. "Estimated Per Capita Water Ingestion and Body Weight in the United States—An Update." EPA-822-R-00-001. Washington, DC: U.S. Environmental Protection Agency. 2004.

Van Iseghem, P. *Geological Disposal of Radioactive Waste—The Challenge of Assessing the Long-Term Safety*. Mol, Belgium: SCK.CEN. 2007.

Vance, R., K.P. Hart, R.A. Day, M.L. Carter, and M. Hambley. "SYNROC Derivatives for the Hanford Waste Remediation Task." *Materials Research Society Symposium Proceedings*. Vol. 465. Warrendale, Pennsylvania: Materials Research Society. pp. 341–349. 1997.

Wang, Y. "Adaptive Waste Forms: The Concept and Its Implications." Presentation at Integrated Radioactive Waste Management in Future Fuel Cycles, Charleston, South Carolina, November 8–12, 2009. New York City, New York: Engineering Conferences International. 2009.

Wilson, C.N. and W.J. Gray. "Measurement of Soluble Nuclide Dissolution Rates From Spent Fuel." *Scientific Basis for Nuclear Waste Management XII*. V.M. Oversby and P.W. Brown, eds. *Materials Research Society Symposium Proceedings*. Vol. 176. Warrendale, Pennsylvania: Materials Research Society. pp. 489–498. 1990.

APPENDIX A
DEFAULT INPUT PARAMETERS

Table A-1. Default parameters for SOAR Waste Form model component			
Parameter Name	Description	Distribution Type and Values	Reference/Rationale
DegRate_HLW_Ceramic	High-Level Waste (HLW) Ceramic Waste Form Degradation Rate (yr ⁻¹)	Log-uniform 1.50 × 10 ⁻⁸ , 2 × 10 ⁻⁶	BSC (2004a), Reeve et al. (1989), Vance et al. (1997), Wang (2009)
DegRate_HLW_Glass	HLW Glass Waste Form Degradation Rate (yr ⁻¹)	Log-uniform 1.5 × 10 ⁻⁶ , 2 × 10 ⁻⁴	BSC (2004a), Iseghem (2007)
DegRate_sMOX_Combined	Spent Mixed Oxide Fuel (sMOX) Waste Form Degradation Rate, Combined Oxic/Anoxic (yr ⁻¹)	Log-uniform 1 × 10 ⁻⁶ , 1 × 10 ⁻³	Shukla et al. (2015), Jung et al. (2011), Carbol et al. (2005)
DegRate_sMOX_Oxic	sMOX Waste Form Degradation Rate, Oxidic Medium (yr ⁻¹)	Log-uniform 1 × 10 ⁻⁶ , 1 × 10 ⁻³	Shukla et al. (2015), Jung et al. (2011), Carbol et al. (2005)
DegRate_sMOX_Anoxic	sMOX Waste Form Degradation Rate, Anoxic Medium (yr ⁻¹)	Log-uniform 1 × 10 ⁻⁷ , 2 × 10 ⁻⁵	Ebert et al. (2002), Wang (2009), Poinssot et al. (2005), Grambow et al. (2000), Carbol et al. (2005). Fractional releases as low as 10 ⁻⁸ 1/yr have been reported, but with very limited verification. A low bound 10 ⁻⁷ 1/yr was selected instead.
DegRate_SNF_Combined	Spent Nuclear Fuel (SNF) Waste Form Degradation Rate, Combined Oxidic/Anoxic (yr ⁻¹)	Log-uniform 1 × 10 ⁻⁶ , 1 × 10 ⁻³	Shukla et al. (2015), Jung et al. (2011)
DegRate_SNF_Oxic	SNF Waste Form Degradation Rate, Oxidic Medium (yr ⁻¹)	Log-uniform 1 × 10 ⁻⁶ , 1 × 10 ⁻³	Shukla et al. (2015), Jung et al. (2011)
DegRate_SNF_Anoxic	SNF Waste Form Degradation Rate, Anoxic Medium (yr ⁻¹)	Log-uniform 1 × 10 ⁻⁸ , 2 × 10 ⁻⁵	Leslie et al. (2007), Ahn and Mohanty (2008), Shoesmith (2000), Shukla et al. (2015), Poinssot et al. (2005), Grambow et al. (2000)

Parameter Name	Description	Distribution Type and Values	Reference/Rationale
HLWc_Inventory	HLW Ceramic Radionuclide Inventory (g) [C-14, Cs-135, I-129, Np-237, Pu-238, Pu-239, Pu-240, Pu-242, Se-79, Tc-99, U-232, U-233, U-234, U-235, U-236, U-238, Th-230, Ra-226, Rn-222, Pb-210]	Constant-vector [0, 7.65×10^2 , 1.02×10^2 , 1.05×10^2 , 1.69, 1.30×10^4 , 3.04×10^2 , 5.84, 0, 0, 8.15×10^{-6} , 1.46×10^{-3} , 3.06×10^1 , 2.73×10^3 , 6.51×10^1 , 1.46×10^4 , 0, 0, 0, 0]	SNL (2007), Tipton (2010). The inventories for Pu-241 and Am-241 were added to the initial inventory of Np-237 to account for contributions from relatively short-lived radionuclides.
HLWg_Inventory	HLW Glass Radionuclide Inventory (g) [C-14, Cs-135, I-129, Np-237, Pu-238, Pu-239, Pu-240, Pu-242, Se-79, Tc-99, U-232, U-233, U-234, U-235, U-236, U-238, Th-230, Ra-226, Rn-222, Pb-210]	Constant-vector [2.91×10^{-1} , 9.47×10^2 , 9.36×10^1 , 5.06×10^2 , 5.31×10^1 , 3.43×10^2 , 3.86×10^1 , 5.44, 1.45×10^2 , 1.36×10^3 , 1.47×10^{-3} , 9.39, 1.79×10^1 , 3.07×10^2 , 5.69×10^1 , 1.41×10^5 , 0, 0, 0, 0]	(DOE, 2009), Tipton (2010). The representative inventory for HLW Glass is derived based upon values taken from DOE (2009). Because there are uncertainties about future inventories for glass waste, a representative bounding glass was created based on DOE (2009, Table 1.5.1-21, pp. 1.5.1-167 through 1.5.1-171). The representative glass waste form for the current approach was derived by selecting the maximum radionuclide inventories from the four glass waste forms (Hanford, Savannah River Site, West Valley, and Idaho) presented in DOE (2009, Table 1.5.1-21). Additionally, the inventories for Pu-241 and Am-241 were added to the initial inventory of Np-237 to account for contributions from relatively short-lived radionuclides.

Table A-1. Default parameters for SOAR Waste Form model component			
Parameter Name	Description	Distribution Type and Values	Reference/Rationale
sMOX_Inventory	sMOX Radionuclide Inventory (g) [C-14, Cs-135, I-129, Np-237, Pu-238, Pu-239, Pu-240, Pu-242, Se-79, Tc-99, U-232, U-233, U-234, U-235, U-236, U-238, Th-230, Ra-226, Rn-222, Pb-210]	Constant-vector [2.58, 7.17×10^3 , 3.09×10^3 , 4.64×10^4 , 1.5×10^3 , 1.03×10^5 , 7.26×10^4 , 1.84×10^4 , 5.42×10^1 , 9.98×10^3 , 1.01×10^{-3} , 2.33×10^{-3} , 9.13×10^1 , 5.62×10^3 , 2.23×10^3 , 8.19×10^6 , 0, 0, 0, 0]	SNL (2007), Tipton (2010). The inventories for Pu-241 and Am-241 were added to the initial inventory of Np-237 to account for contributions from relatively short-lived radionuclides.
SNF_Inventory	SNF Radionuclide Inventory (g) [C-14, Cs-135, I-129, Np-237, Pu-238, Pu-239, Pu-240, Pu-242, Se-79, Tc-99, U-232, U-233, U-234, U-235, U-236, U-238, Th-230, Ra-226, Rn-222, Pb-210]	Constant-vector [1.35, 4.36×10^3 , 1.73×10^3 , 1.54×10^4 , 1.52×10^3 , 4.32×10^4 , 2.05×10^4 , 5.28×10^3 , 4.19×10^1 , 7.55×10^3 , 1.02×10^{-2} , 5.76×10^{-2} , 1.75×10^3 , 6.26×10^4 , 3.84×10^4 , 7.82×10^6 , 0, 0, 0, 0]	DOE (2009), Tipton (2010). Inventories for Pu-241 and Am-241 were added to the initial inventory of Np-237 to account for contributions from relatively short-lived radionuclides.
UnboundFraction_sMOX_C14	C-14 Unbound Fraction for sMOX (Instant Release Fraction from gap/grain inventory)	Constant 0.1	Jain et al. (2004), Tipton (2010)
UnboundFraction_sMOX_Cs135	Cs-135 Unbound Fraction for sMOX (Instant Release Fraction from gap/grain inventory)	Triangular 0.0088, 0.025, 0.058	Leslie et al. (2007), Tipton (2010)

Parameter Name	Description	Distribution Type and Values	Reference/Rationale
UnboundFraction_sMOX_I129	I-129 Unbound Fraction for sMOX (Instant Release Fraction from gap/grain inventory)	Triangular 0.0054, 0.11, 0.32	Leslie et al. (2007), Tipton (2010)
UnboundFraction_sMOX_Se79	Se-79 Unbound Fraction for sMOX (Instant Release Fraction from gap/grain inventory)	Triangular 0.0088, 0.025, 0.058	Leslie et al. (2007), Tipton (2010)
UnboundFraction_sMOX_Tc99	Tc-99 Unbound Fraction for MOX (Instant Release Fraction from gap/grain inventory)	Triangular 0.0005, 0.0013, 0.0028	Leslie et al. (2007), Tipton (2010)
UnboundFraction_SNF_C14	C-14 Unbound fraction for SNF (Instant Release Fraction from gap/grain inventory)	Constant 0.1	Jain et al. (2004), Tipton (2010)
UnboundFraction_SNF_Cs135	Cs-135 Unbound Fraction for SNF (Instant Release Fraction from gap/grain inventory)	Triangular 0.0088, 0.025, 0.058	Leslie et al. (2007), Tipton (2010)
UnboundFraction_SNF_I129	I-129 Unbound Fraction for SNF (Instant Release Fraction from gap/grain inventory)	Triangular 0.0054, 0.11, 0.32	Leslie et al. (2007), Tipton (2010)
UnboundFraction_SNF_Se79	Se-79 Unbound Fraction for SNF (Instant Release Fraction from gap/grain inventory)	Triangular 0.0088, 0.025, 0.058	Leslie et al. (2007), Tipton (2010)
UnboundFraction_SNF_Tc99	Tc-99 Unbound Fraction for SNF (Instant Release Fraction from gap/grain inventory)	Triangular 0.0005, 0.0013, 0.0028	Leslie et al. (2007), Tipton (2010)

Parameter Name	Description	Distribution Type and Values	Reference/Rationale
CS_GC_Anox	Carbon steel, corrosion rate, anoxic medium ($\mu\text{m}/\text{yr}$)	log-normal Median = 1 $\mu\text{m}/\text{yr}$ Geometric St. Dev. = 2.69	Pitting corrosion is not obvious in anoxic conditions. Thus, a pitting enhancement factor of 1 was considered for the general corrosion rates for anoxic conditions. The low and high bound corrosion rates are considered to be 0.1 and 10 $\mu\text{m}/\text{yr}$ for anoxic conditions (Jung et al., 2011; Bennett and Gens, 2008; Johnson and King, 2008; Féron et al., 2008; Ahn and Soo, 1995; Ahn and Leslie, 1998; Taniguchi et al., 2004; Foct et al., 2004; Kursten et al., 2004a,b; Foct and Gras, 2003). Corrosion rates were assumed to follow a log-normal distribution, and the range [0.1 to 10 $\mu\text{m}/\text{yr}$] was considered to be a 98% confidence interval (i.e., 0.1 and 10 $\mu\text{m}/\text{yr}$ were assumed to be the 0.01 and 0.99 quantiles, respectively). The median of the log-normal distribution is 1 $\mu\text{m}/\text{yr}$; and the geometric standard deviation is 2.69.
CS_GC_Ox	Carbon steel, corrosion rate, oxic medium ($\mu\text{m}/\text{yr}$)	Uniform 10, 100	Corrosion rates in oxic environments are higher than in anoxic environments, in the range of 10 to 100 $\mu\text{m}/\text{yr}$ (Jung et al., 2011; Bennett and Gens, 2008; Johnson and King, 2008; Féron et al., 2008; Ahn and Soo, 1995; Ahn and Leslie, 1998; Taniguchi et al., 2004; Foct et al., 2004; Kursten et al., 2004a,b; Foct and Gras, 2003). The literature reports pitting enhancement factors of 1–3. A pitting enhancement factor of 1.5 was considered to define the general corrosion rates for oxic conditions. The estimated bounds for the corrosion rate, 10 and 100 $\mu\text{m}/\text{yr}$, include pitting effects.

Parameter Name	Description	Distribution Type and Values	Reference/Rationale
Cu_GC_Anox	Copper, corrosion rate, anoxic medium. ($\mu\text{m}/\text{yr}$)	Uniform 0.004, 0.02	<p>Wersin et al. (1994) predicted a corrosion rate lower bound of $0.0001 \mu\text{m}/\text{yr}$ considering a pitting enhancement factor of 5 based on thermodynamic modeling. SKB (2010a) concluded that the corrosion depth is less than $100 \mu\text{m}$ over a million year period considering several corrosion processes. The Canadian Nuclear Waste Management Organization estimated a corrosion depth of 1.27 mm over a million year period (Scully and Edwards, 2013). However, there is no direct measurement of the lowest corrosion rate reported in the literature to confirm the thermodynamic calculation. Uncertainty remains on the effect of chloride, prevailing sulfide concentration, and the effect of bacteria. Because of the existing uncertainties, a slightly higher corrosion rate than found in the literature was chosen for the low bound ($0.004 \mu\text{m}/\text{yr}$).</p> <p>Wersin et al. (1994) reported a high corrosion rate of $0.02 \mu\text{m}/\text{yr}$ based on thermodynamic calculation considering a pitting enhancement factor of 5. The enhancement factor depends on the sulfide concentration and the effect of bacteria, which are uncertain.</p>
Cu_GC_Ox	Copper, corrosion rate, oxic medium ($\mu\text{m}/\text{yr}$)	Log-uniform 0.04, 7	Wersin et al. (1994) determined a range of corrosion rates between 0.04 and $7 \mu\text{m}/\text{yr}$, considering pitting enhancement factors between 5 and 100. The enhancement factor depends on the prevailing sulfide concentration and the effect of bacteria, which are uncertain.

Parameter Name	Description	Distribution Type and Values	Reference/Rationale
HS_Concentration	Concentration of hydrogen sulfide (HS ⁻) in groundwater (mol/L)	Log-uniform 10 ⁻⁵ , 10 ⁻³	<p>Studies by SKB indicate low concentrations of sulfides in groundwater (approximately 10⁻⁵ M), arising mainly from decomposition of pyrite, as well as reducing bacteria and Fe(II) catalysis of sulfate reduction (Scully and Hicks, 2012).</p> <p>Swedish and Finnish studies suggest groundwater in repository settings contains sulfide concentrations in the range of (0 to 3) × 10⁻³ mol/L at repository closure to (0 to 0.3) × 10⁻⁴ mol/L 10,000 years into the future. For Swedish repository conditions, sulfide concentrations are expected to be in the range 10⁻⁷ to 10⁻⁴ M (King et al., 2010; Rosborg and Werme, 2008).</p> <p>In the Canadian program, the concentration of hydrogen sulfide in the repository setting has been reported to be approximately in the range of 5 × 10⁻⁵ to 10⁻³ M (Scully and Edwards, 2013).</p> <p>A distribution ranging from 10⁻⁵ to 10⁻³ M is recommended based on the Finnish, Swedish, and Canadian studies.</p>
LC_FailureTime_Period_I	Failure time by localized corrosion (LC) for Period I (assumed that all LC-affected waste packages fail at the same time) (yr)	Log-uniform 30, 280	<p>Period I is an early period during which the waste package may experience localized corrosion. In a repository located in reducing media, a transient oxidizing period—during which the chance for localized corrosion is higher—could develop before the return to long-term reducing conditions. Taniguchi et al. (2004) reported that for a hypothetical geological repository for high-level radioactive waste in Japan, the period until environmental conditions return from oxidizing to reducing is expected to be less than 100 years; possibly around 30 years. However, Wersin et al. (1994) also reported a maximum period of 280 years for oxidizing conditions. In the SOAR model, it is assumed that localized corrosion could initiate during the oxidizing period. This parameter defines the time at which the affected waste packages fail by localized corrosion. Based on the work by Wersin et al. (1994), failure by localized corrosion is assumed to occur at a time between 30 and 280 years.</p>

Parameter Name	Description	Distribution Type and Values	Reference/Rationale
LC_FailureTime_Period_II	Failure time by localized corrosion (LC) for Period II (assumed that all LC-affected waste packages fail at the same time) (yr)	Log-uniform 280, 10 ⁵	Period II is a late period during which the waste package may experience localized corrosion. For a repository located in reducing media, this parameter defines the time at which the affected waste packages fail from localized corrosion after the return of the repository to reducing conditions.
LC_FractionAreaBreached	Fraction of waste package area breached by localized corrosion (unitless)	Log-triangular 0.001, 0.1216, 0.2	According to literature information on stainless steel pitting corrosion in chloride solution, the maximum breach area for stainless steel waste packages would not exceed 5 percent of the total area. To estimate the rate of metal dissolution reactions on anodic sites, it is conservatively assumed that the cathodic area is at least five times that of anodic sites. This is because both oxygen and water reduction reactions occur at much slower rates compared to metal dissolution reactions at anodic sites. An upper bound of 20 percent damage is considered feasible. A log-triangular distribution is considered, ranging from 0.001 to 0.2, with mid-point adjusted for the mean to be exactly 0.05.
SS_GC_Anox	Stainless steel, corrosion rate, anoxic medium ($\mu\text{m}/\text{yr}$)	Log-uniform 0.003, 0.1	<p>A low bound for the corrosion rate equal to 0.003 $\mu\text{m}/\text{yr}$ was estimated based on Kursten et al. (2004b, Table 4-34). This low-bound rate is near the resolution limit of the weight loss analysis method used to determine corrosion rates.</p> <p>The high bound of 0.1 $\mu\text{m}/\text{yr}$ was estimated based on corrosion studies performed in cementitious backfill material. Kursten et al. (2004b) concluded that the long-term anoxic corrosion rate of stainless steel at all repository temperatures are less than 0.01 $\mu\text{m}/\text{yr}$. Based on <i>in-situ</i> corrosion studies relevant to the Belgian disposal concept in clay, Kursten et al. (2004b) determined that the maximum corrosion rate was 0.15 $\mu\text{m}/\text{yr}$ at 170 °C [338 °F], with most of the corrosion rates less than 0.1 $\mu\text{m}/\text{yr}$. Based on these limited data for anoxic conditions, it is reasonable to assume that the maximum corrosion rate is 0.1 $\mu\text{m}/\text{yr}$. Selecting a log-normal distribution for the stainless steel corrosion rate skewed toward the lower end is reasonable.</p>

Parameter Name	Description	Distribution Type and Values	Reference/Rationale
SS_GC_Ox	Stainless steel, corrosion rate, oxic medium ($\mu\text{m}/\text{yr}$)	Log-uniform 0.01, 3	<p>A low bound for the corrosion rate equal to $0.01 \mu\text{m}/\text{yr}$ was estimated based on work by Kursten et al. (2004b, Table 4-34). This low rate is near the resolution limit of the weight loss analysis method to determine corrosion rates.</p> <p>A high bound equal to $3 \mu\text{m}/\text{yr}$ was estimated based on corrosion studies performed in cementitious backfill material summarized in Kursten et al. (2004b, Table 4-54 and Figure 4-72). Tests were conducted at pH of 1.9–13 and temperatures of $30\text{--}80^\circ\text{C}$ [$86\text{--}176^\circ\text{F}$]. The corrosion rate increased with decreasing pH. At pH of 4 and 80°C [176°F], the corrosion rate was $2.6 \mu\text{m}/\text{yr}$. Based on other data from international geological repository programs, $3 \mu\text{m}/\text{yr}$ appears to be a reasonable bounding value under various environmental conditions. Most of the data are distributed at the lower end (McCright et al., 1987, Glass et al., 1984, BSC, 2004b).</p> <p>Selecting a distribution for the stainless steel corrosion rate skewed toward the lower end is reasonable.</p>
SS_Prob_LC_Period_I_Oxic	Fraction of stainless steel waste packages failed by localized corrosion during Period I in oxic environment (unitless)	Triangular 0.25, 0.45, 0.5	<p>Probability of localized corrosion, per waste package, during Period I (see parameter LC_FailureTime_Period_I for Period I definition) in a repository in oxidizing conditions. Stainless steel has a greater chance of exhibiting localized corrosion in an oxidizing repository. Based on the arguments for parameter SS_Prob_LC_Period_I_Anoxic, 50 percent probability for localized corrosion is a reasonable upper bound. A triangular distribution biased towards an upper end of 0.5 is assumed for this parameter.</p>

Table A-2. Default parameters for SOAR Waste Package model components			
Parameter Name	Description	Distribution Type and Values	Reference/Rationale
SS_Prob_LC_Period_I_Anoxic	Fraction of stainless steel waste packages failed by localized corrosion during Period I in anoxic environment (unitless)	Triangular 0, 0.125, 0.25	Probability of localized corrosion, per waste package, during Period I (see parameter LC_FailureTime_Period_I for Period I definition) for a repository in reducing conditions. Period I is the transient oxidizing period prior to stable reducing period, Period II. 50 percent probability for localized corrosion to occur is a reasonable estimate, based on water compositions and 1,000 ppm chloride concentration. The backfill diffusive barrier could limit the chloride concentration in contact with stainless steel, so a 50 percent probability for backfill to limit water contact is assumed. Estimated fraction = $(0.5 \times 0.5) = 0.25$. A symmetric triangular distribution is used to define the fraction of waste packages affected by localized corrosion, with an upper bound at 0.25.
SS_Prob_LC_Period_II_Oxic	Fraction of stainless steel waste packages failed by localized corrosion during Period II in oxic environment (unitless)	Constant 0	Probability of localized corrosion, per waste package, during Period II (see parameter LC_FailureTime_Period_II for Period II definition) for a repository in oxidizing conditions. It is assumed that all of the LC damage occurred during Period I; thus, this parameter is assigned a value of 0.
SS_Prob_LC_Period_II_Anoxic	Fraction of stainless steel waste packages failed by localized corrosion during Period II in anoxic environment (unitless)	Uniform 0.01, 0.1	Probability of localized corrosion, per waste package, during Period II (see parameter LC_FailureTime_Period_II for Period II definition) for a repository in reducing conditions. Localized corrosion for reducing environments is less likely, but the backfill may be less effective at protecting against localized corrosion. A uniform distribution with a 5 percent average probability was assumed.
Ti_GC_Anox	Titanium, corrosion rate, anoxic medium ($\mu\text{m}/\text{yr}$)	Log-uniform 0.008, 0.2	The general corrosion rates are based on literature review of titanium corrosion rates in possible repository conditions from various disposal programs. Germany proposed using Ti 99.8-Pd alloy (which is similar to Titanium Grade 7) as the container material in rock-salt. Corrosion rates in rock-salt brine were higher than those obtained from other media because of the more aggressive nature of the rock-salt brine. A range of corrosion rates estimated for the titanium drip shield for the proposed Yucca Mountain repository covers a wide range of environmental conditions and experimental uncertainty (SNL, 2008). Other data reported are very close to this range (Brossia et al., 2001; BSC, 2004b; Blackwood et al., 1988; Hua and Gordon, 2004; Schutz, 2005, 2003; Nakayama et al., 2008). Data in oxidizing and reducing conditions are similar.

Parameter Name	Description	Distribution Type and Values	Reference/Rationale
Ti_GC_Ox	Titanium, corrosion rate, oxic medium ($\mu\text{m}/\text{yr}$)	Log-uniform 0.008, 0.2	See rationale for Ti_GC_Anox.
WP_Thickness_CS	Carbon steel waste package thickness (cm)	Constant 10	Various repository programs have reported 3–25 cm [1.2–9.8 in] as the carbon steel container thickness. The rounded average value of 10 cm [3.9 in] is chosen.
WP_Thickness_Cu	Copper waste package thickness (cm)	Constant 2.5	Canada proposes 2.5 cm [1 in] and both Finland and Sweden propose 5 m [2 in], based on Kursten et al. (2004b, Table 1-1). The thinner value of 2.5 cm [1 in] was chosen as the container thickness.
WP_Thickness_SS	Stainless steel waste package thickness (cm)	Constant 5	Based on the inner container for the proposed Yucca Mountain repository, because data are not available from other repository programs.
WP_Thickness_Ti	Titanium waste package thickness (cm)	Constant 1	Based on data from repository programs. Canada proposes 6.35 mm [0.25 in]; Germany proposes 3–4 mm [0.12–0.16 in]; the proposed Yucca Mountain drip shield thickness is 15 mm [0.59 in]. 10 mm [0.39 in] is considered a reasonable value.
X_Prob_LC_Period_I	Fraction of waste packages failed by localized corrosion during Period I (X=Cu, CS, Ti)	Constant 0	Probability of localized corrosion, per waste package, during Period I (see parameter LC_FailureTime_Period_I for Period II definition) in a repository in oxidizing media. This probability parameter is used for all materials except stainless steel (the stainless steel probability is defined in separate parameters).
X_Prob_LC_Period_II	Fraction of waste packages failed by localized corrosion during Period II (X=Cu, CS, Ti)	Constant 0	Probability of localized corrosion, per waste package, during Period II (see parameter LC_FailureTime_Period_II for Period II definition) in a repository in reducing media. This probability parameter is used for all materials except stainless steel (the stainless steel probability is defined in separate parameters).

Table A-3. Default Parameters for SOAR Near Field Model Component			
Parameter Name	Description	Distribution Type & Values	Reference/Rationale
BF_Porosity	Initial porosity of the buffer unit (unitless)	Constant 0.44	SKB (2006, Table A-8). Treated as constant for this model because variability is small compared to uncertainty in K_d values.
BF_SpecificDensity	Buffer specific density (kg/m^3)	Constant 2000	SKB (2006, Table A-8). Treated as constant for this model because variability is small compared to uncertainty in K_d values.
BF_dispersivityFraction	Dispersivity fraction of a buffer unit after cracking (unitless)	Uniform 0.05, 0.15	Typical range of dispersivity is around 10 percent of the pathway length
BFtoFrac_dispersivity Fraction	Dispersivity fraction of transition region (unitless)	Uniform 0.1, 0.2	Typical range of dispersivity is around 10 percent of the pathway length.
Dc_C_BF	Diffusivity of C in buffer material (m^2/s)	Uniform 3×10^{-12} , 3×10^{-11}	SKB (2006, Table A-11). Uniform distribution selected to equally weight full range of uncertainty. Note that range of values for diffusivity is smaller than for positively charged species because carbonate species and organic acids are subject to anion exclusion.
Dc_C_Free	Diffusivity of C in free water (m^2/s)	Constant 1.2×10^{-9}	SKB (2006, Table A-40). Recommended diffusion coefficients in free solution are on the order of $10^{-9} \text{ m}^2/\text{s}$, consistent with diffusion coefficients of electrolytes and nonelectrolytes in Weast (1986) at 25 °C [77 °F].
Dc-Cs_BF	Diffusivity of Cs in buffer material (m^2/s)	Uniform 4.94×10^{-11} , 1.91×10^{-10}	SKB (2006, Table A-11). Uniform distribution selected to equally weight full range of uncertainty.
Dc-Cs_Free	Diffusivity of Cs in free water (m^2/s)	Constant 2.1×10^{-9}	SKB (2006, Table A-40). Recommended value for diffusivities in free solution. The recommended diffusion coefficients in free solution are on the order of $10^{-9} \text{ m}^2/\text{s}$, which is consistent with diffusion coefficients of electrolytes and nonelectrolytes in Weast (1986) at 25 °C [77 °F].
Dc_I_BF	Diffusivity of I in buffer material (m^2/s)	Uniform 3×10^{-12} , 3×10^{-11}	SKB (2006, Table A-11). Uniform distribution selected to equally weight full range of uncertainty. Note that range of values for iodide in buffer is smaller than for positively charged species because iodide is subject to anion exclusion.
Dc_I_Free	Diffusivity of I in free water (m^2/s)	Constant 8.3×10^{-10}	SKB (2006, Table A-40). Recommended value for diffusivities in free solution. The recommended diffusion coefficients in free solution are on the order of $10^{-9} \text{ m}^2/\text{s}$, which is consistent with diffusion coefficients of electrolytes and nonelectrolytes in Weast (1986) at 25 °C [77 °F].

Table A-3. Default Parameters for SOAR Near Field Model Component			
Parameter Name	Description	Distribution Type & Values	Reference/Rationale
Dc_Np_BF	Diffusivity of Np in buffer material (m ² /s)	Uniform 4.94 × 10 ⁻¹¹ , 1.91 × 10 ⁻¹⁰	SKB (2006, Table A-11). Uniform distribution selected to equally weight full range of uncertainty.
Dc_Np_Free	Diffusivity of Np in free water (m ² /s)	Constant 10 ⁻⁹	SKB (2006, Table A-40). Recommended value for diffusivities in free solution. The recommended diffusion coefficients in free solution are on the order of 10 ⁻⁹ m ² /s, which is consistent with diffusion coefficients of electrolytes and nonelectrolytes in Weast (1986) at 25 °C [77 °F].
Dc_Pu_BF	Diffusivity of Pu in buffer material (m ² /s)	Uniform 4.94 × 10 ⁻¹¹ , 1.91 × 10 ⁻¹⁰	SKB (2006, Table A-11). Uniform distribution selected to equally weight full range of uncertainty.
Dc_Pu_Free	Diffusivity of Pu in free water (m ² /s)	Constant 10 ⁻⁹	SKB (2006, Table A-40). Recommended value for diffusivities in free solution. The recommended diffusion coefficients in free solution are on the order of 10 ⁻⁹ m ² /s, which is consistent with diffusion coefficients of electrolytes and nonelectrolytes in Weast (1986) at 25 °C [77 °F].
Dc_Se_BF	Diffusivity of Se in buffer material (m ² /s)	Uniform 3 × 10 ⁻¹² , 3 × 10 ⁻¹¹	SKB (2006, Table A-11). Uniform distribution selected to equally weight full range of uncertainty.
Dc_Se_Free	Diffusivity of Se in free water (m ² /s)	Constant 2.1 × 10 ⁻⁹	SKB (2006, Table A-40). Recommended value for diffusivities in free solution. The recommended diffusion coefficients in free solution are on the order of 10 ⁻⁹ m ² /s, which is consistent with diffusion coefficients of electrolytes and nonelectrolytes in Weast (1986) at 25 °C [77 °F].
Dc_Tc_BF	Diffusivity of Tc in buffer material (m ² /s)	Uniform 4.94 × 10 ⁻¹¹ , 1.91 × 10 ⁻¹⁰	SKB (2006, Table A-11). Uniform distribution selected to equally weight full range of uncertainty.
Dc_Tc_Free	Diffusivity of Tc in free water (m ² /s)	Constant 10 ⁻⁹	SKB (2006, Table A-40). Recommended value for diffusivities in free solution. The recommended diffusion coefficients in free solution are on the order of 10 ⁻⁹ m ² /s, which is consistent with diffusion coefficients of electrolytes and nonelectrolytes in Weast (1986) at 25 °C [77 °F].
Dc_U_BF	Diffusivity of U in buffer material (m ² /s)	Uniform 4.94 × 10 ⁻¹¹ ,	SKB (2006, Table A-11). Uniform distribution selected to equally weight full range of uncertainty.

Table A-3. Default Parameters for SOAR Near Field Model Component			
Parameter Name	Description	Distribution Type & Values	Reference/Rationale
		1.91×10^{-10}	
Dc_U_Free	Diffusivity of U in free water (m ² /s)	Constant 10^{-9}	SKB (2006, Table A-40). Recommended value for diffusivities in free solution. The recommended diffusion coefficients in free solution are on the order of 10^{-9} m ² /s, which is consistent with diffusion coefficients of electrolytes and nonelectrolytes in Weast (1986) at 25 °C [77 °F].
Dc_Th_BF	Diffusivity of Th in buffer material (m ² /s)	Uniform 4.94×10^{-11} , 1.91×10^{-10}	SKB (2006, Table A-11). Uniform distribution selected to equally weight full range of uncertainty.
Dc_Th_Free	Diffusivity of Th in free water (m ² /s)	Constant 1.5×10^{-10}	SKB (2006, Table A-40). Recommended value for diffusivities in free solution. The recommended diffusion coefficients in free solution are on the order of 10^{-9} m ² /s, which are consistent with diffusion coefficients of electrolytes and nonelectrolytes in Weast (1986) at 25 °C [77 °F].
Dc_Ra_BF	Diffusivity of Ra in buffer material (m ² /s)	Uniform 4.94×10^{-11} , 1.91×10^{-10}	SKB (2006, Table A-11). Uniform distribution selected to equally weight full range of uncertainty.
Dc_Ra_Free	Diffusivity of Ra in free water (m ² /s)	Constant 8.9×10^{-10}	SKB (2006, Table A-40). Recommended value for diffusivities in free solution. The recommended diffusion coefficients in free solution are on the order of 10^{-9} m ² /s, which are consistent with diffusion coefficients of electrolytes and nonelectrolytes in Weast (1986) at 25 °C [77 °F].
Dc_Rn_BF	Diffusivity of Rn in buffer material (m ² /s)	Uniform 4.94×10^{-11} , 1.91×10^{-10}	SKB (2006, Table A-11). Uniform distribution selected to equally weight full range of uncertainty.
Dc_Rn_Free	Diffusivity of Rn in free water (m ² /s)	Constant 9.6×10^{-10}	Lide (2005). Value listed is for diffusion of radon gas at 15 °C, which is the estimated temperature at repository depth used by SKB in SR-Can (Duro et al., 2006).
Dc_Pb_BF	Diffusivity of Pb in buffer material (m ² /s)	Uniform 4.94×10^{-11} , 1.91×10^{-10}	SKB (2006, Table A-11). Uniform distribution selected to equally weight full range of uncertainty.

Parameter Name	Description	Distribution Type & Values	Reference/Rationale
Dc_Pb_Free	Diffusivity of Pb in free water (m ² /s)	Constant 3.6 × 10 ⁻¹⁰	Van Der Leer et al. (2002). The recommended diffusion coefficients in free solution are on the order of 10 ⁻⁹ m ² /s, which are consistent with diffusion coefficients of electrolytes and nonelectrolytes in Weast (1986) at 25 °C [77 °F].
f_DiffLengthToFrac ture	Fraction to compute the effective diffusive distance to the nearest fracture (unitless)	Uniform 0.1, 0.2	Stothoff (2010)
Kd_C_BF_Red	K _d of C in bentonite buffer, reducing conditions (m ³ /kg)	Constant 0	SKB (2006, Table A-12) gives zero value (nonsorbing) for carbon.
Kd_C_BF_Ox	K _d of C in bentonite buffer, oxidizing conditions (m ³ /kg)	Constant 0	SKB (2006, Table A-12) gives zero value (nonsorbing) for carbon.
Kd_Cs_BF_Red	K _d of Cs in bentonite buffer, reducing conditions (m ³ /kg)	Triangular 0.018, 0.11, 0.6	SKB (2006, Table A-12) provides a range of minimum to maximum recommended values for bentonite buffer.
Kd_Cs_BF_Ox	K _d of Cs in bentonite buffer, oxidizing conditions (m ³ /kg)	Triangular 0.018, 0.11, 0.6	SKB (2006, Table A-12) provides a range of minimum to maximum recommended values for bentonite buffer.
Kd_I_BF_Red	K _d of I in bentonite buffer, reducing conditions (m ³ /kg)	Constant 0	SKB (2006, Table A-12) gives zero value (nonsorbing) for iodine.
Kd_I_BF_Ox	K _d of I in bentonite buffer, oxidizing conditions (m ³ /kg)	Constant 0	SKB (2006, Table A-12) gives zero value (nonsorbing) for iodine.
Kd_Np_BF_Red	K _d of Np in bentonite buffer, reducing conditions (m ³ /kg)	Triangular 4, 63, 1113	SKB (2006, Table A-12) provides a range of minimum to maximum recommended values for bentonite buffer. For reducing conditions, Np(IV) is assumed.
Kd_Np_BF_Ox	K _d of Np in bentonite buffer, oxidizing conditions (m ³ /kg)	Triangular 0.004, 0.02, 0.2	SKB (2006, Table A-12) provides a range of minimum to maximum recommended values for bentonite buffer. For oxidizing conditions, Np(V) is assumed.
Kd_Pu_BF_Red	K _d of Pu in bentonite buffer, reducing conditions (m ³ /kg)	Triangular 4, 63, 1111	SKB (2006, Table A-12) provides a range of minimum to maximum recommended values for bentonite buffer. For reducing conditions, the range for Pu(IV) is specified here.

Table A-3. Default Parameters for SOAR Near Field Model Component			
Parameter Name	Description	Distribution Type & Values	Reference/Rationale
Kd_Pu_BF_Ox	K _d of Pu in bentonite buffer, oxidizing conditions (m ³ /kg)	Triangular 0.002, 0.02, 0.2	SKB (2006, Table A-12) provides ranges of minimum to maximum recommended values for bentonite buffer for Pu(V) and for Pu(VI). The ranges do not quite overlap, with Pu(V) values from 0.002 to 0.2 and Pu(VI) values from 0.3 to 28. The range and SKB "best estimate" for Pu(V) are specified in the triangular distribution used here.
Kd_Se_BF_Red	K _d of Se in bentonite buffer, reducing conditions (m ³ /kg)	Triangular 0.003, 0.04, 0.4	SKB (2006, Table A-12) provides a range of minimum to maximum recommended values for bentonite buffer. For reducing conditions, Se(IV) is assumed.
Kd_Se_BF_Ox	K _d of Se in bentonite buffer, oxidizing conditions (m ³ /kg)	Constant 0	SKB (2006, Table A-12) gives zero value (nonsorbing) for Se(VI).
Kd_Tc_BF_Red	K _d of Tc in bentonite buffer, reducing conditions (m ³ /kg)	Triangular 2.3, 63, 1764	SKB (2006, Table A-12) provides a range of minimum to maximum recommended values for bentonite buffer. For reducing conditions, Tc(IV) is assumed.
Kd_Tc_BF_Ox	K _d of Tc in bentonite buffer, oxidizing conditions (m ³ /kg)	Constant 0	SKB (2006, Table A-12) gives zero value (nonsorbing) for Tc(VII), which is assumed for oxidizing conditions.
Kd_U_BF_Red	K _d of U in bentonite buffer, reducing conditions (m ³ /kg)	Triangular 3.6, 63, 1113	SKB (2006, Table A-12) provides a range of minimum to maximum recommended values for bentonite buffer. For reducing conditions, range for U(IV) is assumed.
Kd_U_BF_Ox	K _d of U in bentonite buffer, oxidizing conditions (m ³ /kg)	Triangular 0.5, 3, 18	SKB (2006, Table A-12) provides range of minimum to maximum recommended values for bentonite buffer. For oxidizing conditions, range for U(VI) is assumed.
Kd_Th_BF_Red	K _d of Th in bentonite buffer, reducing conditions (m ³ /kg)	Triangular 6, 63, 700	SKB (2006, Table A-12) provides a range of minimum to maximum values for bentonite buffer. A triangular probability distribution was recommended by SKB (2006, Section 5.4).
Kd_Th_BF_Ox	K _d of Th in bentonite buffer, oxidizing conditions (m ³ /kg)	Triangular 6, 63, 700	SKB (2006, Table A-12) provides a range of minimum to maximum values for bentonite buffer. A triangular probability distribution was recommended by SKB (2006, Section 5.4).
Kd_Ra_BF_Red	K _d of Ra in bentonite buffer, reducing conditions (m ³ /kg)	Triangular 0.001, 0.005, 0.03	SKB (2006, Table A-12) provides a range of minimum to maximum values for bentonite buffer. A triangular probability distribution was recommended by SKB (2006, Section 5.4).

Table A-3. Default Parameters for SOAR Near Field Model Component			
Parameter Name	Description	Distribution Type & Values	Reference/Rationale
Kd_Ra_BF_Ox	K _d of Ra in bentonite buffer, oxidizing conditions (m ³ /kg)	Triangular 0.001, 0.005, 0.03	SKB (2006, Table A-12) provides a range of minimum to maximum values for bentonite buffer. A triangular probability distribution was recommended by SKB (2006, Section 5.4).
Kd_Rn_BF_Red	K _d of Rn in bentonite buffer, reducing conditions (m ³ /kg)	Constant 0	SKB (2006, Table A-12) gives a zero value (no sorption) for Rn.
Kd_Rn_BF_Ox	K _d of Rn in bentonite buffer, oxidizing conditions (m ³ /kg)	Constant 0	SKB (2006, Table A-12) gives a zero value (no sorption) for Rn.
Kd_Pb_BF_Red	K _d of Pb in bentonite buffer, reducing conditions (m ³ /kg)	Triangular 12, 74, 457	SKB (2006, Table A-12) provides a range of minimum to maximum values for bentonite buffer. A triangular probability distribution was recommended by SKB (2006, Section 5.4).
Kd_Pb_BF_Ox	K _d of Pb in bentonite buffer, oxidizing conditions (m ³ /kg)	Triangular 12, 74, 457	SKB (2006, Table A-12) provides a range of minimum to maximum values for bentonite buffer. A triangular probability distribution was recommended by SKB (2006, Section 5.4).
Solubility_C_Ox	C solubility in buffer, oxidizing conditions (mg/L)	Log-uniform 8, 8.50 × 10 ²	Duro et al. (2006, Table 8-1). Value for oxidizing conditions is based on the table column for groundwater at atmospheric conditions (pO ₂ = 0.2 atm), indicating a maximum dissolved C concentration of 7.1 × 10 ⁻³ mol/L with CaCO ₃ acting as the solubility-limiting solid phase. This converts to a value of 85 mg/L C. To consider uncertainty, the range given evaluates approximately one order of magnitude above and below this value.
Solubility_C_Red	C solubility in buffer, reducing conditions (mg/L)	Log-uniform 4.8, 4.80 × 10 ²	Duro et al. (2006, Table 8-1). Value for reducing conditions is based on the table column for bentonite porewater, indicating a maximum dissolved C concentration of 3.99 × 10 ⁻³ mol/L with CaCO ₃ acting as the solubility-limiting solid phase. This converts to a value of 48 mg/L C. To consider uncertainty, the range given evaluates approximately one order of magnitude above and below this value.
Solubility-Cs_Ox	Cs solubility in buffer, oxidizing conditions (mg/L)	Constant -1	Duro et al. (2006, Table 8-1) indicates there is no solubility limit for Cs. The entered value of -1 tells the GoldSim model that this is the case.

Table A-3. Default Parameters for SOAR Near Field Model Component			
Parameter Name	Description	Distribution Type & Values	Reference/Rationale
Solubility_Cs_Red	Cs solubility in buffer, reducing conditions (mg/L)	Constant -1	Duro et al. (2006, Table 8-1) indicates there is no solubility limit for Cs. The entered value of -1 tells the GoldSim model that this is the case.
Solubility_I_Ox	I solubility in buffer, oxidizing conditions (mg/L)	Constant -1	No reference was available for iodine solubility in oxidizing waters. Based on Duro et al. (2006), which indicates no solubility limit for Cs and Tc, it seems reasonable to assume the same for iodine. The entered value of -1 tells the GoldSim model that this is the case.
Solubility_I_Red	I solubility in buffer, reducing conditions (mg/L)	Constant -1	No reference available for iodine solubility. Basecase assumes no solubility limit. The entered value of -1 tells the GoldSim model that this is the case.
Solubility_Np_Ox	Np solubility in buffer, oxidizing conditions (mg/L)	Log-uniform 0.4, 40	Duro et al. (2006, Table 8-1). Value for oxidizing conditions is based on the table column for groundwater at atmospheric conditions ($pO_2 = 0.2$ atm), indicating a maximum dissolved Np concentration of 1.7×10^{-5} mol/L with Np_2O_5 acting as the solubility-limiting phase, which converts to 4 mg/L Np. To consider uncertainty, the range given evaluates approximately one order of magnitude above and below this value.
Solubility_Np_Red	Np solubility in buffer, reducing conditions (mg/L)	Log-uniform 2.6×10^{-5} , 2.6×10^{-3}	Duro et al. (2006, Table 8-1). Value for reducing conditions is based on the table column for bentonite porewater, indicating a maximum dissolved Np concentration of 1.1×10^{-9} mol/L with NpO_2 acting as the solubility-limiting solid phase, which converts to 2.6×10^{-4} mg/L Np. To consider uncertainty, the range given evaluates one order of magnitude above and below this value.
Solubility_Pu_Ox	Pu solubility in buffer, oxidizing conditions (mg/L)	Log-uniform 5.4, 540	Duro et al. (2006, Table 8-1). Value for oxidizing conditions is based on the table column for groundwater at atmospheric conditions ($pO_2 = 0.2$ atm), indicating a maximum dissolved Pu concentration of 2.2×10^{-4} mol/L with $Pu(OH)_4$ acting as the solubility-limiting solid phase. This converts to 54 mg/L Pu. To consider uncertainty, the range given evaluates one order of magnitude above and below this value.
Solubility_Pu_Red	Pu solubility in buffer, reducing conditions (mg/L)	Log-uniform 0.3, 30	Duro et al. (2006, Table 8-1). Value for reducing conditions is based on the table column for bentonite porewater, indicating a maximum dissolved Pu concentration of 1.3×10^{-5} mol/L with $PuOHCO_3$ acting as the solubility-limiting solid phase. This converts to about 3 mg/L

Table A-3. Default Parameters for SOAR Near Field Model Component			
Parameter Name	Description	Distribution Type & Values	Reference/Rationale
			Pu. To consider uncertainty, the range given evaluates approximately one order of magnitude above and below this value.
Solubility_Se_Ox	Se solubility in buffer, oxidizing conditions (mg/L)	Constant -1	Duro et al. (2006, Table 8-1). Value for oxidizing conditions is based on the table column for groundwater at atmospheric conditions ($pO_2 = 0.2$ atm). For Se, this table indicates no solubility limit under these conditions. The entered value of -1 tells the GoldSim model that this is the case.
Solubility_Se_Red	Se solubility in buffer, reducing conditions (mg/L)	Log-uniform 10^{-6} , 10^{-4}	Duro et al. (2006, Table 8-1). Value for reducing conditions is based on the table column for bentonite porewater, indicating a maximum dissolved Se concentration of 1.3×10^{-10} mol/L with FeSe acting as the solubility-limiting solid phase. This converts to about 1.0×10^{-5} mg/L Se. To consider uncertainty, the range given evaluates approximately one order of magnitude above and below this value.
Solubility_Tc_Ox	Tc solubility in buffer, oxidizing conditions (mg/L)	Constant -1	Duro et al. (2006, Table 8-1). Value for oxidizing conditions is based on the table column for groundwater at atmospheric conditions ($pO_2 = 0.2$ atm), for which Tc is listed as having no solubility limit. The entered value of -1 tells the GoldSim model that this is the case.
Solubility_Tc_Red	Tc solubility in buffer, reducing conditions (mg/L)	Log-uniform 4×10^{-5} , 4×10^{-3}	Duro et al. (2006, Table 8-1). Value for reducing conditions is based on the table column for bentonite porewater, indicating a maximum dissolved Tc concentration of 4.4×10^{-9} mol/L with $TcO_2 \cdot 1.6H_2O$ acting as the solubility-limiting solid phase. This converts to about 4×10^{-4} mg/L Tc. To consider uncertainty, the range given evaluates approximately one order of magnitude above and below this value.
Solubility_U_Ox	U solubility in buffer, oxidizing conditions (mg/L)	Log-uniform 0.0405, 4.05	Duro et al. (2006, Table 8-1). Value for oxidizing conditions is based on the table column for groundwater at atmospheric conditions ($pO_2 = 0.2$ atm), indicating a maximum dissolved U concentration of 1.7×10^{-6} mol/L with uranophane acting as the solubility-limiting solid phase. This converts to about 0.405 mg/L U. To consider uncertainty, the range given evaluates approximately one order of magnitude above and below this value.
Solubility_U_Red	U solubility in buffer, reducing conditions (mg/L)	Log-uniform 2.4×10^{-3} , 0.24	Duro et al. (2006, Table 8-1). Value for reducing conditions is based on the table column for bentonite porewater, indicating a maximum dissolved U concentration of $1. \times 10^{-7}$ mol/L with $UO_2 \cdot 2H_2O$ acting as the solubility limiting solid phase. This translates to about 0.024 mg/L U. To consider uncertainty, the range given evaluates approximately one order of magnitude above and below this value.

Parameter Name	Description	Distribution Type & Values	Reference/Rationale
Solubility_Th_Ox	Th solubility in buffer, oxidizing conditions (mg/L)	Log-uniform 1.8×10^{-2} , 1.8	Duro et al. (2006, Table 8-1). Value for oxidizing conditions is based on the table column for groundwater at atmospheric conditions ($pO_2 = 0.2$ atm), indicating a maximum dissolved Th concentration of 7.9×10^{-7} mol/L with $ThO_2:2H_2O$ acting as the solubility-limiting solid phase. This converts to about 1.8×10^{-1} mg/L Th. To consider uncertainty, the range given evaluates approximately one order of magnitude above and below this value.
Solubility_Th_Red	Th solubility in buffer, reducing conditions (mg/L)	Log-uniform 2.3×10^{-2} , 2.3	Duro et al. (2006, Table 8-1). Value for reducing conditions is based on the table column for bentonite porewater, indicating a maximum dissolved Th concentration of 10^{-6} mol/L with $ThO_2:2H_2O$ acting as the solubility-limiting solid phase. This converts to about 2.3×10^{-1} mg/L Th. To consider uncertainty, the range given evaluates approximately one order of magnitude above and below this value.
Solubility_Ra_Ox	Ra solubility in buffer, oxidizing conditions (mg/L)	Log-uniform 2.2×10^{-3} , 2.2×10^{-1}	Duro et al. (2006, Table 8-1). Value for reducing conditions is based on the table column for bentonite porewater, indicating a maximum dissolved Ra concentration of 9.8×10^{-8} mol/L with $RaSO_4$ acting as the solubility-limiting solid phase. This converts to about 2.2×10^{-2} mg/L Ra. To consider uncertainty, the range given evaluates approximately one order of magnitude above and below this value.
Solubility_Ra_Red	Ra solubility in buffer, reducing conditions (mg/L)	Log-uniform 9×10^{-4} , 9×10^{-2}	Duro et al. (2006, Table 8-1). Value for reducing conditions is based on the table column for bentonite porewater, indicating a maximum dissolved Ra concentration of 4×10^{-8} mol/L with $RaSO_4$ acting as the solubility-limiting solid phase. This converts to about 9×10^{-3} mg/L Ra. To consider uncertainty, the range given evaluates approximately one order of magnitude above and below this value.
Solubility_Rn_Ox	Rn solubility in buffer, oxidizing conditions (mg/L)	Constant -1	No solubility limit is assumed for Rn, a short-lived gas phase. The entered value of -1 tells the GoldSim model that this is the case.
Solubility_Rn_Red	Rn solubility in buffer, reducing conditions (mg/L)	Constant -1	No solubility limit is assumed for Rn, a short-lived gas phase. The entered value of -1 tells the GoldSim model that this is the case.

Table A-3. Default Parameters for SOAR Near Field Model Component			
Parameter Name	Description	Distribution Type & Values	Reference/Rationale
Solubility_Pb_Ox	Pb solubility in buffer, oxidizing conditions (mg/L)	Log-uniform 10 ⁻² , 1.0	The EPA "Technical Factsheet on Lead" (EPA, 2014) reports an estimated solubility of Pb in water of 100 ppb (approximately 0.1 mg/L) at pH 6.5, and 10 ppb at pH 8. Reference waters in Duro et al. (2006) for oxidizing groundwater conditions have pH values of about 7. To address uncertainty, the specified range extends one order of magnitude above and below a nominal value of 0.1 mg/L.
Solubility_Pb_Red	Pb solubility in buffer, reducing conditions (mg/L)	Log-uniform 10 ⁻² , 1.0	The EPA "Technical Factsheet on Lead" (EPA, 2014) reports an estimated solubility of Pb in water of 100 ppb (approximately 0.1 mg/L) at pH 6.5, and 10 ppb at pH 8. Reference waters in Duro et al. (2006) for buffer water under reducing conditions have pH values of about 7. To address uncertainty, the specified range extends one order of magnitude above and below a nominal value of 0.1 mg/L.

Table A-4. Default parameters for SOAR Far Field model component			
Parameter Name	Description	Distribution Type & Values	Reference/Rationale
Density_Fractured	Bulk density of fractured rocks (kg/m ³)	Uniform 2000, 2500	SKB (2006, p. 125) suggests a generic value of 2,600 kg/m ³ [162 lb/ft ³] is appropriate for modeling because natural variability is not significant.
Density_Porous	Bulk density of porous media (kg/m ³)	Uniform 2100, 2900	Range of values is consistent with values published in Nirex Limited United Kingdom (2007; Table 6.3) for several potential clay host rocks for waste disposal concepts in Europe.
Density_Sediments	Bulk density of sediments (kg/m ³)	Uniform 1750, 2070	DOE (2008, Table 6.3.10-2). The mean value for the bulk density of alluvium is 1,910 kg/m ³ with a standard deviation of 78. The range given approximates the mean plus or minus two standard deviations.
FF_DispersivityFraction	Dispersivity expressed as a fraction of the length of the far-field transport pathway (unitless)	Constant 0.1	General practice assumes dispersion length is 10 percent of path length.
FF_L1_Fracture_Aperture	Effective aperture of fractures in leg 1 (m)	Log-uniform 10 ⁻⁶ , 10 ⁻²	Effective fracture apertures are difficult to characterize and, therefore, highly uncertain. For the base case we assume log-uniform distribution for a median value of 0.1 mm (10 ⁻⁴ m) [0.039 in] with two orders of magnitude uncertainty on either side.
FF_L1_Fracture_Separation	Distance between fractures with advective flow, Leg 1 (m)	Log-uniform 5, 500	SKB (2006, Tables 6-42 and 6-3) provides average flowing interval frequencies for several granite borehole logs. Results indicate mean fracture spacings as low as 3 m [9.8 ft] to as high as 600 m [1,968 ft], but most average spacings are on the order of several tens of meters. Log-uniform distribution from 5 to 500 m [16 to 1,640 ft] provides a reasonable approximation of these results with median value of 50 m [164 ft].
FF_L1_Hydraulic_K_PM	Hydraulic conductivity for porous rocks/soils (e.g., clay, siltstone) of leg 1 (m/s)	Log-triangular 10 ⁻¹⁴ , 10 ⁻⁹ , 10 ⁻⁶	NEA (2005)
FF_L1_Hydraulic_K_Sed	Hydraulic conductivity for sedimentary rocks/soils of leg 1 (m/yr)	Log-uniform 5,500	DOE (2007, Table 7-4) indicates K _{sat} for combined test intervals in Well EWDP-19D were 55 m/yr [0.5 ft/d]. DOE (2007, Figure 7-4) plots results of other tests in alluvium and indicates uncertainty within an order of magnitude above and below this value. Log-uniform distribution selected to give median of 50 m/yr [164 ft/yr] and equal weight to each order of magnitude.

Table A-4. Default parameters for SOAR Far Field model component			
Parameter Name	Description	Distribution Type & Values	Reference/Rationale
FF_L1_Matrix_Perimeter_f	Matrix Perimeter Fraction of far-field leg 1 (unitless)	Uniform 0.1, 1	Used to define active perimeter for transversal mass exchange with the matrix. Uniform distribution from 0.1 to 1.0 accounts for potential for most flow to be channeled within as little as 10 percent of the fracture volume.
FF_L2_Fracture_Aperture	Effective aperture of fractures in leg 2 (m)	Log-uniform 10^{-6} , 10^{-2}	Effective fracture apertures are difficult to characterize and, therefore, highly uncertain. For the base case we assume log-uniform distribution for a median value of 0.1 mm (10^{-4} m) [0.039 in] with two orders of magnitude uncertainty on either side.
FF_L2_Fracture_Separation	Distance between major fractures with advective flow, Leg 2 (m)	Log-uniform 5, 500	SKB (2006, Tables 6-42 and 6-3) provides average flowing interval frequencies for several granite borehole logs. Results indicate mean fracture spacings as low as 3 m [9.84 ft] to as high as 600 m [1,968 ft], but most average spacings are on the order of several tens of meters. Log-uniform distribution from 5 to 500 m [16 to 1,640 ft] provides a reasonable approximation of these results with median value of 50 m [164 ft].
FF_L2_Hydraulic_K_PM	Hydraulic conductivity for porous rocks/soils (e.g., clay, siltstone) of leg 2 (m/s)	Log-triangular 10^{-14} , 10^{-9} , 10^{-6}	NEA (2005)
FF_L2_Hydraulic_K_Sed	Hydraulic conductivity for sedimentary rocks/soils of leg 2 (m/yr)	Log-uniform 5,500	DOE (2007, Table 7-4) indicates K_{sat} for combined test intervals in Well EWDP-19D were 55 m/yr [0.5 ft/d]. DOE (2007, Figure 7-4) plots results of other tests in alluvium and indicates uncertainty within an order of magnitude above and below this value. Log-uniform distribution selected to give median of 50 m/yr [164 ft/yr] and equal weight to each order of magnitude.
FF_L2_Matrix_Perimeter_f	Matrix Perimeter Fraction of far-field leg 2 (unitless)	Uniform 0.1, 1	Used to define active perimeter for transversal mass exchange with the matrix. Uniform distribution from 0.1 to 1.0 accounts for potential for most flow to be channeled within as little as 10 percent of the fracture volume.
FF_L3_Fracture_Aperture	Effective aperture of fractures in leg 3 (m)	Log-uniform 10^{-6} , 10^{-2}	Effective fracture apertures are difficult to characterize and, therefore, highly uncertain. For the base case we assume log-uniform distribution for a median value of 0.1 mm (10^{-4} m) [0.039 in] with two orders of magnitude uncertainty on either side.

Table A-4. Default parameters for SOAR Far Field model component			
Parameter Name	Description	Distribution Type & Values	Reference/Rationale
FF_L3_Fracture_Separation	Distance between major fractures with advective flow, Leg 3 (m)	Log-uniform 5, 500	SKB (2006, Tables 6-42 and 6-3) provides average flowing interval frequencies for several granite borehole logs. Results indicate mean fracture spacings as low as 3 m [9.8 ft] to as high as 600 m [1,968 ft], but most average spacings are on the order of several tens of meters. Log-uniform distribution from 5 to 500 m [16.4 to 1,640 ft] provides a reasonable approximation of these results with median value of 50 m [164 ft].
FF_L3_Hydraulic_K_PM	Hydraulic conductivity for porous rocks/soils (clay, siltstone etc.) of leg 3 (m/s)	Log-triangular 10^{-14} , 10^{-9} , 10^{-6}	NEA (2005).
FF_L3_Matrix_Perimeter_f	Matrix Perimeter Fraction of far-field leg 3 (unitless)	Uniform 0.1, 1	Used to define active perimeter for transversal mass exchange with the matrix. Uniform distribution from 0.1 to 1.0 accounts for potential for most flow to be channeled within as little as 10 percent of the fracture volume.
FF_L3_Hydraulic_K_Sed	Hydraulic conductivity for sedimentary rocks/soils of leg 2 (m/yr)	Log-uniform 5,500	DOE (2007, Table 7-4) indicates K_{sat} for combined test intervals in Well EWDP-19D were 55 m/yr [0.5 ft/d]. DOE (2007, Figure 7-4) plots results of other tests in alluvium and indicates uncertainty within an order of magnitude above and below this value. Log-uniform distribution selected to give median of 50 m/yr [164 ft/yr] and equal weight to each order of magnitude.
Kd_C_Fractured_Red	K_d of C in fractured rock, reducing conditions (m^3/kg)	Constant 0	Treated as nonsorbing anion.
Kd_C_Fractured_Ox	K_d of C in fractured rock, oxidizing conditions (m^3/kg)	Constant 0	Treated as nonsorbing anion.
Kd_C_Porous_Red	K_d of C in porous media, reducing conditions (m^3/kg)	Log-triangular 10^{-4} , 3×10^{-3} , 1.0	Values from Nirex Limited United Kingdom (2003, Table C.8) for clay-rich rocks. Section C.4.1 of Nirex Limited United Kingdom (2003) recommended sampling a log-triangular distribution.
Kd_C_Porous_Ox	K_d of C in porous media, oxidizing conditions (m^3/kg)	Constant 0	Treated as nonsorbing anion.

Table A-4. Default parameters for SOAR Far Field model component			
Parameter Name	Description	Distribution Type & Values	Reference/Rationale
Kd_C_Sed_Red	K _d of C in sediment, reducing conditions (m ³ /kg)	Uniform 0, 2.0	Brady et al. (2009, Table 5).
Kd_C_Sed_Ox	K _d of C in sediment, oxidizing conditions (m ³ /kg)	Constant 0	DOE (2008, Section 6.3.10.2) identifies as nonsorbing.
Kd_Cs_Fractured_Red	K _d of Cs in fractured rock, reducing conditions (m ³ /kg)	Cumulative 0, 4 × 10 ⁻⁴ 0.25, 10 ⁻² 0.75, 0.14 1.0, 2	SKB (2006, Table A-43) range of high and low values for Cs(I) for granitic rock in saline waters. The values are specified as [percentile, value] pairs.
Kd_Cs_Fractured_Ox	K _d of Cs in fractured rock, oxidizing conditions (m ³ /kg)	Cumulative 0, 4 × 10 ⁻⁴ 0.25, 10 ⁻² 0.75, 0.14 1.0, 2	SKB (2006, Table A-43) range of high and low values for Cs(I) for granitic rock in saline waters. The values are specified as [percentile, value] pairs.
Kd_Cs_Porous_Red	K _d of Cs in porous media, reducing conditions (m ³ /kg)	Log-triangular 10 ⁻³ , 5.0, 100	Values from Nirex Limited United Kingdom (2003, Table C.8) for clay-rich rocks. Section C.4.1 of Nirex Limited United Kingdom (2003) recommended sampling a log-triangular distribution.
Kd_Cs_Porous_Ox	K _d of Cs in porous media, oxidizing conditions (m ³ /kg)	Log-triangular 10 ⁻³ , 5.0, 100	Values from Nirex Limited United Kingdom (2003, Table C.8) for clay-rich rocks. Section C.4.1 of Nirex Limited United Kingdom (2003) recommended sampling a log-triangular distribution.
Kd_Cs_Sed_Red	K _d of Cs in sediment, reducing conditions (m ³ /kg)	Log-uniform 0.1, 1.0	DOE (2008, Table 6.3.10-2) provides minimum and maximum for range. Log-uniform distribution gives equal weight to each order of magnitude of uncertainty range.
Kd_Cs_Sed_Ox	K _d of Cs in sediment, oxidizing conditions (m ³ /kg)	Log-uniform 0.1, 1.0	DOE (2008, Table 6.3.10-2) provides minimum and maximum for range. Log-uniform distribution gives equal weight to each order of magnitude of uncertainty range.
Kd_I_Fractured_Red	K _d of I in fractured rock, reducing conditions (m ³ /kg)	Constant 0	Treated as nonsorbing anion.
Kd_I_Fractured_Ox	K _d of I in fractured rock, oxidizing conditions (m ³ /kg)	Constant 0	Treated as nonsorbing anion.

Table A-4. Default parameters for SOAR Far Field model component			
Parameter Name	Description	Distribution Type & Values	Reference/Rationale
Kd_I_Porous_Red	K _d of I in porous media, reducing conditions (m ³ /kg)	Constant 0	Value from Nirex Limited United Kingdom (2003, Table C.8) for clay-rich rocks.
Kd_I_Porous_Ox	K _d of I in porous media, oxidizing conditions (m ³ /kg)	Constant 0	Treated as nonsorbing anion.
Kd_I_Sed_Red	K _d of I in sediment, reducing conditions (m ³ /kg)	Uniform 0, 0.1	Brady et al. (2009, Table 5).
Kd_I_Sed_Ox	K _d of I in sediment, oxidizing conditions (m ³ /kg)	Constant 0	DOE (2008, Section 6.3.10.2) identifies iodine as nonsorbing.
Kd_Np_Fractured_Red	K _d of Np in fractured rock, reducing conditions (m ³ /kg)	Cumulative 0, 4.7 × 10 ⁻² 0.25, 0.32 0.75, 2.8 1.0, 20	SKB (2006, Table A-43) range of high and low values for Np(IV) for granitic rock in saline waters. The values are specified as [percentile, value] pairs.
Kd_Np_Fractured_Ox	K _d of Np in fractured rock, oxidizing conditions (m ³ /kg)	Cumulative 0, 2 × 10 ⁻³ 0.25, 1.1 × 10 ⁻² 0.75, 4.4 × 10 ⁻² 1.0, 0.22	SKB (2006, Table A-43) range of high and low values for Np(V) for granitic rock in saline waters. The values are specified as [percentile, value] pairs.
Kd_Np_Porous_Red	K _d of Np in porous media, reducing conditions (m ³ /kg)	Log-triangular 10 ⁻² , 2.0, 50.0	Values from Nirex Limited United Kingdom (2003, Table C.8) for Np(IV) in clay-rich rocks. Nirex Limited United Kingdom recommended sampling a log-triangular distribution.
Kd_Np_Porous_Ox	K _d of Np in porous media, oxidizing conditions (m ³ /kg)	Log-triangular 10 ⁻⁴ , 5 × 10 ⁻² , 5	Values from Nirex (2003, Table C.8) for Np(V) in clay-rich rocks. Nirex Limited United Kingdom recommended sampling a log-triangular distribution.
Kd_Np_Sed_Red	K _d of Np in sediment, reducing conditions (m ³ /kg)	Log-uniform 1.8 × 10 ⁻³ , 1.3 × 10 ⁻²	DOE (2008, Table 6.3.10-2) provides minimum and maximum for range. Log-uniform distribution gives equal weight to each order of magnitude of uncertainty range.
Kd_Np_Sed_Ox	K _d of Np in sediment, oxidizing conditions (m ³ /kg)	Log-uniform 1.8 × 10 ⁻³ , 1.3 × 10 ⁻²	DOE (2008, Table 6.3.10-2) provides minimum and maximum for range. Log-uniform distribution gives equal weight to each order of magnitude of uncertainty range.

Parameter Name	Description	Distribution Type & Values	Reference/Rationale
Kd_Pu_Fractured_Red	K _d of Pu in fractured rock, reducing conditions (m ³ /kg)	Triangular 1,5,10	SKB (2006, Table A-44) range of high and low values for Pu(III, IV) for granitic rock in saline waters.
Kd_Pu_Fractured_Ox	K _d of Pu in fractured rock, oxidizing conditions (m ³ /kg)	Triangular 1, 5,10	SKB (2006, Table A-44) range of high and low values for Pu(III, IV) for granitic rock in saline waters.
Kd_Pu_Porous_Red	K _d of Pu in porous media, reducing conditions (m ³ /kg)	Log-triangular 0.01, 50, 1,000	Values from Nirex Limited United Kingdom (2003, Table C.8) for Pu(IV) in clay-rich rocks. Nirex recommended sampling a log-triangular distribution.
Kd_Pu_Porous_Ox	K _d of Pu in porous media, oxidizing conditions (m ³ /kg)	Log-uniform 5 × 10 ⁻² , 0.3	Values for Kd_Pu_Sed_Ox have been used here. DOE (2008, Table 6.3.10-2) provides minimum and maximum for range. Log-uniform distribution gives equal weight to each order of magnitude of uncertainty range.
Kd_Pu_Sed_Red	K _d of Pu in sediment, reducing conditions (m ³ /kg)	Log-uniform 5 × 10 ⁻² , 0.3	DOE (2008, Table 6.3.10-2) provides minimum and maximum for range but makes no distinction about redox conditions. Log-uniform distribution gives equal weight to each order of magnitude of uncertainty range.
Kd_Pu_Sed_Ox	K _d of Pu in sediment, oxidizing conditions (m ³ /kg)	Log-uniform 5 × 10 ⁻² , 0.3	DOE (2008, Table 6.3.10-2) provides minimum and maximum for range but makes no distinction about redox conditions. Log-uniform distribution gives equal weight to each order of magnitude of uncertainty range. These estimates may need to be checked in some other reference for a difference between Pu(IV) and Pu(VI).
Kd_Se_Fractured_Red	K _d of Se in fractured rock, reducing conditions (m ³ /kg)	Constant 10 ⁻³	SKB (1999, Table 2-13) for granitic rock.
Kd_Se_Fractured_Ox	K _d of Se in fractured rock, reducing conditions (m ³ /kg)	Constant 10 ⁻³	SKB (1999, Table 2-13) for granitic rock.
Kd_Se_Porous_Red	K _d of Se in porous media, reducing conditions (m ³ /kg)	Log-triangular 10 ⁻⁶ , 6.4 × 10 ⁻² , 2	Values from Nirex Limited United Kingdom (2003, Table C.8) for Se(-II) in clay-rich rocks. Nirex recommended sampling a log-triangular distribution.
Kd_Se_Porous_Ox	K _d of Se in porous media, oxidizing conditions (m ³ /kg)	Log-triangular 10 ⁻⁶ , 3.2 × 10 ⁻² , 1	Values from Nirex Limited United Kingdom (2003, Table C.8) for Se(IV, VI) in clay-rich rocks. Nirex recommended sampling a log-triangular distribution.

Table A-4. Default parameters for SOAR Far Field model component			
Parameter Name	Description	Distribution Type & Values	Reference/Rationale
Kd_Se_Sed_Red	K _d of Se in sediment, reducing conditions (m ³ /kg)	Log-uniform 1 × 10 ⁻³ , 5 × 10 ⁻²	DOE (2008, Table 6.3.10-1) provides minimum and maximum for range. Log-uniform distribution gives equal weight to each order of magnitude of uncertainty range.
Kd_Se_Sed_Ox	K _d of Se in sediment, oxidizing conditions (m ³ /kg)	Log-uniform 10 ⁻³ , 5 × 10 ⁻²	DOE (2008, Table 6.3.10-1) provides minimum and maximum for range. Log-uniform distribution gives equal weight to each order of magnitude of uncertainty range.
Kd_Tc_Fractured_Red	K _d of Tc in fractured rock, reducing conditions (m ³ /kg)	Constant 0	Treated as nonsorbing anion.
Kd_Tc_Fractured_Ox	K _d of Tc in fractured rock, oxidizing conditions (m ³ /kg)	Constant 0	Treated as nonsorbing anion.
Kd_Tc_Porous_Red	K _d of Tc in porous media, reducing conditions (m ³ /kg)	Log-triangular 10 ⁻⁴ , 0.5, 250	Minimum and "best estimate" are from Nirex Limited United Kingdom (2003, Table C.8) for Tc(IV) in clay-rich rocks. Maximum estimate is from EPA (2004a). Nirex recommended sampling a log-triangular distribution (maximum Nirex value was 50), so the distribution approach is preserved here with the EPA value as a maximum.
Kd_Tc_Porous_Ox	K _d of Tc in porous media, oxidizing conditions (m ³ /kg)	Log-triangular 10 ⁻⁶ , 5 × 10 ⁻² , 0.5	Values from Nirex Limited United Kingdom (2003, Table C.8) for Tc(VII) in clay-rich rocks. Nirex recommended sampling a log-triangular distribution.
Kd_Tc_Sed_Red	K _d of Tc in sediment, reducing conditions (m ³ /kg)	Uniform 0, 1.0	Brady et al. (2009, Table 5).
Kd_Tc_Sed_Ox	K _d of Tc in sediment, oxidizing conditions (m ³ /kg)	Constant 0	DOE (2008, Section 6.3.10.2) identifies as nonsorbing.
Kd_U_Fractured_Red	K _d of U in fractured rock, reducing conditions (m ³ /kg)	Cumulative 0, 4.8 × 10 ⁻² 0.25, 1.1 0.75, 13 1.0, 280	SKB (2006, Table A-43) range of high and low values for U(IV) for granitic rock in saline waters. The values are specified as [percentile, value] pairs.
Kd_U_Fractured_Ox	K _d of U in fractured rock, oxidizing conditions (m ³ /kg)	Cumulative 0, 5 × 10 ⁻⁴ 0.25, 1.5 × 10 ⁻³ 0.75, 1.6 × 10 ⁻² 1.0, 0.12	SKB (2006, Table A-43) range of high and low values for U(VI) for granitic rock in saline waters. The values are specified as [percentile, value] pairs.

Table A-4. Default parameters for SOAR Far Field model component			
Parameter Name	Description	Distribution Type & Values	Reference/Rationale
Kd_U_Porous_Red	K _d of U in porous media, reducing conditions (m ³ /kg)	Log-triangular 1, 10, 5 × 10 ³	Values from Nirex Limited United Kingdom (2003, Table C.8) for U(IV) in clay-rich rocks. Nirex recommended sampling a log-triangular distribution.
Kd_U_Porous_Ox	K _d of U in porous media, oxidizing conditions (m ³ /kg)	Log-triangular 10 ⁻⁴ , 0.1, 50	Values from Nirex Limited United Kingdom (2003, Table C.8) for U(VI) in clay-rich rocks. Nirex recommended sampling a log-triangular distribution.
Kd_U_Sed_Red	K _d of U in sediment, reducing conditions (m ³ /kg)	Uniform 1.7 × 10 ⁻³ , 8.9 × 10 ⁻³	DOE (2008, Table 6.3.10-2) provides minimum and maximum for range, but makes no distinction between U(IV) and U(VI).
Kd_U_Sed_Ox	K _d of U in sediment, oxidizing conditions (m ³ /kg)	Uniform 1.7 × 10 ⁻³ , 8.9 × 10 ⁻³	DOE (2008, Table 6.3.10-2) provides minimum and maximum for range, but makes no distinction between U(IV) and U(VI).
Kd_Th_Fractured_Red	K _d of Th in fractured rock, reducing conditions (m ³ /kg)	Cumulative 0, 0.5 0.25, 0.79 0.75, 2.4 1.0, 10	SKB (2006, Table A-43) range of high, low, and "best estimate" values for Th(IV) for granitic rock in saline waters. The values are specified as [percentile, value] pairs.
Kd_Th_Fractured_Ox	K _d of Th in fractured rock, oxidizing conditions (m ³ /kg)	Cumulative 0, 0.5 0.25, 0.79 0.75, 2.4 1.0, 10	SKB (2006, Table A-43) range of high, low, and "best estimate" values for Th(IV) for granitic rock in saline waters. The values are specified as [percentile, value] pairs.
Kd_Th_Porous_Red	K _d of Th in porous media, reducing conditions (m ³ /kg)	Log-triangular 0.001, 1.0, 100	Values from Nirex Limited United Kingdom (2003, Table C.8) for Th in clay-rich rocks. Nirex recommended sampling a log-triangular distribution.
Kd_Th_Porous_Ox	K _d of Th in porous media, oxidizing conditions (m ³ /kg)	Log-triangular 0.001, 1.0, 100	Values from Nirex Limited United Kingdom (2003, Table C.8) for Th in clay-rich rocks. Nirex recommended sampling a log-triangular distribution.
Kd_Th_Sed_Red	K _d of Th in sediment, reducing conditions (m ³ /kg)	Log uniform 0.8, 60.0	Brady et al. (2009, Table 5). Log-uniform distribution gives equal weight to each order of magnitude of uncertainty range.
Kd_Th_Sed_Ox	K _d of Th in sediment, oxidizing conditions (m ³ /kg)	Log uniform 0.8, 60.0	Brady et al. (2009, Table 5). Log-uniform distribution gives equal weight to each order of magnitude of uncertainty range.

Table A-4. Default parameters for SOAR Far Field model component			
Parameter Name	Description	Distribution Type & Values	Reference/Rationale
Kd_Ra_Fractured_Red	K _d of Ra in fractured rock, reducing conditions (m ³ /kg)	Cumulative 0, 6.4 × 10 ⁻³ 0.25, 9.9 × 10 ⁻² 0.75, 2.3 1.0, 2.6	SKB (2006, Table A-43) range of high, low, and “best estimate” values for Ra(II) for granitic rock in saline waters. The values are specified as [percentile, value] pairs.
Kd_Ra_Fractured_Ox	K _d of Ra in fractured rock, oxidizing conditions (m ³ /kg)	Cumulative 0, 6.4 × 10 ⁻³ 0.25, 9.9 × 10 ⁻² 0.75, 2.3 1.0, 2.6	SKB (2006, Table A-43) range of high, low, and “best estimate” values for Ra(II) for granitic rock in saline waters. The values are specified as [percentile, value] pairs.
Kd_Ra_Porous_Red	K _d of Ra in porous media, reducing conditions (m ³ /kg)	Log-triangular 0.01, 2, 1000	Values from Nirex Limited United Kingdom (2003, Table C.8) for Ra in clay-rich rocks. Nirex recommended sampling a log-triangular distribution.
Kd_Ra_Porous_Ox	K _d of Ra in porous media, oxidizing conditions (m ³ /kg)	Log-triangular 0.01, 2, 1000	Values from Nirex Limited United Kingdom (2003, Table C.8) for Ra in clay-rich rocks. Nirex recommended sampling a log-triangular distribution.
Kd_Ra_Sed_Red	K _d of Ra in sediment, reducing conditions (m ³ /kg)	Log uniform 0.10, 1.00	DOE (2008, Table 6.3.10-1) provides minimum and maximum for range. Log-uniform distribution gives equal weight to each order of magnitude of uncertainty range.
Kd_Ra_Sed_Ox	K _d of Ra in sediment, oxidizing conditions (m ³ /kg)	Log uniform 0.10, 1.00	DOE (2008, Table 6.3.10-1) provides minimum and maximum for range. Log-uniform distribution gives equal weight to each order of magnitude of uncertainty range.
Kd_Rn_Fractured_Red	K _d of Rn in fractured rock, reducing conditions (m ³ /kg)	Constant 0	Treated as nonsorbing gas.
Kd_Rn_Fractured_Ox	K _d of Rn in fractured rock, oxidizing conditions (m ³ /kg)	Constant 0	Treated as nonsorbing gas.
Kd_Rn_Porous_Red	K _d of Rn in porous media, reducing conditions (m ³ /kg)	Constant 0	Treated as nonsorbing gas.
Kd_Rn_Porous_Ox	K _d of Rn in porous media, oxidizing conditions (m ³ /kg)	Constant 0	Treated as nonsorbing gas.

Table A-4. Default parameters for SOAR Far Field model component			
Parameter Name	Description	Distribution Type & Values	Reference/Rationale
Kd_Rn_Sed_Red	K _d of Rn in sediment, reducing conditions (m ³ /kg)	Constant 0	Treated as nonsorbing gas.
Kd_Rn_Sed_Ox	K _d of Rn in sediment, oxidizing conditions (m ³ /kg)	Constant 0	Treated as nonsorbing gas.
Kd_Pb_Fractured_Red	K _d of Pb in fractured rock, reducing conditions (m ³ /kg)	Truncated Log-normal 2.51 × 10 ⁻² , 3.63, 2.05 × 10 ⁻³ , 0.31	SKB (2010b, Table 2-4). Low (2.5 percentile) and high (97.5 percentile) distribution of the range of values for Pb(II) for granitic rock in saline waters. The values are specified as [mean, standard deviation, minimum, maximum].
Kd_Pb_Fractured_Ox	K _d of Pb in fractured rock, oxidizing conditions (m ³ /kg)	Truncated Log-normal 2.51 × 10 ⁻² , 3.63, 2.05 × 10 ⁻³ , 0.31	SKB (2010b, Table 2-4). Low (2.5 percentile) and high (97.5 percentile) distribution of the range of values for Pb(II) for granitic rock in saline waters. The values are specified as [mean, standard deviation, minimum, maximum].
Kd_Pb_Porous_Red	K _d of Pb in porous media, reducing conditions (m ³ /kg)	Log-triangular 0.1, 5, 1000	Values from Nirex Limited United Kingdom (2003, Table C.8) for Pb in clay-rich rocks. Nirex recommended sampling a log-triangular distribution.
Kd_Pb_Porous_Ox	K _d of Pb in porous media, oxidizing conditions (m ³ /kg)	Log-triangular 0.1, 5, 1000	Values from Nirex Limited United Kingdom (2003, Table C.8) for Pb in clay-rich rocks. Nirex recommended sampling a log-triangular distribution.
Kd_Pb_Sed_Red	K _d of Pb in sediment, reducing conditions (m ³ /kg)	Log uniform 0.1, 5.0	McKinley and Scholtis (1992, Table 8). Log-uniform distribution gives equal weight to each order of magnitude in the range.
Kd_Pb_Sed_Ox	K _d of Pb in sediment, oxidizing conditions (m ³ /kg)	Log uniform 0.1, 5.0	McKinley and Scholtis (1992, Table 8). Log-uniform distribution gives equal weight to each order of magnitude in the range.
Porosity_Fractured	Porosity of fractured rocks (unitless)	Uniform 6.8 × 10 ⁻⁴ , 1.5 × 10 ⁻³	SKB (2006). Table A-42 indicates log-10 mean porosity for three different granites ranging from -2.84 to -3.17.
Porosity_Porous	Porosity of porous media (unitless)	Uniform 0.05, 0.4	NEA (2005, Figure 23).
Porosity_Sediments	Porosity of sediments (unitless)	Uniform 0.07, 0.3	DOE (2008, Table 6.3.10-2). Porosity of differentiated valley fill mean value of 0.18 with standard deviation of 0.051. Range given is mean ±2-sigma.

Table A-5. Default parameters for SOAR Biosphere model component			
Parameter Name	Description	Distribution Type & Values	Reference/Rationale
Ingestion_Dose_Coefficient	Radiological dose to an adult from the ingestion of a unit activity of radionuclides in the vector (Sv/Bq) [C-14, Cs-135, I-129, Np-237, Pu-238, Pu-239, Pu-240, Pu-242, Se-79, Tc-99, U-232, U-233, U-234, U-235, U-236, U-238, Th-230, Ra-226, Rn-222, Pb-210]	Constant-vector [5.8×10^{-10} , 2×10^{-9} , 1.1×10^{-7} , 1.1×10^{-7} , 2.3×10^{-7} , 2.5×10^{-7} , 2.5×10^{-7} , 2.4×10^{-7} , 2.9×10^{-9} , 6.4×10^{-10} , 3.30×10^{-7} , 5.1×10^{-8} , 4.9×10^{-8} , 4.7×10^{-8} , 4.7×10^{-8} , 4.5×10^{-8} , 2.1×10^{-7} , 2.8×10^{-7} , 3.8×10^{-8} , 6.9×10^{-7}]	ICRP (1996, Table A.1). Value for Rn-222 was obtained from U.S. National Research Council (1999).
WaterFlowToBiosphere	Water flow rate to the biosphere (ac-ft/yr)	Triangular 370, 1980, 5770	Used to calculate radionuclide concentrations in water available at the interface between the far field and biosphere. USDA (2008, Table 11)
Water_Consumption_Rate	Population-averaged consumption rate of well water (L/yr)	Beta 380, 262, 24, 1023	For adults in the United States. EPA (2004b, Table A1, Appendix E, p. E-4)

References

- Ahn, T. and B. Leslie. "Corrosion Products of Steels in High-Level Waste Management at the Proposed Yucca Mountain Repository." NUDOC 9808060163. ML031671314. Washington, DC: U.S. Nuclear Regulatory Commission. 1998.
- Ahn, T. and S. Mohanty. NUREG-1914, "Dissolution Kinetics of Commercial Spent Nuclear Fuels in the Potential Yucca Mountain Repository Environment." ML083120074. Washington, DC: U.S. Nuclear Regulatory Commission. 2008.
- Ahn, T. and P. Soo. "Corrosion of Low-Carbon Cast Steel in Concentrated Synthetic Groundwater at 80 to 150 C." *Waste Management*. Vol. 15, No. 7. pp. 471-476. 1995.
- Bennett, D.G. and R. Gens. "Overview of European Concepts for High-Level Waste and Spent Fuel Disposal With Special Reference Waste Container Corrosion." Proceedings of the Third International Workshop on Long-Term Prediction of Corrosion Damage in Nuclear Waste Systems, University Park, Pennsylvania, May 14-18, 2007. D. Féron, and D.D. Macdonald, eds. *Journal of Nuclear Materials*. Vol. 379. pp 1-8. 2008.
- Blackwood, D.J., L.M. Peter, and D.E. Williams. "Stability and Open Circuit Breakdown of the Passive Oxide Film on Titanium." *Electrochimica Acta*. Vol. 33. pp. 1143-1149. 1988.
- Brady, P.V., B.W. Arnold, G.A. Freeze, P.N. Swift, S.J. Bauer, J.L. Kanney, R.P. Rechar, and J.S. Stein. "Deep Borehole Disposal of High-Level Radioactive Waste." SAND2009-4401. Albuquerque, New Mexico: Sandia National Laboratories. August 2009.
- Brossia, C.S., L. Browning, D.S. Dunn, O.C. Moghissi, O. Pensado, and L. Yang. "Effect of Environment on the Corrosion of Waste Package and Drip Shield Materials." CNWRA 2001-03. San Antonio, Texas: Center for Nuclear Waste Regulatory Analyses. 2001.
- BSC. "Defense HLW Glass Degradation Model." ANL-EBS-MD-000016. Rev. 02, ACN 001, ERD 001, ERD, 002. Las Vegas, Nevada: Bechtel SAIC Company, LLC. 2004a.
- BSC. "Aqueous Corrosion Rates for Waste Package Materials." ANL-DSD-MD-000001, Rev. 01, ACN 001, ERD 01, ERD 02. Las Vegas, Nevada: Bechtel SAIC Company, LLC. 2004b.
- Carbol, P., J. Cobos-Sabathe, J.-P. Glatz, C. Ronchi, V. Rondinella, D.H. Wegen, T. Wiss, A. Loida, V. Metz, B. Kienzler, K. Spahiu, B. Grambow, and J. Quiones. "The Effect of Dissolved Hydrogen on the Dissolution of ²³³U Doped UO₂(s), High Burn-up Spent Fuel and MOX Fuel." A.M.E. Valiente, Tech. Rep. TR-05-09. Svensk Kärnbränslehantering AB. Stockholm, Sweden: Swedish Nuclear Fuel and Waste Management Company. 2005.
- DOE. DOE/RW-0573, "Yucca Mountain Repository License Application." Rev. 1. ML090700817. Las Vegas, Nevada: DOE, Office of Civilian Radioactive Waste Management. 2009.
- DOE. "Total System Performance Assessment Model/Analysis for the License Application." MDL-WIS-PA-000005. Rev. 00. Las Vegas, Nevada: U.S. Department of Energy, Office of Civilian Radioactive Waste Management. 2008.

DOE. "Saturated Zone Site-Scale Flow Model." MDL-NBS-HS-000011. Rev. 03. Las Vegas, Nevada: U.S. Department of Energy, Office of Civilian Radioactive Waste Management. 2007.

Duro, L., M. Grivé, E. Cera, X. Gaona, C. Domènech, and J. Bruno. "Determination and Assessment of the Concentration Limits to Be Used in SR-Can." SKB Technical Report TR-06-32. Stockholm Sweden: Swedish Nuclear Fuel and Waste Management Co. December 2006.

Ebert, W.L., M.A. Lewis, T.L. Barber, and S.G. Johnson. "Accounting for EBR-II Metallic Waste Form Degradation in TSPA." Scientific Basis for Nuclear Waste Management XXVI. R.J. Finch and D.B. Bullen, eds. Materials Research Society Symposium Proceedings. Vol. 757. Warrendale, Pennsylvania: Materials Research Society. pp. 71-80. 2002.

EPA. "Technical Factsheet on: Lead." National Primary Drinking Water Regulations. Washington, DC: U.S. Environmental Protection Agency. <<http://www.epa.gov/ogwdw/pdfs/factsheets/ioc/tech/lead.pdf>>. 2014. (28th April 2014).

EPA. "Volume III—Review of Geochemistry and Available K_d Values for Americium, Arsenic, Curium, Iodine, Neptunium, Radium, and Technetium." EPA 402-R-04-002C. Washington, DC: U.S. Environmental Protection Agency. 2004a. <<http://www.epa.gov/radiation/cleanup/402-r-99-004.html#vol3>>.

EPA. "Estimated Per Capita Water Ingestion and Body Weight in the United States—An Update." EPA-822-R-00-001. Washington, DC: U.S. Environmental Protection Agency. October 2004b.

Féron, D., D. Crusset, and J.-M. Gras. "Corrosion Issues in Nuclear Waste Disposal." Proceedings of the Third International Workshop on Long-Term Prediction of Corrosion Damage in Nuclear Waste Systems, University Park, Pennsylvania, May 14-18, 2007. D. Féron and D. D. Macdonald, eds. *Journal of Nuclear Materials*. Vol. 379. pp. 16-23. 2008.

Foct, F., J. Cabrea, W. Dridi, and S. Savoye. "Corrosion behavior of Carbon Steel in the Tournemire Clay." Proceedings of the Second International Workshop on Prediction of Long-Term Corrosion Behavior in Nuclear Waste Systems. Chatenay-Malabry, France: European Federation of Corrosion. pp. 68-77. 2004.

Foct, F. and J.-M. Gras. "Semi-Empirical Model for Carbon Steel Corrosion in Long Term Geological Nuclear Waste Disposal." Proceedings of the First International Workshop on Long-Term Corrosion Behavior in Nuclear Waste Systems (ECF 36). D. Féron and D. Macdonald, eds. Cadarache, France: Maney Publishing. pp. 91-102. 2003.

Grambow, B., A. Loida, A. Martinez-Esparza, P. Diaz-Arocas, J. de Pablo, J.-L. Paul, G. Marx, J.-P. Paul, G. Marx, J.-P. Glatz, K. Lemmens, K. Ollila, and H. Christensen. "Source Term for Performance Assessment of Spent Fuel as a Waste Form." EUR 19140. Luxembourg, Germany: European Atomic Energy Community. 2000.

Glass, R.S., G.E. Overturf, R.E. Garrison, and R.D. McCright. "Electrochemical Determination on the Corrosion Behavior of Candidate Alloys Proposed for Containment of High Level Nuclear Waste in Tuff." UCID-20174. Livermore, California: Lawrence Livermore National Laboratory. 1984.

Hua, F. and G. Gordon. "Corrosion Behavior of Alloy 22 and Ti Grade 7 in a Nuclear Waste Repository Environment." *Corrosion*. Vol. 60. pp. 764–777. 2004.

ICRP. International Commission on Radiological Protection. "Age-Dependent Doses to Members of the Public from Intake of Radionuclides: Part 5, Compilation of Ingestion and Inhalation Dose Coefficients." *Annals of the ICRP* Vol. 26/1, Publication 72. Tarrytown, New York: Elsevier Science, Inc. 1996.

Iseghem, P.V. "Geological Disposal of Radioactive Waste—The Challenge of Assessing the Long-term Safety." BNS Evening Lecture April 26, 2007. Brussels, Belgium: SCK•CEN. 2007.

Jain, V., G. Cragolino, and L. Howard. "A Review Report on High Burnup Spent Nuclear Fuel—Disposal Issues." ML043020321. San Antonio, Texas: Center for Nuclear Waste Regulatory Analyses. 2004.

Johnson, L. and F. King. "The effect of the Evolution of Environmental Conditions on the Corrosion Evolutionary Path in a Repository for Spent Fuel and High-Level Waste in Opalinus Clay." Proceedings of the Third International Workshop on Long-Term Prediction of Corrosion Damage in Nuclear Waste Systems, University Park, Pennsylvania, May 14–18, 2007. D. Féron, and D.D. Macdonald, eds. *Journal of Nuclear Materials*. Vol. 379. pp 9–5. 2008.

Jung, H., T. Ahn, and X. He. "Representation of Copper and Carbon Steel Waste Package Degradation in a Generic Performance Assessment Model." Proceedings of the 2011 International High-Level Radioactive Waste Management Conference. Albuquerque, New Mexico: American Nuclear Society. 2011.

Jung, H., T. Ahn, K. Axler, R. Pabalan, and D. Pickett. "Corrosion of SIMFUEL in Aerated Carbonate Solution Containing Calcium and Silicate." San Antonio, Texas: Center for Nuclear Waste Regulatory Analyses. 2011.

King, F., C. Lilja, K. Pedersen, P. Pitkänen, and M. Vähänen. "An Update of the State-of-the-Art Report on the Corrosion of Copper Under Expected Conditions in a Deep Geologic Repository." Stockholm, Sweden: SKB Technical Report, TR-10-67. 2010.

Kursten, B., E. Smailos, I. Azarate, L. Wermer, N.R. Smart, G. Marx, M.A. Cunado, and G. Santarini. "Corrosion Evaluation of Metallic HLW/ Spent Fuel Disposal Containers—Review." Proceedings of the Second International Workshop on Prediction of Long-Term Corrosion Behavior in Nuclear Waste Systems. Chatenay-Malabry, France: European Federation of Corrosion. pp. 153–161. 2004a.

Kursten, B., E. Smailos, I. Azkarate, L. Werme, N.R. Smart, and G. Santarini. "COBECOMA—State-of-the-art Document on the Corrosion Behaviour of Container Materials." FIKW–CT–20014–20138 Final Report. Brussels, Belgium: European Commission. 2004b.

Leslie, B., C. Grossman, and J. Durham. "Total-System Performance Assessment (TPA) Version 5.1 Module Description and User Guide." ML072710060. San Antonio, Texas: Center for Nuclear Waste Regulatory Analyses. 2007.

Lide, D.R., ed. "Diffusion of Gases in Water." *CRC Handbook of Chemistry and Physics*, Internet Version 2005. Boca Raton, Florida. CRC Press. <<http://www.hbcernetbase.com>>

McCright, R.D., W.G. Halsey, and R.A. Van Konynenburg. "Progress Report on the Results of Testing Advanced Conceptual Design Metal Barrier Materials under Relevant Environmental Conditions for a Tuff Repository." UCID-21044. Livermore, California: Lawrence Livermore National Laboratory. 1987.

McKinley, I.G. and A. Scholtis. "Compilation and Comparison of Radionuclide Sorption Databases Used in Recent Performance Assessments. Proceedings: Workshop on Radionuclide Sorption From the Safety Evaluation Perspective. Paris, France: OECD/NEA. pp. 21-55. 1992.

Nakayama, G., Y. Sakakibara, Y. Taniyama, H. Cho, T. Jintoku, S. Kawakami, and M. Takemoto. "The Long-Term Behaviors of Passivation and Hydride Layer of Commercial Grade Pure Titanium in TRU Waste Disposal Environments." Vol. 379. pp. 174-180. 2008.

NEA. "Clay Club Catalogue of Characteristics of Argillaceous Rocks." Radioactive Waste Management ISBN 92-64-01067. NEA No. 4436, OECD 2005. Paris, France: Nuclear Energy Agency. 2005.

Nirex Limited United Kingdom. "Generic Repository Studies: Assessment of Repository Designs in Clays and Evaporites." Report No. J01 v2. Oxfordshire, United Kingdom: Nirex Limited United Kingdom. March 2007.

Nirex Limited United Kingdom. "Generic Repository Studies: Generic Postclosure Performance Assessment." Report No. N/080. Oxfordshire, United Kingdom: Nirex Limited United Kingdom. July 2003.

Poinssot, C., C. Ferry, M. Kelm, B. Grambow, A. Martinez, L. Johnson, Z. Andriambololona, J. Bruno, C. Cacho, J.M. Cavedon, H. Christensen, C. Corbel, C. Jegou, K. Lemmens, A. Loida, P. Lovera, F. Miserque, J. de Pablo, A. Poulesquen, J. Quinones, V. Rondinella, K. Spahiu, and D.H. Wegen. "Spent Fuel Stability Under Repository Conditions—Final Report of the European Project." European Commission, 5th Euratom Framework Programme 1998-2002. 2005.

Reeve, K.D., D.M. Levins, B.W. Seatonberry, R.K. Ryan, K.P. Hart, and G.T. Stevens. "Fabrication and Leach Testing of SYNROC Containing Actinides and Fission Products." Material Research Society Symposium Proceedings. Warrendale, Pennsylvania: Material Research Society. Vol. 127. pp. 223-230. 1989.

Rosborg, B. and L. Werme. "The Swedish Nuclear Waste Program and the Long-Term Corrosion Behaviour of Copper." *Journal of Nuclear Materials*. Vol. 379. Pp. 142-153. 2008.

Schutz, R.W. "Corrosion of Titanium and Titanium Alloys." *ASM Handbook—Vol. 13B: Corrosion*. Materials Park, Ohio: ASM International. 2005.

Schutz, R.W. "Platinum Metal Additions to Titanium: A Highly Effective Strategy for Enhancing Corrosion Resistance." *Corrosion*. Vol. 59. pp. 1,043-1,057. 2003.

Scully, J.R. and M. Edwards. "Review of the NWMO Copper Corrosion Allowance." NWMO TR-2013-04. Toronto Canada: Nuclear Waste Management Organization. May 2013.

Scully, J.R. and T.W. Hicks. "Technical Note 2012:21, Initial Review Phase for SKBs Safety Assessment SR-Site: Corrosion of Copper." Stockholm, Sweden. Swedish Radiation Safety Authority (SSM). July 31, 2012.

Shoesmith, D.W. "Fuel Corrosion Processes Under Waste Disposal Conditions." *Journal of Nuclear Materials*. Vol. 282. pp. 1–31. 2000.

Shukla, P., T. Ahn, J. McMurry, M. J. Rubal, D. Daruwalla, and Y.-M. Pan. "Hydrogen Effects on Dissolution of Spent Nuclear Fuel in Reducing Repository Conditions." San Antonio, Texas: Center for Nuclear Waste Regulatory Analyses. 2015.

SKB. "Corrosion Calculations Report for the Safety Assessment SR-Site." Technical Report TR–10–66. Svensk Kärnbränslehantering AB. Stockholm, Sweden: Swedish Nuclear Fuel and Waste Management Co. December 2010a.

SKB. "Radionuclide Transport Report for the Safety Assessment SR-Site." Technical Report TR–10–50. Stockholm Sweden: Swedish Nuclear Fuel and Waste Management Co. December 2010b.

SKB. "Data Report for the Safety Assessment SR-Can." Technical Report TR–06–25. S. Kärnbränslehantering, ed. Stockholm Sweden: Swedish Nuclear Fuel and Waste Management Co. November 2006.

SKB. "Deep Repository for Spent Nuclear Fuel—SR 97-Post-Closure Safety." Main Report—Volume II. S. Kärnbränslehantering, ed. Stockholm Sweden: Swedish Nuclear Fuel and Waste Management Co. November 1999.

SNL. "General and Localized Corrosion of the Drip Shield." ANL–EBS–MD–000004. Rev 02, Add 01, ERD 02. Las Vegas, Nevada: Sandia National Laboratories. 2008.

SNL. "MOX Spent Nuclear Fuel and LaBS Glass for TSPA–LA." ANL–WIS–MD–000022. Rev. 01. Las Vegas, Nevada: Sandia National Laboratories. 2007.

Stothoff, S. "Integrated Spent Fuel Management Program Analyses." Scientific Notebook No. 1038E. San Antonio, Texas: CNWRA. 2010.

Taniguchi, N., M. Kawasaki, S. Kawakami, and M. Kubota. "Corrosion Behavior of Carbon Steel in Contact with Bentonite under Anaerobic Condition." Proceedings of the Second International Workshop on Long-Term Corrosion Behavior in Nuclear Waste Systems. Chatenay-Malabry, France: European Federation of Corrosion. pp. 24–34. 2004.

Tipton, E.L. "Flexible Performance Assessment—Scoping of Options and Analyzing Risk (FPA–SOAR)." Scientific Notebook No. 1036E. San Antonio, Texas: CNWRA. 2010.

USDA. "2008 Farm and Ranch Irrigation Survey, Volume 3, Special Studies, Part 1, 2007 Census of Agriculture." U.S. Department of Agriculture, National Agricultural Statistics Service. 2008. <http://www.agcensus.usda.gov/Publications/2007/Online_Highlights/Farm_and_Ranch_Irrigation_Survey/fris08.pdf> (10 February 2010).

U.S. National Research Council. "Risk Assessment of Radon in Drinking Water." Committee on Risk Assessment of Exposure to Radon in Drinking Water, Board on Radiation Effects Research, Commission on Life Sciences. Washington, D.C.: U.S. National Research Council, National Academy Press. Table 4.5, p. 75. 1999.

Vance, R., K.P. Hart, R.A. Day, M.L. Carter, and M. Hambley. "SYNROC Derivatives for the Hanford Waste Remediation Task." Material Research Society Symposium Proceedings. Vol. 465. Warrendale, Pennsylvania: Material Research Society. pp. 341–349. 1997.

Van Der Leer, D., N.P. Weatherill, R.J. Sharp, and C.R. Hayes. "Modelling the Diffusion of Lead Into Drinking Water." Vol. 26. pp. 681–699. 2002.

Wang, Y. "Adaptive Waste Forms: The Concept and Its Implications." Presentation at Integrated Radioactive Waste Management in Future Fuel Cycles, Charleston, South Carolina, USA, November 8–12, 2009. New York City, New York: Engineering Conferences International. 2009.

Weast, R.C. *CRC Handbook of Chemistry and Physics*. Boca Raton, Florida: CRC Press, Inc. 1986.

Wersin, P., S. Kastriot, and J. Bruno. "Kinetic Modeling of Bentonite-Canister Interaction—Long-Term Predictions of Copper Canister Corrosion Under Oxidic and Anoxic Conditions." SKB TR 94–25. Cerdanyola, Spain: MBT. *Tecnología Ambiental*. September 1994.

APPENDIX B
GLOSSARY

GLOSSARY

Abstraction: Reduction and representation of the essential components of a feature, event, or process into a simplified form for inclusion in a model. An abstraction is intended to maximize the use of limited computational resources while allowing a sufficient range of sensitivity and uncertainty analyses.

Advection: The process in which solutes, particles, or molecules are transported by the motion of flowing fluid.

Ambient: Undisturbed, natural conditions.

Anoxic: Pertaining to the minimal or no oxygen present in groundwater.

Aqueous: Pertaining to water, such as aqueous phase, aqueous species, or aqueous transport.

Backfill: Materials used to fill in an excavated, open area after emplacement of waste.

Breach: A penetration in the waste package.

Cell: GoldSim term to refer to a model element representing a chamber with a uniformly mixed mass or solute within a given volume. The mass transfer between connected cells is controlled by concentration gradients or by flow rates.

Cell Pathway: GoldSim term to refer to a group of connected cells (representing a one-, two-, or three-dimensional geometry), with mass transfers between cells regulated by concentration gradients or by flow rates.

Cladding: The metal outer sheath of a fuel rod generally made of a zirconium alloy intended to protect the uranium dioxide pellets, which are the nuclear fuel, from direct contact with reactor coolants or neutron moderators and dissolution by exposure to high temperature water under operating conditions in a reactor.

Colloid: As applied to radionuclide migration, a colloidal system is a group of large molecules or small particles having at least one dimension with the size range of 10^{-9} to 10^{-6} m [3.9×10^{-7} to 3.9×10^{-4} in] that are suspended in a solvent. Colloids that are transported in groundwater can be filtered out of the water in small pore spaces or very narrow fractures because of the large size of those colloids.

Conceptual Model: A set of descriptive features used to characterize a system or subsystem for a given purpose in a model. These features are compatible with one another and fit the existing data within the purpose of the model.

Corrosion: The deterioration of a material, usually a metal, as a result of a chemical or electrochemical reaction with its environment.

Criticality: The condition in which a fissile material sustains a chain reaction. It occurs when the number of neutrons present in one generation cycle equals the number generated in the previous cycle. The state is considered critical when a self-sustaining nuclear chain reaction is ongoing.

Diffusion: (i) The spreading or dissemination of a substance caused by concentration gradients. (ii) The gradual mixing of the molecules of two or more substances because of molecular random thermal motion.

Diffusive Transport: Movement of solutes because of their concentration gradient. It is the process in which substances in the groundwater move through the subsurface by means of diffusion due to concentration gradients.

Dispersion: (i) The tendency of a solute (substance dissolved in groundwater) to spread out away from the fluid bulk motion. (ii) The macroscopic outcome of the actual movement of individual solute particles through a porous medium. Dispersion causes dilution of solutes, including radionuclides, in groundwater and is usually an important mechanism for spreading contaminants in low-velocity flows. In similitude to diffusion, dispersion is associated with concentration gradients, but the mechanism driving dispersion is non-ideal fluid motion (deviations from plug flow), as opposed to molecular random thermal motion in diffusion.

Disruptive Event: An off-normal event, such as volcanic activity, seismic activity, and nuclear criticality in the case of the potential geologic disposal system. Disruptive events have two possible effects: (i) direct release of radioactivity or (ii) alteration of the nominal behavior of the system.

Dissolution: (i) Change from a solid to a liquid state. (ii) Dissolving a substance in a solvent.

Distribution: See Probability Distribution.

Drip Shield: A metallic structure placed along the extension of the emplacement area and above the waste packages to prevent seepage water from directly dripping onto the waste package outer surface.

Effective Porosity: The fraction of a porous medium volume available for fluid flow or solute transport. The effective porosity is less than or equal to the total void space (porosity).

Equilibrium: The state of a chemical system in which the phases do not undergo any further change in properties or proportions with time; the system is under a balance in which the net rate of addition or depletion of masses or phases is zero.

Events: (i) Occurrences that have a specific starting time and, usually, duration much shorter than the time span being simulated in a model. (ii) Uncertain occurrences that take place within a short time relative to the time frame of the model.

Features: Physical, chemical, thermal, or temporal components of a system or site.

Flow: The movement of a fluid such as air, water, or magma. Flow and transport are processes that can move radionuclides from a geologic disposal system to the biosphere.

Flow Pathway: The subsurface course that water or a solute (including radionuclides) would follow in a given groundwater velocity field, governed principally by hydraulic gradients.

Fracture: A discontinuity in rock along which loss of cohesion has occurred. It is often caused by the stresses that cause folding and faulting. Fractures may act as fast paths for groundwater movement.

General Corrosion: A type of corrosion attack (deterioration) approximately uniformly distributed over a metal surface; also called uniform corrosion.

Geochemical: Characterizing the distribution and amounts of the chemical elements in minerals, ores, rocks, soils, water, and the atmosphere; the movement of the elements in nature on the basis of their properties.

Geologic Disposal System: A set of engineered components integrated within natural, geologic formations and with a function to isolate radioactive waste for a long period of time.

Groundwater: Water contained in pores or fractures in either the unsaturated or saturated zones below ground level.

High-Level Waste: A waste form produced by separating fissile material from fission products in spent nuclear fuel; the nonuseable material from current recycling technology.

Hydrologic: Pertaining to the properties, distribution, and circulation of water on the surface of the land, in the soil and underlying rocks, and in the atmosphere.

Isothermal: Having a constant temperature.

Localized Corrosion: Corrosion at discrete sites (e.g., pitting and crevice corrosion).

Matrix: Rock material and its pore space exclusive of fractures.

Matrix Diffusion: The process by which molecular or ionic solutes, such as radionuclides in ground water, move from areas of higher concentration to areas of lower concentration. This movement is through the pore spaces of the rock material as opposed to movement through the fractures.

Model: A depiction or representation of a system, phenomenon, or process, including any hypotheses required to describe the system or explain the phenomenon or process. Examples are conceptual, physical, mathematical, and numerical models.

Near Field: The area and conditions within a geologic disposal system, including the rock, immediately surrounding the waste packages. The region within a geologic disposal system where the natural hydrogeologic system has been significantly impacted by the excavation of a geologic disposal system and the emplacement of waste.

Oxic: Pertaining to the presence of oxygen in groundwater.

Oxidation State: The chemical state of a radionuclide as a function of the number of electrons. The oxidation state is lower in reducing environments than in oxidizing environments.

Parameter: Quantitative properties (e.g., data, values), together with principles or equations governing the behavior of a system, that are major constituents of computer codes for a mathematical or numerical model.

Pathway: A potential route by which radionuclides might reach the biosphere and pose a threat to humans.

Performance: A quantitative or qualitative result of the long-term evolution of a component, combination of components, or the whole geologic disposal system.

Permeability: The ability of a material to transmit fluid through its pores when subjected to a difference in pressure (pressure gradient).

Phase: A physically homogeneous and distinct portion of a material system, such as the gaseous, liquid, and solid phases of a substance.

Pipe: GoldSim term to refer to a model element that implements a solution to the one-dimensional dispersive-advective mass-balance equation, with a zero concentration initial condition, defined release rate (mass/time) as boundary condition at the inlet (position $x=0$), and release rate at the outlet computed as output.

Pipe pathway: GoldSim term to refer to a group of connected pipes to simulate transport through complex geometries, where each pipe represents a physical segment that can be approximated as a one-dimensional transport pathway.

Pitting Corrosion: Localized corrosion of a metal surface, confined to a small area, that takes the form of cavities named pits.

Porosity: The ratio of openings, or voids, to the total volume of a soil or rock expressed as a numeric fraction or as a percentage. See also *effective porosity*.

Probability: The chance that an outcome will occur from the set of possible outcomes. Statistical probability examines actual events and can be verified by observation or sampling. Knowledge of the exact probability of an event is usually limited by the inability to know, or compile, the complete set of possible outcomes over time and space.

Probability Distribution: The set of outcomes (values) and their corresponding probabilities for a random variable.

Processes: A series of actions that have gradual, continuous interactions with the system being modeled.

Radiolysis: Dissociation of molecules by the action of radiation.

Radionuclide: Radioactive type of atom with an unstable nucleus that spontaneously decays, usually emitting ionizing radiation in the process.

Receptor: An individual for whom radiological doses are calculated or measured.

Redox: Pertaining to the magnitude that a system is reducing or oxidizing.

Retardation: Slowing radionuclide movement in groundwater by mechanisms that include sorption of radionuclides, diffusion into rock matrix pores, and microfractures.

Risk: The probability that an undesirable event will occur, multiplied by the consequences of the undesirable event.

Rock Matrix: See *Matrix*.

Scenario: A well-defined, connected sequence of features, events, and processes that can be thought of as a storyboard of a possible future condition of a geologic disposal system. Scenarios can be undisturbed, in which case the performance would be the expected behavior for the system. Scenarios can also be disturbed, if altered by alternative failure modes.

Scoping Tool: A model specifically developed to gain preliminary risk and performance insights on a geologic disposal system.

Sorption: The binding, on a microscopic scale, of one substance to another. A term that includes both adsorption and absorption. The sorption of dissolved radionuclides onto solids or waste package materials by means of close-range chemical or physical forces is potentially an important process in a geologic disposal system. Sorption is a function of the chemistry of the radioisotopes, the fluid in which they are carried, and the mineral material they encounter along the flow path.

Sorption Coefficient (K_d): Coefficient characterizing the affinity by which one substance binds to another.

Source Term: Types and amounts of radionuclides that are the source of a potential release.

Spent Nuclear Fuel: Fuel that has been withdrawn from a nuclear reactor following irradiation, the constituent elements of which have not been separated by reprocessing. This fuel is more radioactive than it was before irradiation and releases significant amounts of heat from the decay of its fission product radionuclides.

Stress Corrosion Cracking: A cracking process that requires the simultaneous action of a corrosive environment, a susceptible material, and sustained (residual or applied) tensile stress. Stress corrosion cracking excludes both the fracture of already corroded sections and the localized corrosion processes that can compromise the metallic structure without the action of residual or applied stress.

Transparency: The ease of understanding the process by which a study was carried out, which assumptions are driving the results, how they were arrived at, and the rigor of the analyses leading to the results. Transparency is achieved when a reader or reviewer has a clear picture of what was done in the analysis, the outcome, and why this outcome was produced.

Transport: A process that allows substances, such as contaminants or radionuclides, to be carried in a fluid through (i) the physical mechanisms of advection, diffusion, and dispersion and (ii) the chemical mechanisms of sorption, leaching, precipitation, dissolution, and complexation. Types of transport include advective, diffusive, and colloidal.

Transport Pathway: A physical region through which substances (e.g., contaminants or radionuclides) can mobilize due to processes such as diffusion and advection.

Uncertainty: How much a calculated or measured value varies from the unknown true value.

Variable: A nonunique property or attribute.

Variability: A measure of how a quantity varies over time or space.

APPENDIX C

SUMMARY OF MODEL UPDATES AND VERIFICATION ACTIVITIES FOR SOAR VERSION 2.0

SUMMARY OF MODEL UPDATES AND VERIFICATION ACTIVITIES FOR SOAR VERSION 2.0

This appendix summarizes the changes to the Scoping of Options and Analyzing Risk (SOAR) model to update it from Version 1.1 to 2.0. This appendix supplements the SOAR user guide and offers examples to clarify changes to the model. The user is referred to the user guide for a detailed description of the SOAR model. Version 2.0 changes to the SOAR code focused on updates to the waste package corrosion model and the buffer material evolution model. Conceptual and coding errors were also addressed, and the model file was migrated to GoldSim Version 11.1. A small number of tests are summarized in this appendix to demonstrate that model updates were properly implemented.

Tests were implemented by a party independent to the model developers. Corresponding test reports were archived on the shared hard drive where the SOAR model resides. No issues were identified during the independent testing. The tester recommended addition of a results element to compare the fraction of waste packages failed and the waste package breach area fraction as functions of time for the different failure mechanisms (general corrosion, localized corrosion, and alternative failure). This recommendation was incorporated in the waste package results dashboard. The independent tester suggested introducing an interrupt command in case invalid inputs are provided by the user in the dashboards. GoldSim 11.1 does not provide the functionality of a complete interrupt. However, a message window is displayed if internal error checking detects a user input error, allowing the user the option of manually aborting the computation.

This appendix compares a series of results from deterministic mean-value runs using SOAR Version 2.0 to results from the SOAR Version 1.1 model. The comparison is intended to provide confidence that model updates have not altered previously developed and tested modules. Changes to the approach to compute the breach area of failed waste packages make it impossible to match previous results, but differences in the results can be explained solely on the basis of model updates. Thus, the effect of model changes is specific to certain modules and results of the SOAR code, and previous general tests and test results remain valid.

Summary of Model Updates

The model updates include

- Migration of the model to GoldSim 11.1.
 - All of the graphic displays are updated to take advantage of GoldSim 11.1 capabilities
- Consolidation of the general corrosion model into a model with fewer model elements and with flexibility to incorporate arbitrary distributions for corrosion rates of waste package materials.
 - In SOAR Version 1.1, the corrosion rate distributions were constrained to uniform, normal, log-uniform, and lognormal
- Implementation of an abstraction for dynamic corrosion, with different constant corrosion rates applied at different times depending on the repository setting conditions (e.g., humid air, oxic groundwater, anoxic groundwater after buffer saturation).

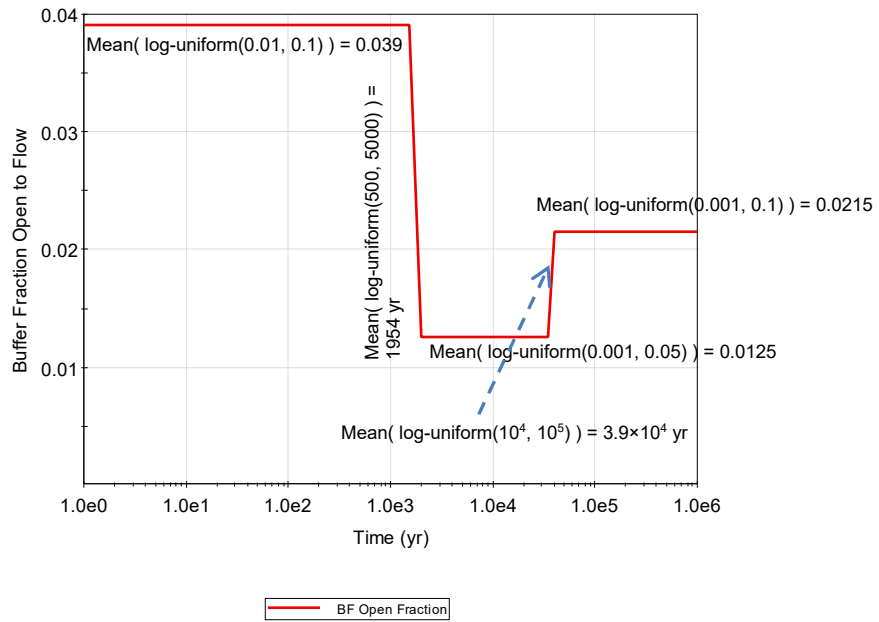
- Implementation of a model for copper corrosion enhanced by hydrogen sulfide, as part of the dynamic corrosion abstraction.
- Development of code to track the fraction of the buffer material open to flow as a function of time, which affects the following processes:
 - Corrosion of the copper canister, if hydrogen sulfide is assumed present in the groundwater, and
 - Radionuclide transport through the buffer material, after failure of the waste packages.
- Correction of a conceptual error in the computation of the waste package breach area fraction. In the revised computation, the fraction is the breach area fraction conditional on failure of the waste package.
- Updated dashboards (user-friendly interfaces for input parameters) for the Waste Form, Waste Package, and Near Field. New parameters were introduced for the buffer degradation abstraction and the hydrogen sulfide copper corrosion model.
- Updated parameter database, with consolidated distributions for the general corrosion model parameters and a new parameter for the hydrogen sulfide concentration in groundwater.
- Inclusion of an event probability factor in the computation of integrated releases (comparable to 40 CFR 191 cumulative release limits).
- Correction of a coding error that set the diffusion coefficient to zero in the region between the buffer material and the host rock, for the radionuclides newly added in Version 1.1 (Th-230, Ra-226, Rn-222, Pb-210).

In the next sections, results are presented that (i) illustrate changes to the buffer material evolution model and to the waste package corrosion model and (ii) provide a comparison to results from the previous SOAR code, Version 1.1.

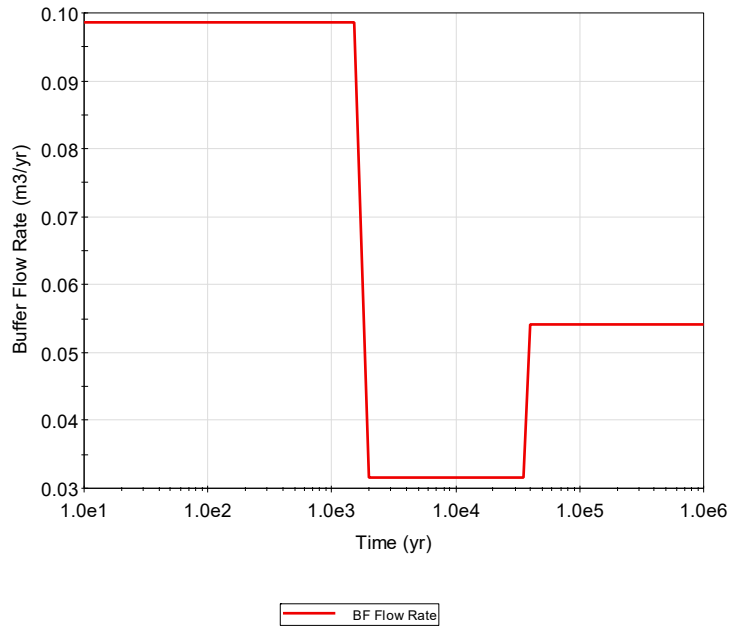
Buffer Material Evolution

Figure C-1 shows an example of the buffer evolution abstraction. The top plot is the fraction of the buffer open to flow, and the bottom plot is the flow through the buffer (which affects the waste package failure time if the material is copper, and always affects radionuclide transport through the buffer). **Error! Reference source not found.** shows the settings in the near-field dashboard for the run in Figure C-1. The average numbers, plateaus, and transition times in the top plot in Figure C-1 were verified based on values in the dashboard settings in **Error! Reference source not found.**

Figure C-3 compares the fraction of waste packages failed versus time for two mean-value runs, one with and one without hydrogen sulfide (HS^-) corrosion. The top plot includes HS^- corrosion effects on copper, and in the bottom plot HS^- effects were disabled. Three different options were independently compared to disable the HS^- corrosion effects: (i) using the “disable” check in the waste package settings dashboard, (ii) setting the concentration of $\text{HS}^- = 0$ with a factor controlled in the waste package settings dashboard, and (iii) disabling the variable flow through the buffer abstraction in the near field settings dashboard. The three different options produced the identical waste package failure fraction versus time (bottom plot of Figure C-3). Therefore, it was verified that the waste package failure in the SOAR code is dependent on the concentration of HS^- in the groundwater and on flow rates through the buffer.



T01.gsp Run: 7:52:03 PM 1/12/2017



T01.gsp Run: 7:52:03 PM 1/12/2017

Figure C-1. Time variation of the Fraction of Buffer Open to flow (top) and the Flow Rate Through the Buffer (Bottom) for a Deterministic Mean-Value Run.

Enable variable flow through the buffer (if unchecked, assumed HS- does not contact the copper WP)

Parameters sampled from log-uniform distributions between min and max values

	Min Value	Max Value
Open BF fraction initial	0.01	0.1
Open BF fraction after saturation	0.001	0.05
BF degradation time [yr]	10000	100000
Open BF fraction after degradation	0.001	0.1

The following times must be in increasing order

- Transition time from humid air to aqueous corrosion
- Buffer saturation time
- Buffer degradation time

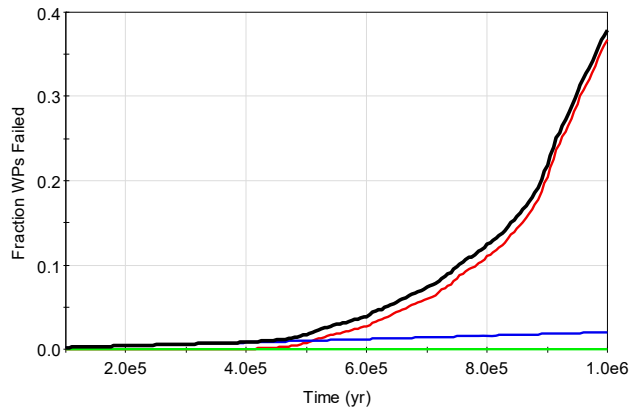
If there is any potential cross-over, the simulation will be stopped.

	Min Value	Max Value
BF saturation time [yr]	500	5000

The humid air transition time is controlled in the Waste Package Settings dashboard.

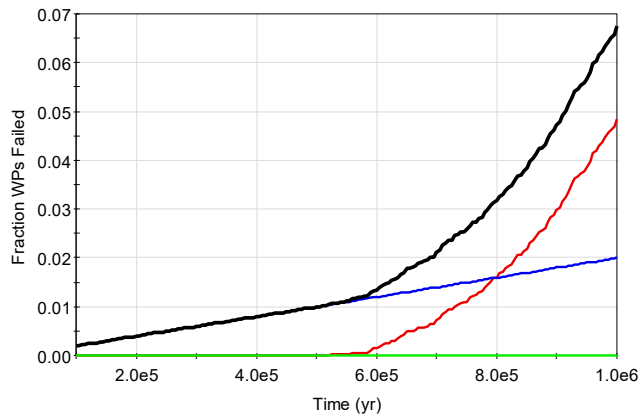
The BF saturation time is assumed to be the transition time from oxic to anoxic conditions in the dynamic general corrosion model

Figure C-2. Settings in the Near-Field dashboard for the run in Figure C-1.



Gen corr Loc corr Alternative Total

T01.gsp Run: 7:52:03 PM 1/12/2017



Gen corr Loc corr Alternative Total

T01_noSulfide.gsp Run: 10:33:35 AM 1/20/2017

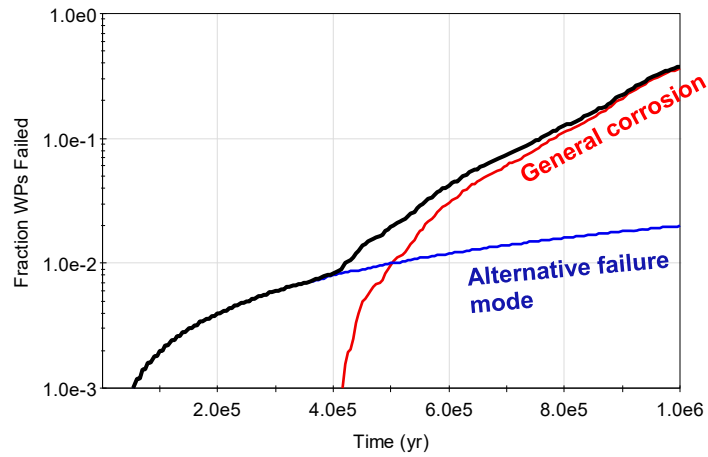
Figure C-3. Examples of Waste Package Failure Versus Time. The Top Plot Includes the Influence of Hydrogen Sulfide (HS^-) on Copper Corrosion. In the Bottom Plot, the Influence of HS^- Was Nullified With Appropriate Settings in the Dashboard.

Waste Package Model

The approach to compute the degraded breach area of a waste package was revised for Version 2.0. Figure C-4 shows an example of a breach area computation. The top plot is the fraction of waste packages failed by multiple failure mechanisms. At times less than 400,000 years, waste package failure is dominated by the alternative modes (from the Alternative Failure Submodule; the waste package failure rates were selected arbitrarily). After 500,000 years, general corrosion becomes the dominant waste package failure mechanism. The bottom plot in Figure C-4 includes the breach area fraction versus time for the different failure mechanisms, as well as the average curve. The average breach area fraction is used in SOAR to define a “representative” waste package and the breached cross section is used to compute rates of radionuclide transfer from the waste package internals into the buffer material.

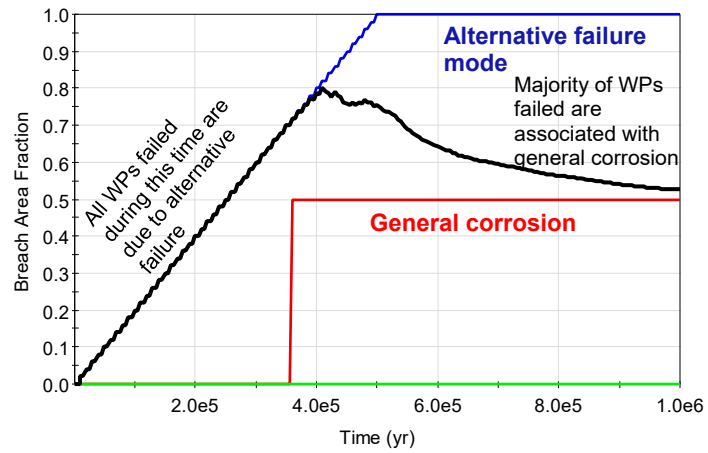
The alternative failure mode considered in the example in Figure C-4 was *multiple-events*. In this mode, multiple events occur at random times, and each time an event occurs, it is conservatively assumed that different waste packages fail. The number of waste packages failed increases depending on the number of events and the event intensity. In this example, the increase with time is approximately linear. For the breach area computation, it is conservatively assumed that the representative waste package for the *multiple-events* mode experiences all of the multiple events, with the corresponding breach area accumulating with time. The approximately linear increase with time in the bottom plot in Figure C-4 for the alternative failure mode curve (blue curve) is due to the assumption of multiple events affecting the same representative waste package. Eventually the blue curve plateaus at 1. The breach area fraction for the representative waste package failed by general corrosion is a simple step function (red curve in the bottom plot in Figure C-4). All of the waste packages failed within a realization by general corrosion are assumed to exhibit the same constant breach area. The total average for the breach area (black curve in the bottom plot in Figure C-4) follows the alternative breach area curve at times less than 400,000 years (because failure is dominated by the alternative failure events) and then bends downwards approaching the general corrosion (dominant failure mode after 500,000 years) breach area fraction red curve. The results in Figure C-4 are consistent with expected trends.

An abstraction was developed allowing for different constant corrosion rates of waste package materials during different periods. The corrosion rate may transition from humid air, to aqueous oxic, to aqueous anoxic. Transition times are defined in the waste package and near field dashboards. In addition, in the case of copper waste packages, copper could be attacked by hydrogen sulfide, depending on the state of the buffer material. In Figure C-4, the transition time from aqueous oxic to anoxic was set to 1,954 years (average buffer material saturation time, derived from the assumed default values in the dashboard in **Error! Reference source not found.**). Figure C-5 includes results from 4 deterministic runs. The buffer saturation time was increased (with respect to the run in Figure C-4) to 3,274 years and to 5,000 years. Oxidic corrosion rates (on the order of 1 $\mu\text{m}/\text{yr}$) are two orders of magnitude higher than the anoxic corrosion rates. Increasing the window of operation of oxidic corrosion by increasing the buffer saturation time (from 1,954 years in Figure C-4, to 3,274 years and to 5,000 years in Figure C-5) has a significant effect on the fraction of waste packages failed by general corrosion. A late inflection in the fraction versus time is noted after 800,000 years, due to buffer degradation and the action of HS^- on the copper material. In the deterministic runs in the bottom plots in Figure C-5, this late enhancement in the corrosion rate was disabled by selecting a late degradation time for the buffer material (close to 10^6 years), and, as expected, the waste package failure fraction versus time does not show the late inflection. Therefore, the results exhibit expected dependencies consistent with the modeled abstraction for waste package corrosion.



Gen corr Loc corr Alternative Total

T02.gsp Run: 11:08:49 AM 1/20/2017

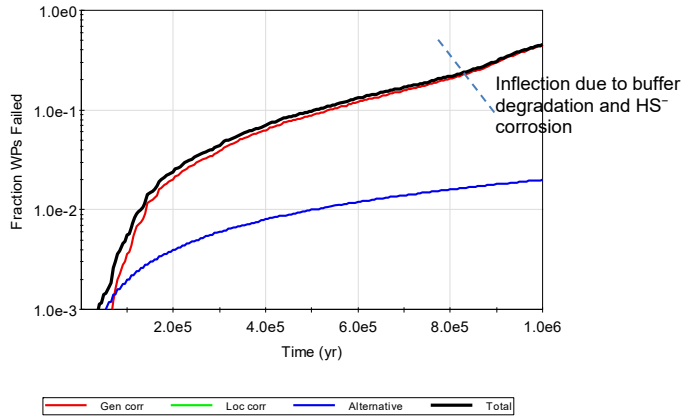


Gen corr Loc corr Alternative Average

T02.gsp Run: 11:08:49 AM 1/20/2017

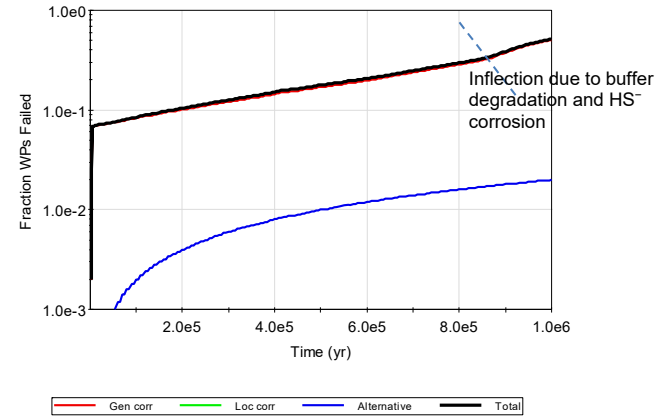
Figure C-4. Fraction of Waste Packages Failed and Breach Area Fraction as Function of Time for a Deterministic Mean-Value Run With the Buffer Saturation Time = 1,954 Years

Buffer saturation time = 3,274 years



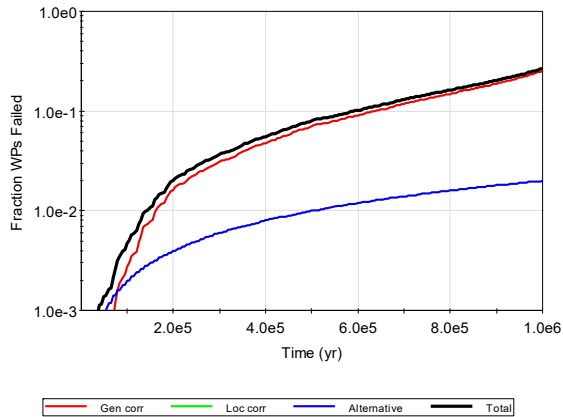
T03_2000.gsp Run: 1:57:18 PM 1/20/2017

Buffer saturation time = 5,000 years



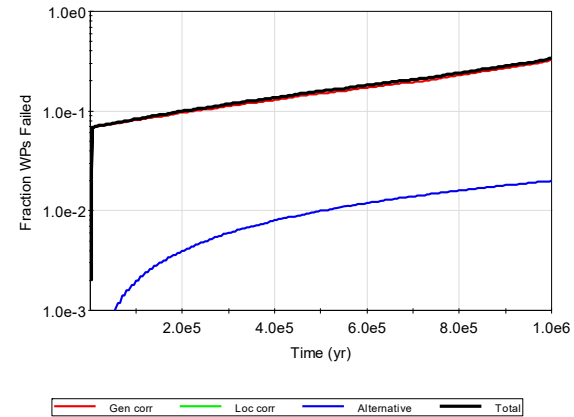
T03_5000.gsp Run: 2:01:32 PM 1/20/2017

Buffer saturation time = 3,274 years; no late buffer degradation



T03_2000b.gsp Run: 1:58:38 PM 1/20/2017

Buffer saturation time = 5,000 years; no late buffer degradation



T03_5000b.gsp Run: 1:59:59 PM 1/20/2017

Figure C-5. Examples of Waste Package Failure Versus Time for Different Selections of Transition Times

Comparison to Results of SOAR Version 1.1 (Regression Testing)

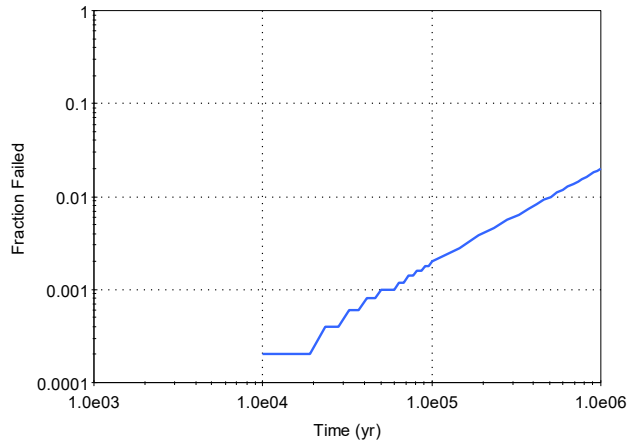
Selected results were compared to Version 1.1 to provide confidence that recent modifications have not altered calculations by previously developed and tested modules. The computation of the breach area fraction was modified for Version 2.0, resulting in higher radionuclide release estimates. The results differ and are expected to differ from previous code versions when identical parameter values and settings are selected, and the changes can be explained.

Figure C-6 compares a few outputs from SOAR Version 2.0 to the corresponding Version 1.1 outputs. The run was a deterministic mean-value run, with copper as the waste package material and with the multiple-events failure mode enabled. The buffer evolution and dynamic corrosion abstractions of SOAR Version 2.0 were disabled, as those models were not available in SOAR Version 1.1. The only mechanism causing waste package failure in this example is the multiple-events mode. The total fraction of waste packages failed is similar, with minor differences due to time-stepping. The breach area fraction is larger in Version 2.0, causing major differences in the radionuclide release rates. Due to the approach for computing the breach area, the breach area fraction versus time exhibits jumps at the events. These jumps are also manifested in the release versus time curves as up-and-down wiggles. The wiggles and oscillations are more evident in the far-field releases of I-129 computed with SOAR Version 2.0, which are propagated all the way to the dose estimates. Those oscillations are not considered anomalous, but are a consequence of the multiple-events model and the approach to compute the breach area. Those oscillations were also present in SOAR Version 1.1, but were less evident because of the smaller magnitude of the breach area fraction.

Figure C-7 shows another comparison of results of mean-value deterministic runs. In this case, stainless steel was selected as waste package material, and localized corrosion was disabled. The waste package failure versus time is identical in both Version 1.1 and 2.0 runs. The breach area fraction versus time differs due to the implementation of the updated approach in Version 2.0 (which results in a larger breach area fraction). As in the previous example, the increase in the area is propagated to estimates of radionuclide release rates. Figure C-7 includes near-field radionuclide release rates and dose estimates. Note that the transition to GoldSim Version 11.1 changed the color schedule of the radionuclide curves. In both cases, I-129 and Cs-135 are contributors to the dose estimates, with similar time evolution in both code versions. In Version 2.0, members of the U-238 decay chain series appear as important dose contributors (Ra-226, Rn-222, and Pb-210). These radionuclides did not appear in Version 1.1 due to a coding error (diffusion coefficients for these radionuclides were inadvertently assigned a value of 0 in the transition region between the buffer and the host rock); this error was corrected in Version 2.0.

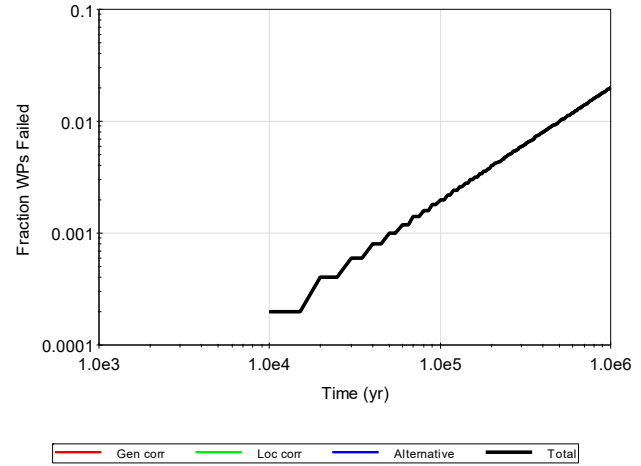
It is concluded that results of Version 2.0 are comparable to results of Version 1.1, with differences that can be explained on the basis of updates to address conceptual and coding errors.

SOAR Version 1.1

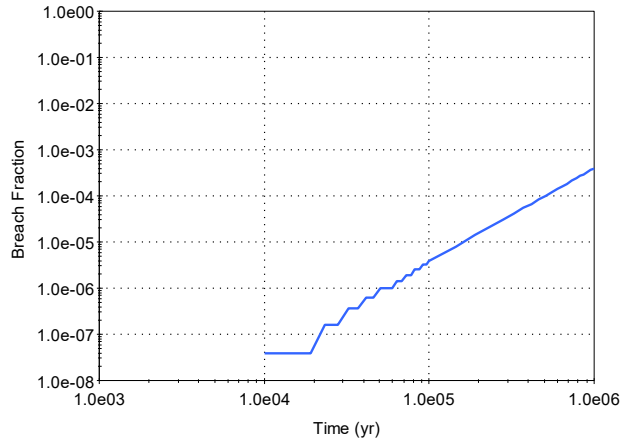


T04_V1.1.gsp Run: 10:52:00 AM 1/27/2017

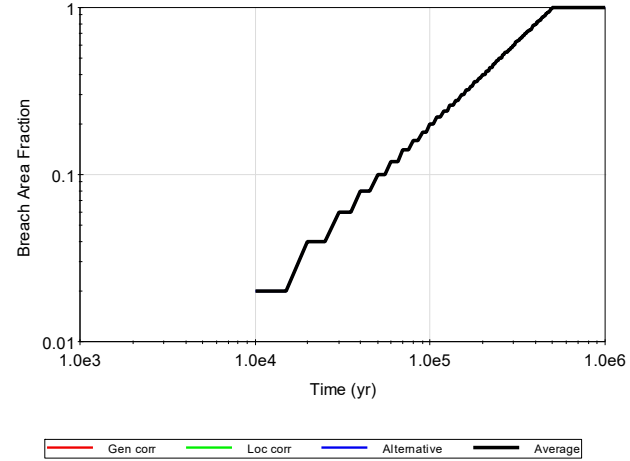
SOAR Version 2.0



T04_V2.0.gsp Run: 10:47:52 AM 1/27/2017



T04_V1.1.gsp Run: 10:52:00 AM 1/27/2017

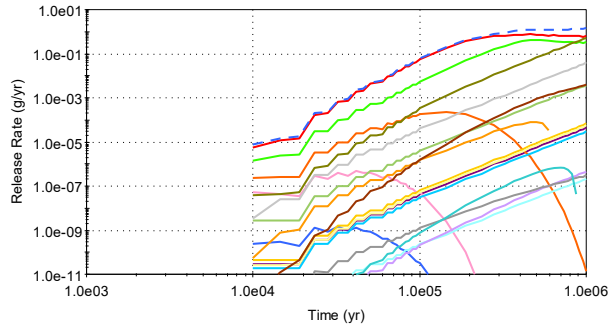


T04_V2.0.gsp Run: 10:47:52 AM 1/27/2017

Figure C-6. Comparison of Outputs of SOAR Versions 1.1 and 2.0 (Multiple-Events Failure Mode)

SOAR Version 1.1

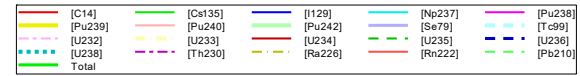
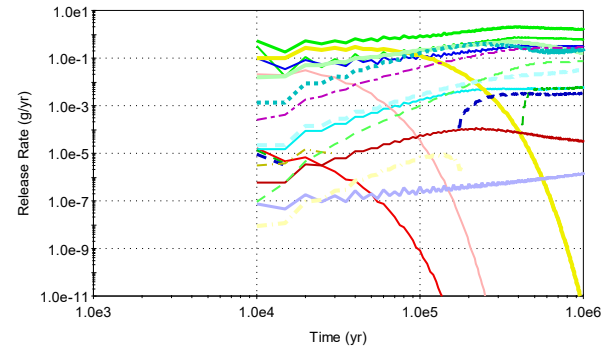
Release Rates from the Waste Package for SNF



T04_V1.1.gsp Run: 10:52:00 AM 1/27/2017

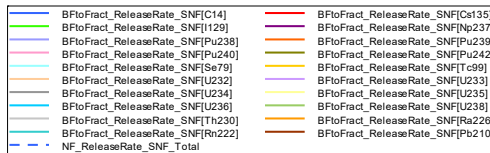
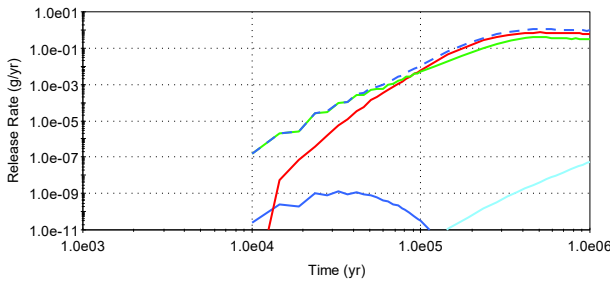
SOAR Version 2.0

Release Rates from the Waste Package for SNF



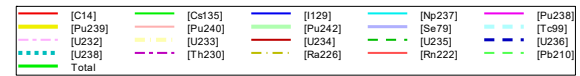
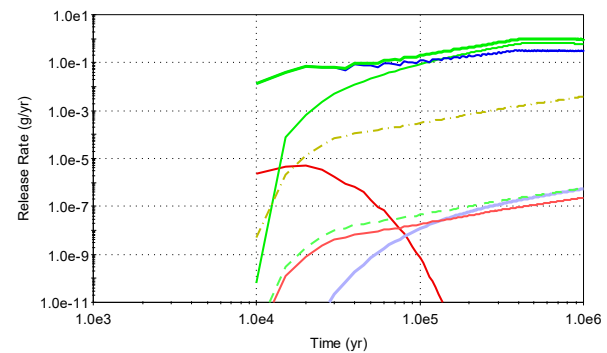
T04_V2.0.gsp Run: 10:47:52 AM 1/27/2017

Release Rates from the Near Field for SNF



T04_V1.1.gsp Run: 10:52:00 AM 1/27/2017

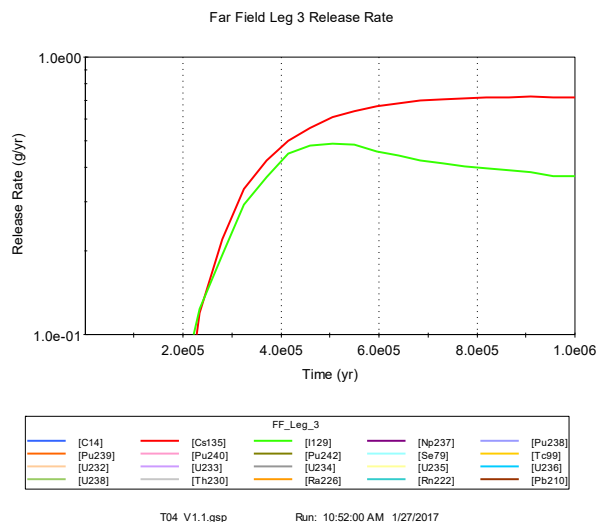
Near-Field SNF Release Rate



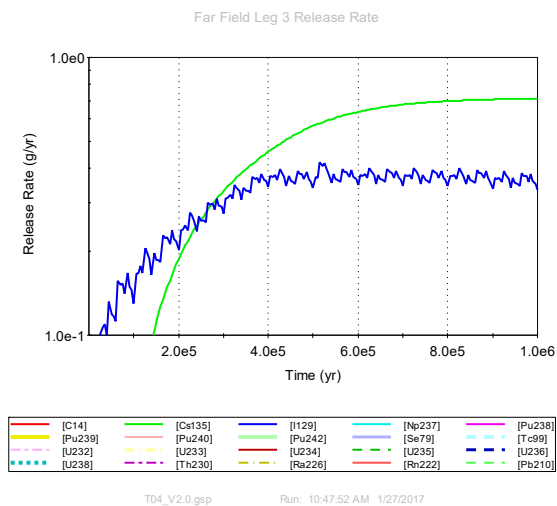
T04_V2.0.gsp Run: 10:47:52 AM 1/27/2017

Figure C-6 (Continued): Comparison of Outputs of SOAR Versions 1.1 and 2.0 (Multiple-Events Failure Mode)

SOAR Version 1.1



SOAR Version 2.0



C-11

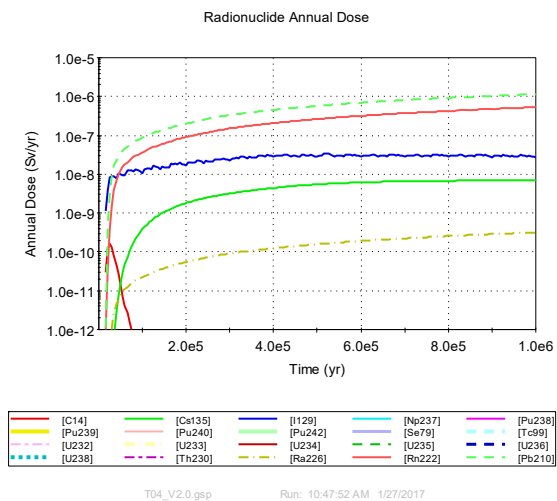
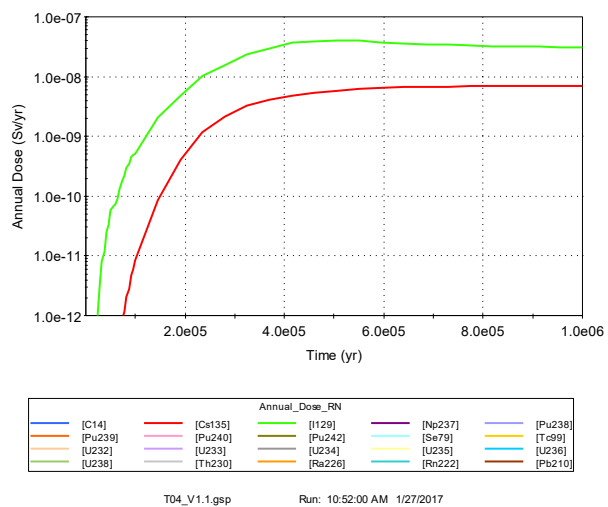
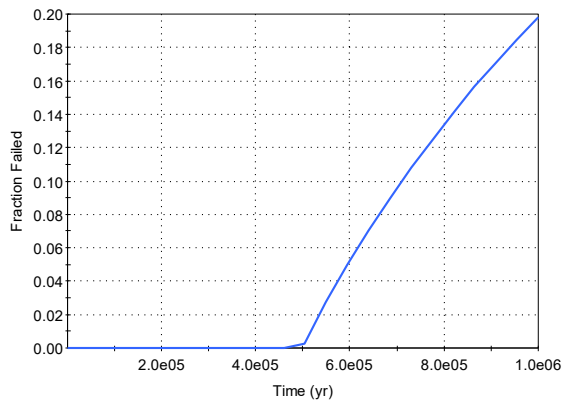


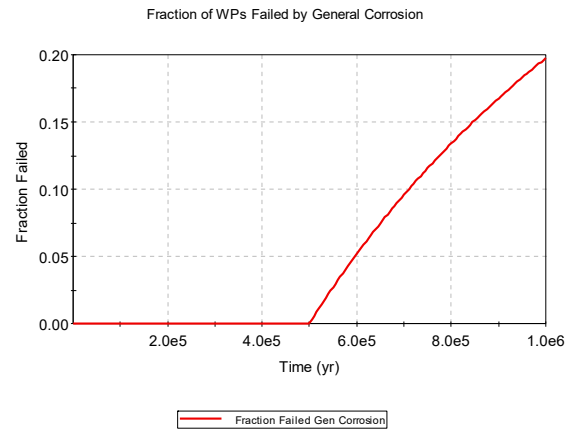
Figure C-6 (Continued): Comparison of Outputs of SOAR Versions 1.1 and 2.0 (Multiple-Events Failure Mode)

SOAR Version 1.1



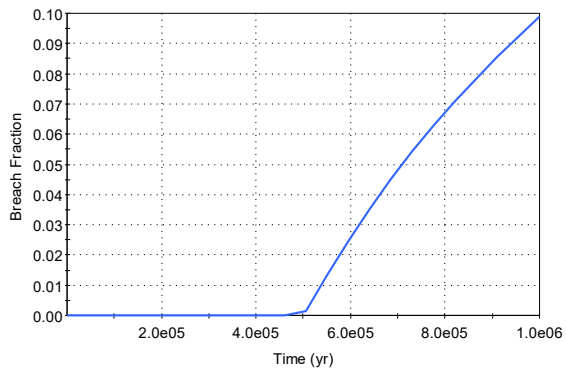
T05_V1.1.gsp Run: 4:11:49 PM 1/20/2017

SOAR Version 2.0



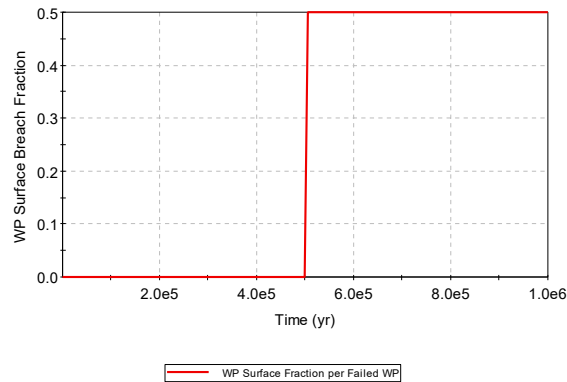
T05_V2.0.gsp Run: 4:16:08 PM 1/20/2017

Waste Package Breach Fraction Implemented



T05_V1.1.gsp Run: 4:11:49 PM 1/20/2017

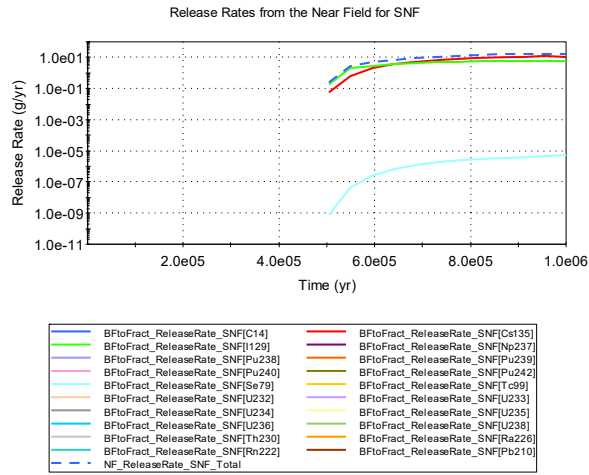
Combined WP Breached Area Fraction



T05_V2.0.gsp Run: 4:16:08 PM 1/20/2017

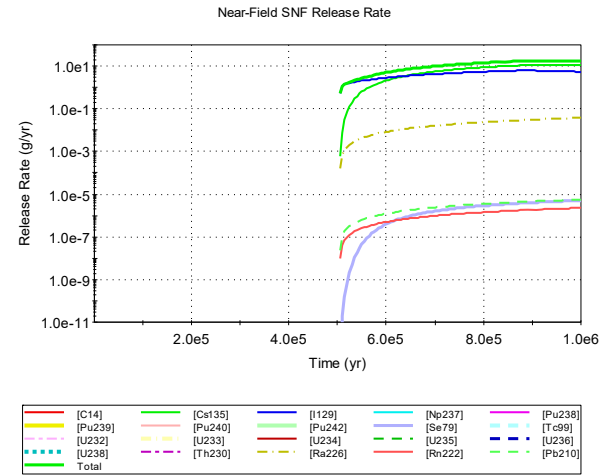
Figure C-7. Comparison of Outputs of SOAR Versions 1.1 and 2.0 (General Corrosion Failure Case)

SOAR Version 1.1



T05_V1.1.gsp Run: 4:11:49 PM 1/20/2017

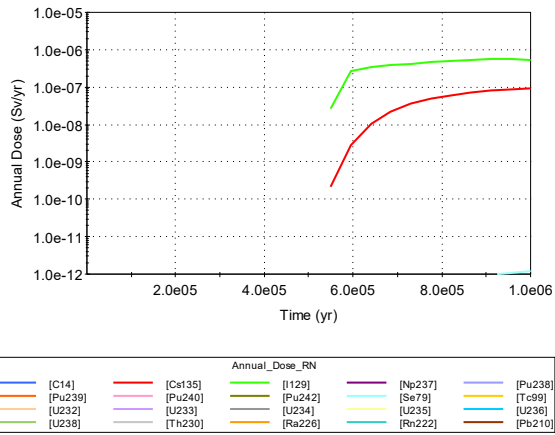
SOAR Version 2.0



T05_V2.0.gsp Run: 4:16:08 PM 1/20/2017

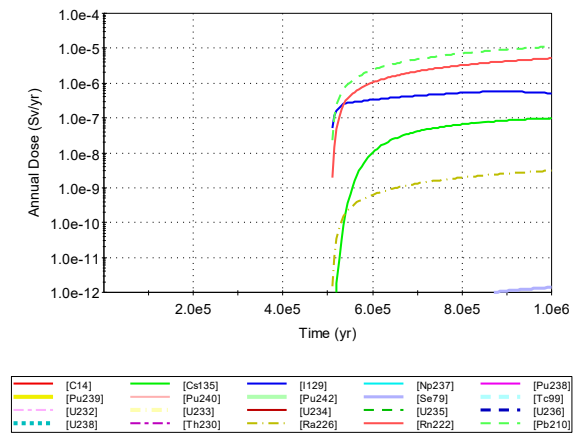
C-13

Radionuclide Annual Dose



T05_V1.1.gsp Run: 4:11:49 PM 1/20/2017

Radionuclide Annual Dose



T05_V2.0.gsp Run: 4:16:08 PM 1/20/2017

Figure C-7 (Continued). Comparison of Outputs of SOAR Versions 1.1 and 2.0 (General Corrosion Failure Case)

Remarks

A number of tests are presented in this summary report to clarify updates to migrate from SOAR Version 1.1 to Version 2.0. An abstraction was implemented in Version 2.0 that allows analyzing scenarios of the evolution of the buffer material and its relationship to waste package failure and radionuclide release. Version 2.0 of the SOAR code includes an explicit dependence of waste package failure on buffer evolution, but only for the case that the waste package material is copper and HS^- is present in the groundwater. Otherwise, waste package failure is modeled as independent of buffer performance. It is recognized that other systems exist wherein degradation of the buffer material is linked to degradation by corrosion of waste package materials.⁵ Radionuclide transport through the buffer material is always dependent on flow through the buffer. Thus, the SOAR Version 2.0 model provides some tools to evaluate the significance of the buffer material to the overall system performance, but the user should exercise caution given the model limitations.

A conceptual error in the manner by which the breach area of the representative waste package was computed in Version 1.1 was identified and fixed in Version 2.0. In SOAR Version 1.1, the breach area was incorrectly computed as the average of the failed and non-failed waste packages; in SOAR Version 2.0, the breach area is the average of the failed waste packages. Consequently, the breach area is significantly larger in Version 2.0. The multiple-events alternative failure mode produces release rates with abrupt oscillations for fast moving radionuclides (i.e., radionuclides with limited or null sorption in the buffer material and host rock, such as I-129), with the oscillations propagating all the way to dose estimates. Those oscillations are predominantly due to stepwise increases in the breach area after an event occurrence. This stepwise increase arises from the conservative assumption that the representative waste package experiences multiple events, accumulating damage. The model could be made less conservative by considering independent sets of waste packages failing after every event, and computing the breach area of the representative waste package as the average breach area of the failed waste packages (taking into account that few waste packages may be affected by multiple events and accumulate damage). The disadvantage of this approach is that it would increase the model complexity, and make the breach area model more difficult to explain, and results more difficult to interpret. A potential advantage of an alternative approach would be a reduction in the release rate versus time oscillations. Moving-window average approaches could be also explored to smooth the breach area versus time curve of the multiple-events alternative failure mode, and reduce oscillations in the release versus time curves.

Because of updates to the approach to compute the waste package breach area (resulting in larger values of the breach area compared to SOAR Version 1.1), results of the previous versions cannot be reproduced when identical input parameters are selected. However, it is possible to fully explain differences on the basis of changes and updates to the SOAR model, as shown in this appendix. Therefore, previous tests and test results remain valid for Version 2.0, so that it is sufficient to verify Version 2.0 by testing just the incremental changes to the SOAR code.

⁵ For example, in a concrete-iron system, iron can be kept passive by alkaline porewater, at least until concrete degrades (e.g., the porewater pH decreases) and iron becomes activated.

APPENDIX D

Test of Feature Pathway to Simulate a Human Intrusion Scenario

This Appendix D documents testing of SOAR Version 2.5 of the Feature Pathway Module, considering a human intrusion scenario. The objective of the test is to demonstrate the flexibility of the Feature Pathway module to simulate diverse systems. Some elements of the human intrusion scenario described by Chu, Lee, and Wang (2010) were adopted; for example

- A single borehole penetrates the repository at 1,000 years.
- The number of spent nuclear fuel waste packages affected by the intrusion is between 1 and 5.
- The intruding borehole flow is 2.55 m³/yr. This flow is residual groundwater flow, not associated with direct water extraction.

The following complementary assumptions were implemented

- The intruding borehole path is 1 km in length.
- The reference cross section is 1 m² (the flow speed is assumed 2.55 m/yr). A larger reference cross section would decrease the flow speed and decrease related releases. The reference cross section is not necessarily the borehole cross section. Flow may occur, for example, through the excavation damage zone. The reference cross section is uncertain, a value of 1 m² was selected for exploratory purposes. The only waste package failure mechanism is human intrusion (i.e., failure by corrosion was disabled).
- The Feature Pathway was used to simulate the human intrusion pathway. The near-field Feature Pathway segment length was set to 0.
- The Main Pathway was exercised in parallel to the Feature Pathway. The buffer was assumed to be an intact diffusive barrier. In the Main Pathway, radionuclides would diffuse through the buffer and through excavated disturbed zone until intercepting a far-field fracture.
- The far field host rock was assumed to be fractured rock. Each of the three legs of the far-field pathway was assumed to be 1 km in length.
- The dose pathway in SOAR is a drinking water pathway for both the Main and Feature Pathways. Other dose pathways related to direct exposure to waste cuttings are not considered in SOAR.

The model was executed in Monte Carlo mode, with a total of 500 realizations. The following figures demonstrate the dashboard selections to emulate a human intrusion scenario. The Waste Package Linear Failure Rate was modified to force waste package failure between 1,000 and 1,001 years (Figure D–1). A total of 7,500 spent nuclear fuel (SNF) waste packages were assumed present in the repository; therefore, 1 and 5 intruded waste packages correspond to 1.33×10^{-4} and 6.67×10^{-4} failed fractions, respectively. After the intrusion event, no diffusive resistance was assigned to the waste package (i.e., the waste package breach fraction was assumed 100 percent). Figure D–2 shows the settings in the Near Field dashboard to emulate direct intersection of the waste package by the intruding borehole. The Near Field Feature Pathway was set to an arbitrarily small length. Figure D–3 displays the settings in the Far Field dashboard for the Feature Pathway. The product of the “aperture” and the “width” define a

reference cross section (=1 m²). The flow velocity times the reference cross section equal the 2.55 m³/yr flow considered by Chu, Lee, and Wang (2010).

Waste Package Linear Failure Rate Inputs	
Start time of waste package failure (year):	<input type="text" value="1000"/> ?
End time of waste package failure (year):	<input type="text" value="1001"/> ?
Waste package failure fraction plateau (minimum fraction):	<input type="text" value="0.000133"/> ?
Waste package failure fraction plateau (maximum fraction):	<input type="text" value="0.000667"/> ?
Minimum waste package breach fraction*:	<input type="text" value="1"/> ?
Maximum waste package breach fraction*:	<input type="text" value="1"/> ?

Figure D-1. Alternative Failure Modes dashboard settings, forcing waste package failure between 1,000 and 1,001 years. The fractions 1.33×10^{-4} and 6.67×10^{-4} correspond to 1 and 5 spent nuclear fuel (SNF) waste packages out of 7,500 in the repository.

(a)

Buffer, Zone 2

Buffer case *See diagram below for Variable Openings case*

	Value
Length [m]	0.5
Inner radius [m]	0.5
Reference height [m]	0.5
Flow factor	1

Flow factor with respect to far-field leg-one flow

(b)

Feature Pathway

Enable Feature Pathway

BF diffusive length [m]	1E-10	<i>Additional diffusive path in buffer to reach the tunnel</i>
Tunnel length [m]	1E-10	
Tunnel cross section [m2]	1	
Enable sorption (0, 1)	0	<i>If disabled, Kd=0 and porosity=1. If enabled, Kd=buffer Kd</i>

Zero concentration far-field discharge cell
*If checked, the far-field discharge cell is fixed at zero concentration.
If unchecked, the discharge rate to the far-field is controlled by the flow rate.*

Define flow through the tunnel of the NF Feature Pathway
*If checked, user-defined flow is selected (next field)
If unchecked, the flow is computed based on the FF Leg 1 flux. Flow factor used to modify the flow.*

Flow rate (m³/yr)

Figure D–2. Near Field dashboard settings. (a) The buffer was assumed to be a diffusive barrier (intact buffer case). (b) A negligible distance of the Feature Pathway length was input to emulate direct borehole intersection of the waste package. The flow rate 2.55 m³/yr is based on data by Chu, Lee, and Wang (2010).

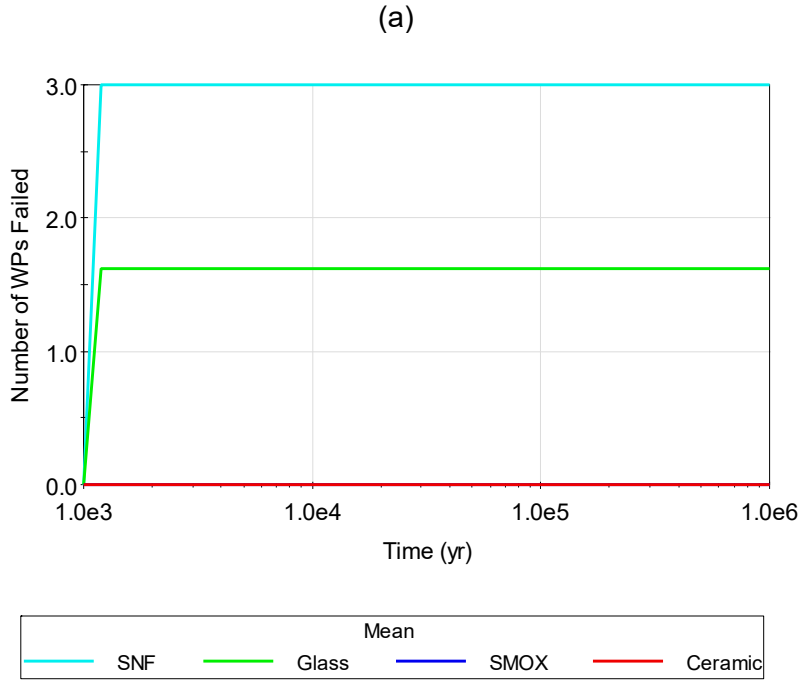
Feature Pathway (e.g., shaft, fault, tunnel)

The Feature Pathway (FP) is an independent pathway with direct release to the biosphere. Water flows through the FP are independently defined by the user. The host rock is assumed consistent with the Leg One host rock. The Near Field FP must be enabled in the Near Field dashboard to activate the Far Field Feature Pathway.

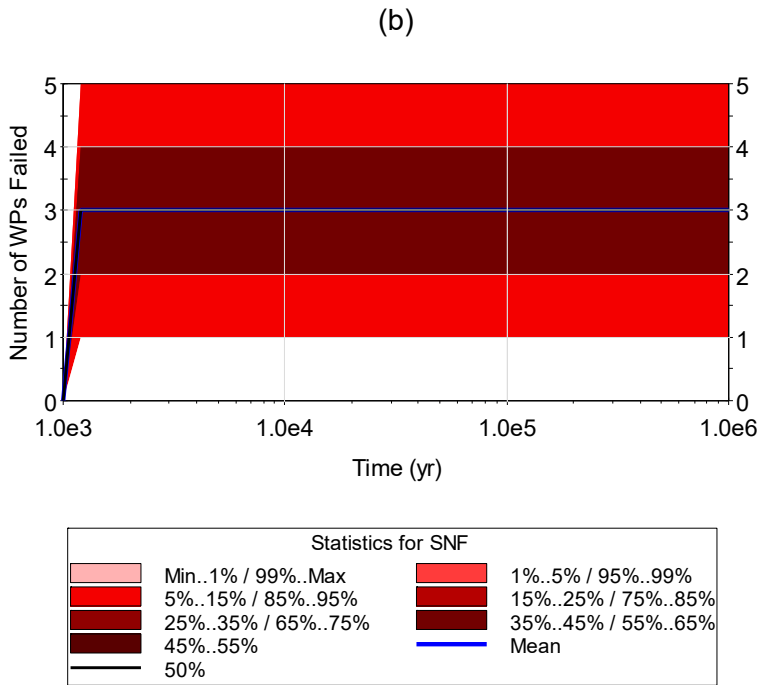
	Value	
Length [m]	1000	
Dispersivity/Length	0.1	
Aperture [m]	1	<i>The aperture controls mass transfer with the matrix, if enabled.</i>
Width [m]	1	<i>Width is perpendicular to the aperture.</i>
Enable matrix diffusion? (0-no, 1=yes)	1	
Flow velocity [m/yr]	2.55	
Water travel time	392.157 yr	

Figure D–3. Far Field dashboard settings.

The following plots show results from the Monte Carlo run. Figure D–4 displays plots of the number of waste packages failed per human intrusion event. The plot in Figure D–4(a) is the average number of waste packages failed. The average of SNF packages is 3, consistent with assumptions by Chu, Lee, and Wang (2010). Only SNF and glass waste form packages are assumed to be affected by the human intrusion. The spent mixed-oxide fuel (sMOX) and ceramic waste form are assumed unaffected by the intrusion event. The products of the waste package intrusion fractions, 1.33×10^{-4} and 6.67×10^{-4} , and the number of sMOX and ceramic waste packages (50 and 100, respectively), are numbers that are less than 0.1; GoldSim rounds those numbers to 0 failed waste packages. Figure D–4(b) is the number of SNF waste packages for the 500 realizations. The number ranges from 1 to 5, following a uniform distribution, with a mean of 3, as expected. Figure D–5 includes plots of near-field and far-field releases, including the Feature and Main Pathways. The near-field release to the far field is dominated by the Feature Pathway [curve labeled To FF (Feature) in Figure D–5(a)]. Note that in the SOAR model, radionuclides are first incorporated in the buffer before splitting into the Main and Feature Pathways. Figure D–5(b) is a plot of far-field releases. The Leg 1, Leg 2, and Leg 3 transfer rates are displayed to show decreasing transfer rates. Activity transfer rates to the biosphere are dominated by the Feature Pathway (human intrusion borehole) before 10,000 years, and then dominated by the Main Pathway after 10,000 years. The reversal of the activity transfer rate is counterintuitive, because the Feature Pathway is dominant in the near field. One explanation for the reversal can be identified by examining the water travel times in the far field (Figure D–6). The distribution of travel times in the Main Pathway is log-uniform, spanning up to eight orders of magnitude. By contrast, the travel time in the far field Feature Pathway is 392 years ($=1,000 \text{ m} / 2.55 \text{ m/yr}$). The large variation of water travel times is an artefact of the simple far-field flow model implemented in SOAR. The user inputs the hydraulic gradient in the Far Field dashboard. The Darcy flux is computed in SOAR based on an effective hydraulic conductivity, computed as a function of the fracture aperture and fracture separation. Flow velocities also depend on the fracture aperture and the fracture spacing (for a given average flux, the flow velocity is higher in systems of narrow fracture aperture or very large fracture spacing). Fracture aperture and fracture spacing are independently sampled in SOAR, giving rise to extreme flow velocities. In reality, flow rates, fracture apertures, and fracture spacing or fracture density are correlated, constraining the range of attainable flow velocities. The SOAR model can be modified to take the water travel time and fracture aperture distributions as inputs, and sample those parameters in correlated manner, to be more consistent with site characteristics. Computations in this appendix were not intended to be realistic, but only exploratory to exhibit properties of the Feature Pathway model.



SOAR_Version_2.0_14_HumanIntrusion_Stochastic_IntactBuffer.gsm Run: 7:13:35 PM 2/19/2019

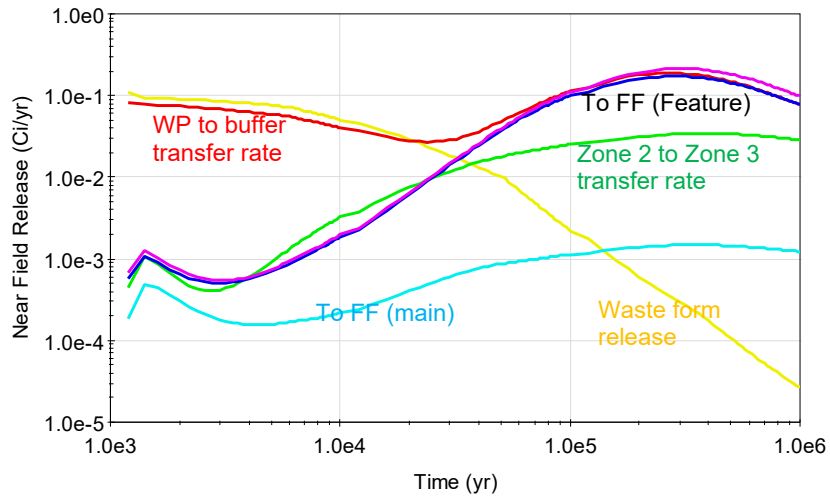


SOAR_Version_2.0_14_HumanIntrusion_Stochastic_IntactBuffer.gsm Run: 7:13:35 PM 2/19/2019

Figure D-4. (a) Average number of waste packages failed per waste form package, and (b) distribution of SNF waste packages failed per human intrusion event.

(a)

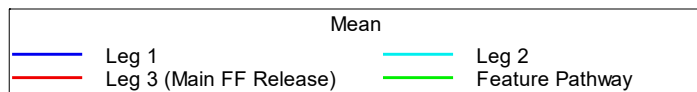
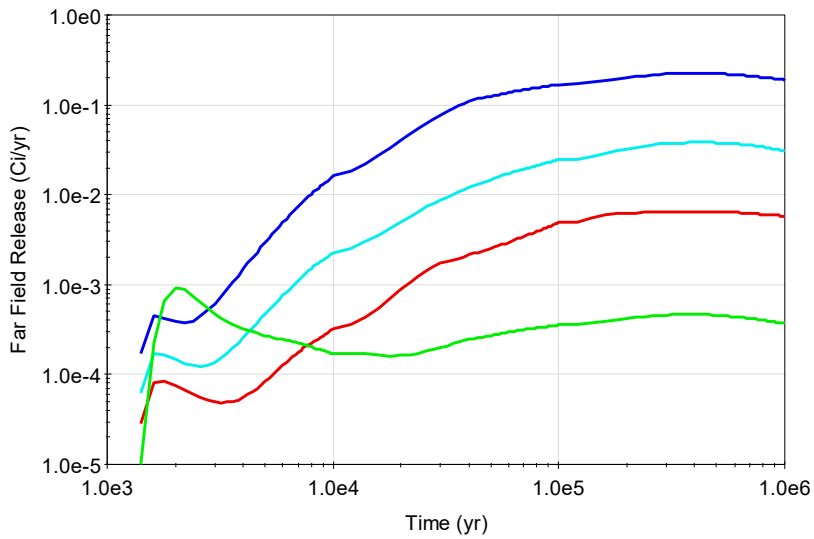
All Waste Forms



SOAR_Version_2.0_14_HumanIntrusion_Stochastic_IntactBuffer.gsm

Run: 7:13:35 PM 2/19/2019

(b)



SOAR_Version_2.0_14_HumanIntrusion_Stochastic_IntactBuffer.gsm

Run: 7:13:35 PM 2/19/2019

Figure D-5. (a) Near Field and (b) Far Field releases.

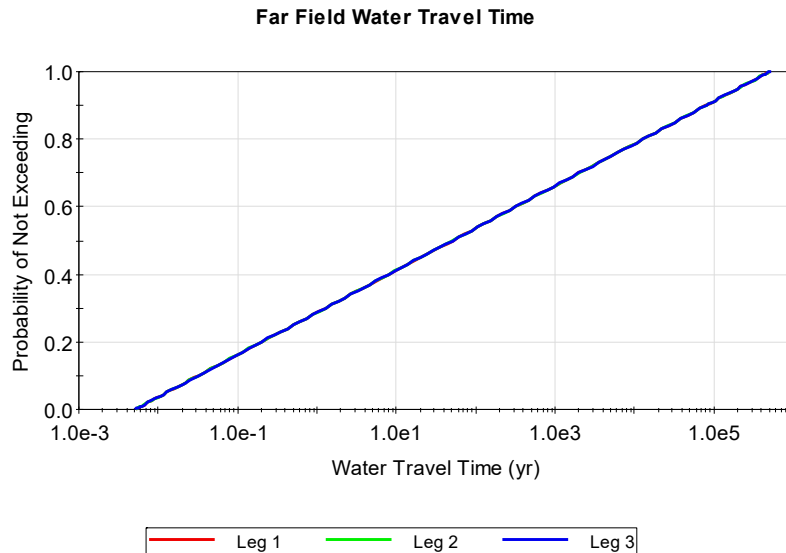
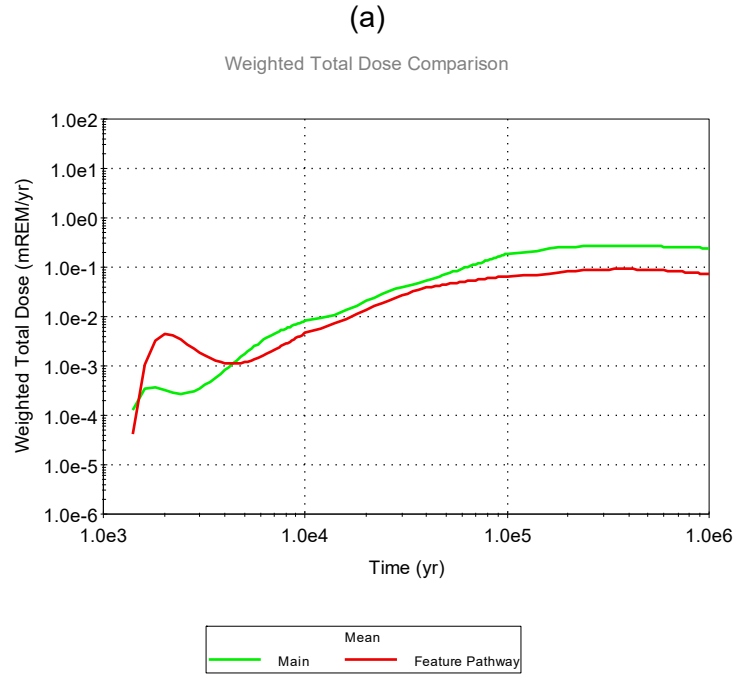


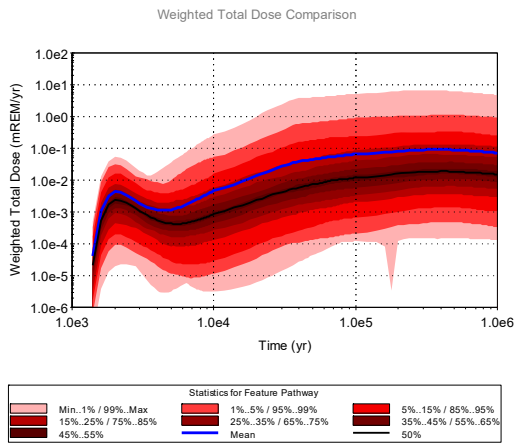
Figure D-6. Water travel times in the Main Pathway of the far field.

Figure D-7 includes dose estimates associated with the human intrusion event and the Main Pathway. The doses are tracked separately in SOAR, because the biosphere system may be different. For example, in the case of the human intrusion scenario, doses are computed directly above the repository site, while in the Main Pathway doses occur at a distance from the site. The SOAR model can be updated to include options to aggregate doses, if needed. The plot in Figure D-7(a) displays the total dose (aggregated over all radionuclides) of the human intrusion and Main Pathway. The doses are comparable at all times; the human intrusion dose is greater than the Main Pathway dose during the first 500 years, and less than the Main Pathway dose afterwards. Figure D-7(b) and (c) shows uncertainty bands in dose estimates. The broader uncertainty band of the Main Pathway is associated in part with the broader variability in performance of the natural system (e.g., water travel time in the far field fractures ranging from a few days to hundreds of thousands of years —Figure D-6). A more realistic representation of site-specific far-field flow may constrain uncertainty in the dose estimates.

The objective of the test documented in this appendix was demonstrating the flexibility of the Feature Pathway model, and SOAR in general, to simulate different release scenarios. The plots displayed in this appendix are all accessible from results dashboards. The corresponding GoldSim model file of the human intrusion scenario is provided with the distribution of SOAR Version 2.5, to allow exploration of additional results.



(b) Dose from human intrusion event (Feature Pathway)



(c) Dose from Main Pathway

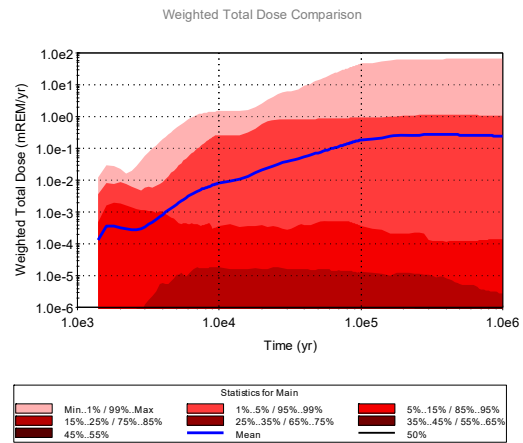


Figure D-7. Dose estimates. (a) Comparison of total dose associated with the human intrusion event (Feature Pathway) and the Main Pathway. Uncertainty band of the (b) human intrusion and (c) Main Pathway dose estimates.

Reference

S. Chu, J.H. Lee, Y. Wang. 2010. "Monte Carlo Simulation for Generic Granite Repository Studies." Report LA-UR-10-08186. Los Alamos National Laboratory.
<http://permalink.lanl.gov/object/tr?what=info:lanl-repo/lareport/LA-UR-10-08186>

APPENDIX E

Input Parameter Database

A Microsoft Access database was prepared to control input parameters of the SOAR model. To facilitate database inputs, users supply information on parameter distributions and values through bridge Excel files. The following Excel files are maintained in a SharePoint server:

- Parameter_Waste_Form-C.xls
- Parameter_Waste_Package-C.xls
- Parameter_Near_Field-C.xls
- Parameter_Far_Field-C.xls
- Parameter_Biosphere-C.xls

The file name refers to the SOAR module name (Waste Form, Waste Package, Near Field, Far Field, and Biosphere). Each Excel file is of the same structure, with worksheets that should be updated in case new parameter information is to be introduced to the parameter database. Table E–1 includes a brief description of the worksheets.

Table E–1. Description of worksheets in Excel files to prepare the SOAR input database

Worksheet name	Description
Name_Entry	Worksheet with the unique parameter names. The column Value_ID is a number indicating the information source row in the Attribute_Entry worksheet
Attribute_Entry	Worksheet with parameter distribution definitions (e.g., uniform, normal, discrete, triangular)
GS_Parameter	Worksheet with a GoldSim-compatible structure. This worksheet is linked to Name_Entry and Attribute_Entry. The user should ensure that new information in those worksheets is properly displayed through linked formulas.
GS_Parameter_Value	Worksheet with a GoldSim-compatible structure. This worksheet is linked to Name_Entry and Attribute_Entry. The user should ensure that new information in those worksheets is properly displayed through linked formulas.
GS_Value_Component	Worksheet with a GoldSim-compatible structure, including values for distribution functions. This worksheet is linked to Name_Entry and Attribute_Entry, except on column A, Value_ID. The user must manually update information in the column Value_ID for consistency with Value_ID in the Attribute_Entry worksheet.
Parameter_Code	Dictionary of parameter codes. This worksheet is for information only; the user should not modify this worksheet.
bFTPA internal	List of radionuclides tracked in the SOAR model. This worksheet must be modified when the list of radionuclides is changed. All parameters that are specified as a set of radionuclides (e.g., inventories and dose coefficients) must be consistently updated, as well as the GoldSim SOAR model file. Changing the list of radionuclides in SOAR can be a labor intensive process, and prone to error.
GoldSim	Dictionary of probability distribution function codes. This worksheet is for information only; the user should not modify this worksheet.

The SOAR database is designed to be incremental, with updated values to be added as new entries, while keeping old information. See the entry for the parameter DegRate_SNF_Anoxic in the file Parameter_Waste_Form-C.xls for an example of a new entry with the same parameter name as an older entry. Adding new entries for updated information is optional; alternatively, it is more straightforward to update existing entries, albeit at the expense of losing previous information. However, SharePoint tracks Excel file versions, and the previous information is still captured in the SharePoint system. It is up to the user to decide whether to add new entries (and preserve old entries in the database), or to simply update existing entries. Old entries become inactive in the SOAR database.

The GoldSim database structure, in general, includes dated entries to facilitate retrieving information pertaining to a specific date or date range within a GoldSim model file. However, the SOAR parameter database was not designed to pass dated entries to a SOAR model file. Instead, each parameter is declared with one unique active entry (or a set of entries for

parameters that are radionuclide vectors). Only the active entry can be retrieved for each parameter. Inactive entries can be identified in the worksheet GS_Parameter, column Parameter_Name, by the presence of curly brackets enclosing a number next to the parameter name (e.g., DegRate_SNF_Anoxic{7}). Retrieval of old information captured in the database requires a database update, to declare a different entry as active for a specific parameter. The active entry for a parameter is declared in the Excel worksheet titled Name_Entry, on the Value_ID column.

The Excel file FPA-SOAR-C.xls is a synthesis file connected to the five support Excel files listed in previous bullets, implementing a GoldSim-compatible syntax or structure. The entries in the file FPA-SOAR-C.xls are automatically updated. This file does not require any modification when the user updated information solely in existing entries in any of the five support files. A straightforward change is required when the user adds new entries to any of the five support files. The change involves adding new rows, and copying existing formulae in other entries to the new rows, to connect to the newly added entries in the support Excel files.

The process to generate the Microsoft Access database is described in the following bullets.

- Step 1: Save the five Excel files and the synthesis file FPA-SOAR-C.xls to a local directory. The formulas in the Excel files point to relative locations, and remain valid in the local directory.
- Step 2: Using Microsoft Access, create a new database and delete any default tables.
- Step 3: Use the Import Spreadsheet Wizard to import the worksheets in the file FPA-SOAR-C.xls (Figure E-1). Select “No primary key” in the Import Spreadsheet Wizard. Repeat the process for each of the three worksheets in the spreadsheet (GS_Parameter, GS_Parameter_Value, GS_Value_Component). At the end of the import process, a database object with three tables will be created (Figure E-2).
- Step 4: Save the newly created database and name it FPA-SOAR.accdb, and close the file.

The following steps describe the approach to make the database accessible to Windows in general, and to GoldSim in particular.

- Step 1: In the Windows Control Panel, locate Administrative Tools.
- Step 2: Locate ODBC Data Sources (32-bit) [Figure E-3(a)]. A computer administrator password may be required to launch ODBC Data Sources (32-bit).
- Step 3: Go to the System Data Source Name (DSN) and click on the “Add...” button, and select “Microsoft Access Driver (*.mdb, *.accdb)” [Figure E-3(b)].
- Step 4: Name the Data Source Name FPA-SOAR.
- Step 5: Then click on the button “Select...” and navigate to the FPA-SOAR.accdb file [Figure E-3(c)]. The new data source will then become available in the System DSN tab [Figure E-3(d)].

The FPA-SOAR database may be tested within the GoldSim model file. For example, locate a stochastic element connected to the database within the SOAR model file. Double click the stochastic element and select the Database tab. Click the “Download Now” button (Figure E-4). If the download is successful, the date in the Status field will reflect the current time (Figure E-4).

Do not check the box “Download data with the most recent Effective Date on or before:” (Figure E-4). As previously stated, FPA-SOAR database does not support retrieval of dated

information. There is only one active entry per parameter from which data can be retrieved, independently of the date.

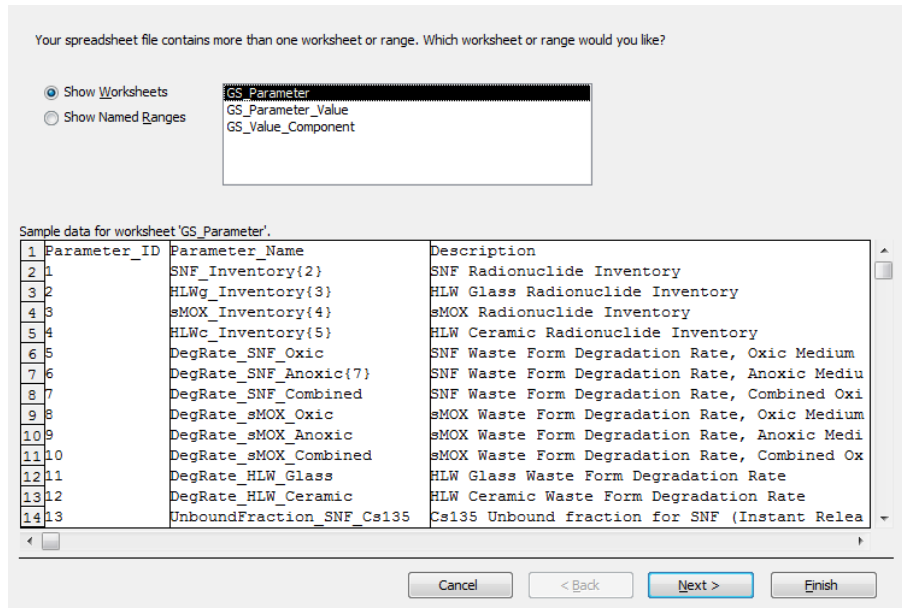


Figure E-1. Import Spreadsheet Wizard in Microsoft Access. The import process must be repeated three times, once for each of the three worksheets (GS_Parameter, GS_Parameter_Value, GS_Value_Component) in the file FPA-SOAR-C.xls.

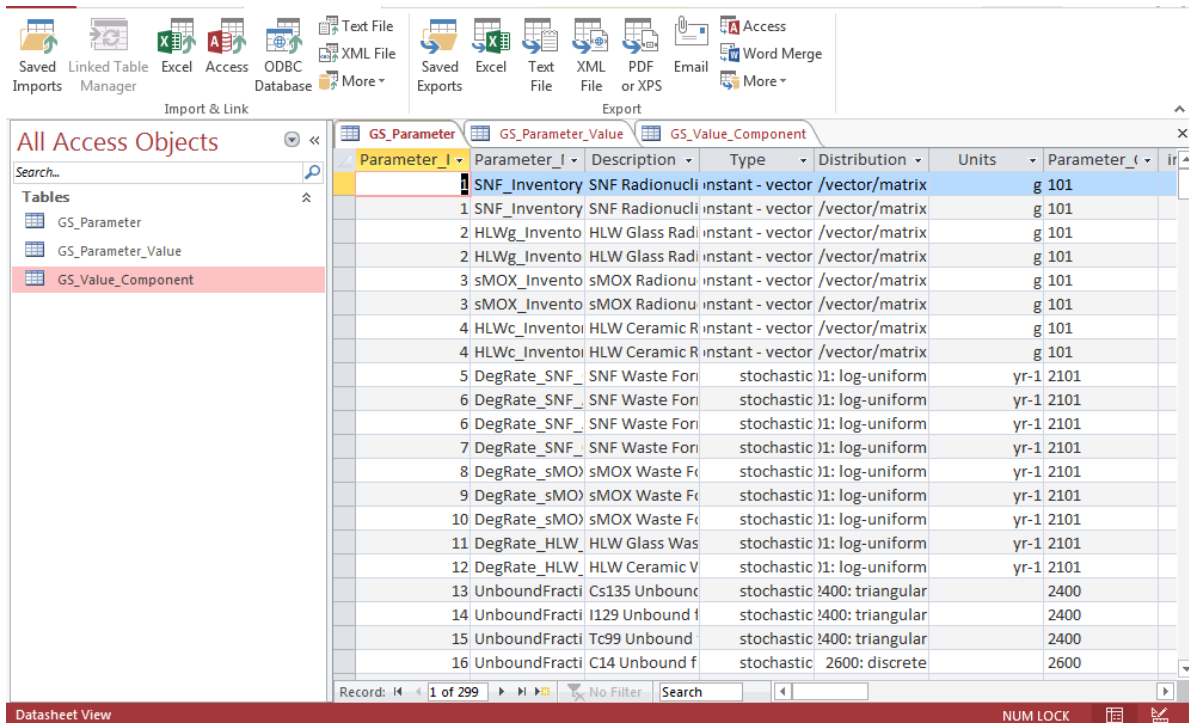


Figure E-2. A database object with three tables is created at the end of the import process.

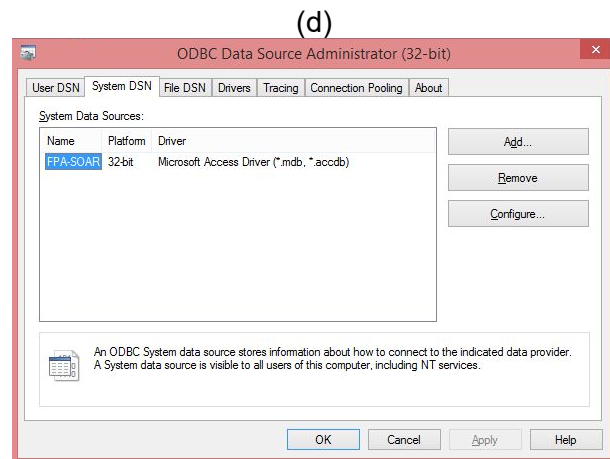
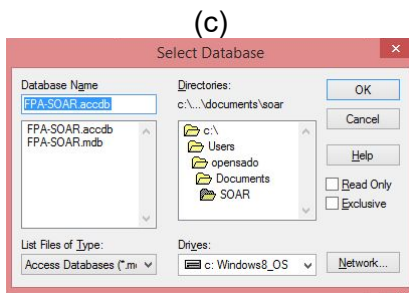
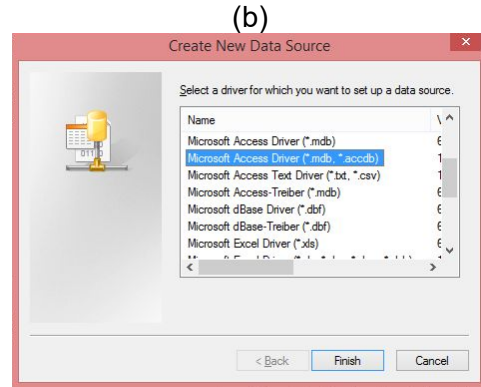


Figure E-3. Process to make accessible a database to Windows and GoldSim.

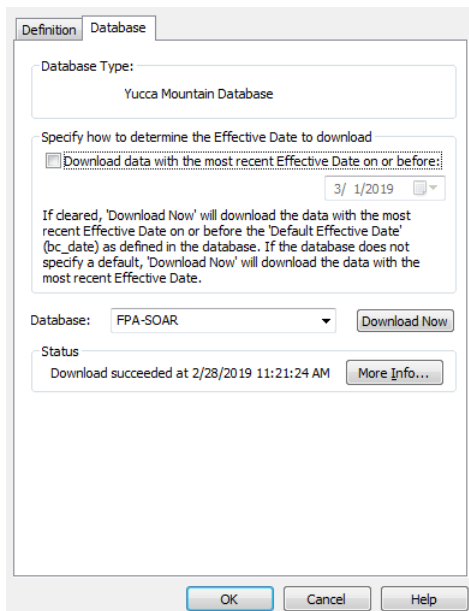


Figure E-4. The FPA-SOAR database can be tested from the Database tab of stochastic element in the SOAR model file.